Elucidation of the structure and biosynthetic pathways of dihydromenthofurolactones as highly potent aroma compounds of basidiomycetes

Cumulative Dissertation

Presented by

Fabio Francesco Brescia, M. Sc.

for the degree of

Doctor rerum naturalium (*Dr. rer. nat.*)

submitted to the

Faculty of Biology and Chemistry

prepared at the

Institute of Food Chemistry and Food Biotechnology

Justus Liebig University Giessen, Germany

2024

This thesis is accepted as a doctoral dissertation in fulfillment of the requirements for the degree of *Doctor rerum naturalium* by the Faculty of Biology and Chemistry, Justus Liebig University Giessen, Germany.

Dean:	Prof. Dr. Holger Zorn
Members of the committee:	Prof. Dr. Holger Zorn
	Prof. Dr. Matthias Wüst
	Prof. Dr. Martin Rühl
	Prof. Dr. Siegfried Schindler
1st Referee:	Prof. Dr. Holger Zorn
	Institute of Food Chemistry and Food Biotechnology
	Justus Liebig University Giessen
2nd Referee:	Prof. Dr. Matthias Wüst
	Institute of Nutritional and Food Science
	University of Bonn

Declaration

I declare that I have completed this dissertation single-handedly without the unauthorized help of a second party and only with the assistance acknowledged therein. I have appropriately acknowledged and cited all text passages that are derived verbatim from or are based on the content of published work of others, and all information relating to verbal communications. I consent to the use of an anti-plagiarism software to check my thesis. I have abided by the principles of good scientific conduct laid down in the charter of the Justus Liebig University Giessen „Satzung der Justus-Liebig-Universität Gießen zur Sicherung guter wissenschaftlicher Praxis“ in carrying out the investigations described in the dissertation.

Date, Place

Signature

Acknowledgements

The practical work of this thesis was carried out between October 2019 and June 2023 at the Institute of Food Chemistry and Food Biotechnology at the Justus Liebig University Giessen under the supervision of Prof. Dr. Holger Zorn. The work was made possible by the contribution and help of a number of people to whom I would like to express my gratitude.

Foremost, I would like to express my deepest gratitude to **Prof. Dr. Holger Zorn**, who allowed me to realize this work. His excellent supervision, the granted trust, the constant scientific input and the high motivation kept me to focus my research objectives.

I would like to thank **Prof. Dr. Matthias Wüst** to be the second supervisor of this thesis. Additionally, I am very thankful to **Prof. Dr. Martin Rühl** for joining the thesis committee and for the great inspiration and fruitful discussions during my thesis. I would also like to thank **Prof. Dr. Siegfried Schindler** for joining the thesis committee.

Dr. Marco Alexander Fraatz owes a lot of thanks, not only for the technical support in the field of gas chromatography, but also for the constant scientific exchange, hours of discussions and support in many ways. Thanks a lot!

Furthermore, I would like to sincerely thank **Dr. Raffael Christoph Wende** for carrying out organic syntheses, the scientific exchange, the good collaboration with the Institute of Organic Chemistry and the support. I would also like to express my gratitude to **Dr. Heike Hausmann** from the Institute of Organic Chemistry for performing the NMR measurements and supporting the structure elucidation. Moreover, I would like to thank **Dr. Flavius Popa** from the Black Forest National Park for the good collaboration.

Additionally, I would like to thank my colleagues for the time we spent at LCB. Besides the hard work, we had plenty of good times. In particular, I would like to thank my documentary zone colleagues Bastian Loderhose, Friederike Bürger, Jean-Philippe Kanter, Niklas Broel, and Suzan Yalman for the advice and making the hard work a little bit easier. The bachelor and master students at the LCB also deserve thank for their work. Particularly noteworthy are Jan Passinger, Maximilian Koch, and Wassilios Pitelas.

The final words go to my parents Mechthild and Raffaele as well as my brother Daniele and my sister Laura for always supporting me. Thank you for your steady support and incentive to continue even in the harder times.

Abstract

Increasing consumer rejection towards non-natural food ingredients is driving the global demand for natural food ingredients, including natural flavors. Many biocatalytic production processes are used in order to meet this demand, offering the advantage that, unlike many chemical syntheses, they often adhere to the principles of green chemistry. As fungi are known to be excellent biocatalysts harboring a broad enzymatic portfolio, research on their potential as natural flavor source is increasingly conducted.

The present work aimed to investigate the structure, biogenesis, and olfactory properties of a highly interesting group of aroma compounds, the bicyclic benzofuran derivatives. *Cystostereum murrayi*, a rarely occurring species found in the Black Forest National Park, was identified to *de novo* form derivatives of the above-mentioned compounds. Volatile compounds produced by the fungus in submerged culture were identified after aroma dilution analysis (ADA) using dynamic headspace extraction (DHS) after sensory evaluation of the culture supernatant. Among the perceived substances were two diastereoisomers of 3,6-dimethyl-2,3,3a,4,5,7a-hexahydrobenzofuran (dill ether). The identification of the three substances with the highest flavor dilution (FD) values was achieved after isolation using preparative HPLC by means of nuclear magnetic resonance (NMR) and high-resolution mass spectrometry (HR-MS). Hereby, the compounds were identified as two diastereoisomers of 3,6-dimethyl-3a,4,5,6,7,7a-hexahydro-3*H*-1-benzofuran-2-one, known as dihydromenthofurolactones (dml), as well as the C3-unsaturated analogue (Δ^3-dml). Semiquantitative analyses revealed comparatively high concentrations of 8 mg L^{-1} (dml **a**), 22 mg L^{-1} (Δ^3-dml), and 86 mg L^{-1} (dml **c**).

As the benzofuran derivatives studied within this work are chiral aroma compounds, their olfactory properties such as odor impression and threshold may differ depending on the investigated enantiomer. Employing chiral analyses by means of enantioselective multidimensional gas chromatography (MDGC) in comparison to authentic standards, either of natural origin or from chemical synthesis, revealed a stereospecific formation (enantiomeric ratio (er) >99.9:0.1) of the respective stereoisomer. Thereby, dill ether and dml differed in the orientation of the methyl group at the C3* position, at which Δ^3-dml contains a double-bond. Noteworthy, the dill ether and lactones' stereochemistry differs significantly at two positions within the tetrahydrofuran ring system, suggesting independent biosynthetic pathways. Indeed, supplementations studies using labeled and non-labeled potential terpenoid precursors suggested dill ether formation via *p*-menth-1-en-9-ol. The latter may thereby be formed as a biotransformation product of limonene, which, however, does not necessarily act as a precursor within the fungus. Analogous precursors could be excluded for the (Δ^3)-dml.

The high FD value determined for dml **a** at comparatively low concentrations indicated a low odor threshold. For the determination, a novel approach by means of direct analysis via gas chromatography-olfactory (GC–O) in conjunction with a flame ionization detector (FID) was established. The determined odor threshold of 1.9 x 10^{-6} ng L^{-1} air represents one of the lowest thresholds known to date.

Additionally, the combination of aroma analysis data and bioinformatics allowed for the identification of an *O*-methyltransferase in *Pleurotus sapidus*, a close relative to the well-known oyster mushroom, involved in aroma biogenesis. The enzyme was heterologously expressed in *Escherichia coli*, crystallized, and enabled the transmethylation of both hydroxylated compounds and a thiol-nucleophile.

Zusammenfassung

Die zunehmende Ablehnung nicht natürlicher Lebensmittelzusätze durch Verbraucher führt zu einer weltweit steigenden Nachfrage nach natürlichen Lebensmittelinhaltsstoffen, einschließlich natürlicher Aromen. Um dieser Nachfrage gerecht zu werden, gewinnen biokatalytische Produktionsverfahren zunehmend an Relevanz. Diese bieten gegenüber der chemischen Synthese zudem oftmals den Vorteil, die Grundsätze der nachhaltigen Chemie (*green chemistry*) zu erfüllen. Pilze, die als exzellente Biokatalysatoren bekannt sind und über ein breites enzymatisches Portfolio verfügen, werden daher zunehmend auf ihr Potenzial als Quelle natürlicher Aromastoffe untersucht.

Ziel der vorliegenden Arbeit war es, die Struktur, Biogenese und Geruchseigenschaften einer hochinteressanten Gruppe von Aromastoffen, den bicyclischen Benzofuranderivaten, zu untersuchen. Mit *Cystostereum murrayi* wurde eine seltene, im Nationalpark Schwarzwald vorkommende, Art identifiziert, die Vertreter der oben genannten Verbindungen *de novo* bildet. Zur Identifizierung der vom Pilz in submerser Kultur gebildeten flüchtigen Verbindungen wurde nach sensorischer Bewertung des Kulturüberstandes eine ADA mittels DHS durchgeführt. Unter den wahrgenommenen Substanzen befanden sich zwei Diastereoisomere von 3,6-Dimethyl-2,3,3a,4,5,7a-hexahydrobenzofuran (Dillether). Die Identifizierung der drei Substanzen mit den höchsten FD-Werten erfolgte nach der Isolierung mittels präparativer HPLC durch NMR und HR-MS. Hierbei wurden die Verbindungen als zwei Diastereomere von 3,6-Dimethyl-3a,4,5,6,7,7a-hexahydro-3*H*-1-benzofuran-2-on, auch bekannt als Dihydromenthofurolactone (dml), sowie das C3-ungesättigte Analogon (Δ^3-dml) identifiziert. Die semiquantitativ ermittelten Konzentrationen im Überstand waren mit 8 mg L^{-1} (dml **a**), 22 mg L^{-1} (Δ^3-dml) und 86 mg L^{-1} (dml **c**) erstaunlich hoch.

Da es sich bei den in dieser Arbeit untersuchten Benzofuranderivaten um chirale Aromastoffe handelt, können sich ihre olfaktorischen Eigenschaften wie Geruchseindruck und -schwelle abhängig vom untersuchten Enantiomer unterscheiden. Chirale Analysen mittels enantioselektiver MDGC und der Vergleich mit authentischen Standards natürlichen oder synthetisierten Ursprungs zeigten eine stereospezifische Bildung (*er* >99,9:0,1) des jeweiligen Stereoisomers. Dabei unterscheiden sich sowohl Dillether als auch dml in der Ausrichtung der Methylgruppe an der C3*-Position, an welcher das Δ^3-dml eine Doppelbindung trägt. Anzumerken ist ferner, dass sich die Stereochemie der Dillether und Lactone an zwei Positionen des Tetrahydrofuran-Ringsystems unterscheidet, was auf unabhängige Biosynthesewege hindeutet. Supplementationsstudien unter Verwendung markierter und nicht-markierter potenzieller Terpenoidvorstufen legten eine Dilletherbildung ausgehend von *p*-Menth-1-en-9-ol nahe. Letzteres kann dabei als Biotransformationsprodukt von Limonen gebildet werden, das jedoch nicht notwendigerweise als Vorstufe innerhalb des Pilzes fungiert. Analoge Vorstufen wurden für die (Δ^3)-dml ausgeschlossen.

Der hohe FD-Wert, der für dml **a** bei vergleichsweise geringer Konzentration ermittelt wurde, deutete auf eine niedrige Geruchsschwelle hin. Für deren Bestimmung wurde eine neuartige Methode mittels direkter Analyse durch GC-FID-O etabliert. Die ermittelte Geruchsschwelle von 1,9 x 10^{-6} ng L^{-1} Luft stellt eine der niedrigsten bisher bekannten Schwellenwerte dar.

Ferner ermöglichte die Kombination von Aromaanalysedaten und Bioinformatik die Identifizierung einer an der Aromastoffbiogenese beteiligten *O*-Methyltransferase in *Pleurotus sapidus*, einem nahen Verwandten des Austernseitlings. Das Enzym wurde heterolog in *E. coli* exprimiert, kristallisiert, und ermöglichte sowohl die Transmethylierung von hydroxylierten Verbindungen als auch eines Thiol-Nukleophils.

List of publications

1. Brescia, F. F.; Pitelas, W.; Yalman, S.; Popa, F.; Hausmann, H. G.; Wende, R. C.; Fraatz, M. A.; Zorn, H. Formation of diastereomeric dihydromenthofurolactones by *Cystostereum murrayi* and aroma dilution analysis based on dynamic headspace extraction. *J. Agric. Food Chem.* **2021**, *69*, 5997−6004.
2. Brescia, F. F.; Koch, M.; Wende, R. C.; Schreiner, P. R.; Zorn, H.; Fraatz, M. A. Structure elucidation of aroma-active bicyclic benzofuran derivatives formed by *Cystostereum murrayi*. *J. Agric. Food Chem*. **2023**, *71*, 7744–7751.
3. Brescia, F. F.; Passinger, J.; Wende, R. C.; Schreiner, P. R.; Zorn, H.; Fraatz, M. A. Determining ultra-low organic molecular odor thresholds in air helps identify the most potent fungal aroma compound. *J. Agric. Food Chem*. **2024**, *72*, 7511–7516.
4. Brescia, F. F.; Korf, L.; Essen, L.-O.; Zorn, H.; Rühl, M. A novel *O*- and *S*-methyltransferase from *Pleurotus sapidus* is involved in flavor formation. *J. Agric. Food Chem*. **2024**, *72*, 6471–6480.

Conference contributions

Poster

1. Brescia, F. F.; Pitelas, W.; Yalman, S.; Popa, F.; Hausmann, H. G.; Wende, R. C.; Fraatz, M. A.; Zorn, H. Aroma dilution analysis (ADA) by means of dynamic headspace analysis of submerged cultivated *Cystostereum murrayi*. 16th Weurman Online, **2020**.
2. Brescia, F. F.; Pitelas, W.; Koch, M.; Popa, F.; Fraatz, M. A.; Wende, R. C.; Zorn, H. Bildung aromaaktiver Benzofuranderivate durch *Cystostereum murrayi*. 50. Deutscher Lebensmittelchemikertag, Hamburg (Germany), **2022**.
3. Brescia, F. F.; Passinger, J.; Wende.; R. C.; Zorn, H.; Fraatz, M. A. Etablierung einer neuartigen Methode zur Geruchsschwellenbestimmung in Luft. 51. Deutsche Lebensmittelchemietage, Bonn (Germany), **2023**.

Presentation

1. Brescia, F. F.; Trapp, T.; Pitelas, W.; Yalman, S. Popa, F.; Wende, R. C.; Fraatz, M. A.; Zorn, H. Biogenesis of aroma-active bicyclic monoterpenoid benzofuran derivatives by fungi of the division Basidiomycota. International Conference of the German Mycological Society (100 years DGfM), Blaubeuren (Germany), **2021**.
2. Brescia, F. F.; Pitelas, W.; Yalman, S.; Popa, F.; Fraatz, M. A.; Zorn, H. Biogenese aromaaktiver Benzofuranderivate durch Pilze der Abteilung Basidiomycota. Regionalverbandstagung Südwest der lebensmittelchemischen Gesellschaft (Online), **2021**.

3. Brescia, F. F.; Pitelas, W.; Koch, M.; Popa, F.; Fraatz, M. A.; Wende, R. C.; Zorn, H. Bildung aromaaktiver Benzofuranderivate durch *Cystostereum murrayi*. 50. Deutscher Lebensmittelchemikertag (Flash Poster Talk), Hamburg (Germany), **2022**.
4. Brescia F. F.; Pitelas, W.; Koch, M.; Fraatz, M. A.; Wende, R.; Zorn, H.; Popa, F. Biogenesis of aroma-active bicyclic benzofuran derivatives by *Cystostereum murrayi*. Bioflavour, Frankfurt am Main (Germany), **2022**.
5. Brescia F. F.; Trapp, T.; Pitelas, W.; Yalman, S.; Popa, F.; Wende, R. C.; Fraatz, M. A.; Zorn, H. Formation of rare aroma-active chiral benzofruan derivatives by fungi of the division Basidiomycota. Summer School 2023, Geisenheim, **2023**.
6. Brescia, F. F.; Korf, L.; Essen L.-O.; Zorn, H.; Rühl, M. Combining aroma- and transcriptomic analyses for the identification of a novel *O*(*S*)-methyltransferase from *Pleurotus sapidus*. 13th Wartburg Symposium on Flavor Chemistry & Biology, Eisenach, **2023**.

Table of contents

List of abbreviations

ADA	aroma dilution analysis
CIS	Cooled Injection System
DHS	dynamic headspace
dml	dihydromenthofurolactone
er	enantiomeric ratio
FD	flavor dilution
FID	flame ionization detector
GC	gas chromatograph/gas chromatography
HR-MS	high-resolution mass spectrometry
MDGC	multidimensional gas chromatograph/ gas chromatography
MS	mass spectrometer/mass spectrometry
NMR	nuclear magnetic resonance
O	olfactory/olfactometry
RI	retention index
SBSE	stir bar sorptive extraction
SPME	solid phase microextraction
TDU	Thermal Desorption Unit
Δ^3-dml	C3-unsaturated dihydromenthofurolactone

1. Introduction

The use and isolation of fragrances and odoriferous substances from natural sources has a long tradition in the history of humankind. As early as at the time of the pharaohs in 5000 B.C., the Egyptians used myrrh, frankincense, cedar wood, and other precious woods for religious rituals. Essential oils, in particular, have been extracted since this ancient times and used extensively in cosmetics, as food flavoring substances, medicine, or aphrodisiacs.[1,2] The large-scale production of such oils began many thousands of years later, during the industrialization in the first half of the 19th century.[3] With the chemical synthesis of vanillin in 1876 by Reimer and Tiemann, the cornerstone of the modern flavor chemistry was laid.[4] Over the following decades, the flavor and fragrance (F&F) industry experienced rapid growth, reaching global sales of € 39 billion in 2022[a]. The constant progress thereby also confronts the F&F industry with new tasks, which include, among others:

- fulfilment of the principles of green chemistry[5] (e. g., use of renewable or upcycled feedstocks for flavor production (water savings, reduction of energy consumption, and land use))[6]
- increase in production efficiency for known molecules and products[7]
- demand for new molecules, fragrant chemicals, and scents with unique flavor, which may also effect consumers psychology positively[7]
- stability, human safety, low-volatility, solubility in aqueous systems[6,7]
- consumers' demand for more sustainable and natural ingredients ("clean-label")[8–10]
- new sources for natural flavors[11]
- establishment and *upscaling* of (new) biotechnological production processes.[12]

Thus, with consumers becoming increasingly health-conscious and rejecting non-natural food ingredients, natural flavorings are highly demanded by the F&F industry. Legally, natural flavoring substances are defined according to the Regulation (EC) No 1334/2008 in European Union as "… substance obtained by appropriate physical, enzymatic or microbiological processes from material of vegetable, animal or microbiological origin…" and "Natural flavoring substances correspond to substances that are naturally present and have been identified in nature".[13] Accordingly, biotechnological production processes that utilize microorganisms for the production of natural flavors are one viable approach, besides the extraction from natural sources. Moreover, these biocatalysts offer the advantage of being frequently more chemo-, regio-, and stereoselective compared to chemical synthesis, which is highly demanded by the F&F industry.[14,15] In addition to commonly used bacteria and yeasts, "higher fungi" are especially suitable for such biotechnological processes, whereby Basidiomycota, a phylum within the kingdom of fungi, are considered as a promising source, last but not least due to the large number of existing species and a versatile enzymatic repertoire.[16]

[a]https://www.statista.com/statistics/482852/market-value-of-the-flavors-and-fragrances-industry-worldwide-by-division/, last accessed October 13, 2023.

1.1 Basidiomycota

The phylum Basidiomycota is one of the nine phylum-level clades within the kingdom of fungi and belongs, together with the Ascomycota, to the Dikarya.[17] So far, more than 40,000 species are known to exist.[18] Taxonomically, the subdivisions *Ustilaginomycotina*, *Pucciniomycotina* and *Agaricomycotina* are distinguished within the phylum.[19] The latter subdivision includes many well-known edible species such as the oyster mushroom (*Pleurotus ostreatus*), the white button mushroom or champignon (*Agaricus bisporus*), the poricini mushroom (*Boletus edulis*), and shiitake (*Lentinula edodes*). Basidiomycota are therefore of great economic importance, as almost all of the edible fungi cultivated on a large scale belong to this phylum.[20–22] In 2013, the global mushroom production reached 34 billion kg, whereby six main genera of the Basidiomycota (*Lentinula*, *Pleurotus*, *Auricularia*, *Agaricus*, *Flammulina* and *Volvariella*) accounted for 90% of the world production.[23] In common parlance, the fruiting bodies formed for sexual reproduction are often used as a synonym for the fungus, whereas in fact the filamentous mycelium represent the vegetative body of the organism.[24] Morphologically, Basidiomycota are generally characterized by their eponymous basidia, which are formed by enlargement of terminal hyphae.[25] After karyogamy of the two existing independent nuclei within the basidia of a dikaryotic mycelium, haploid basidiospores are formed which, after germination, can form a monokaryotic mycelium.[25] Due to genetic recombination, the resulting monokaryotic mycelia thereby may differ from the original mycelium.[26,27] This effect has been observed, for example, for various monokaryotic strains of *Pleurotus sapidus*, which differed, e. g., in their growth rate, the aroma profile as well as enzymatic activities compared to the original dikaryotic fungus and also in-between the different monokaryons.[28–30]

In addition to the nutritional value of some Basidiomycota, the organisms produce numerous secondary metabolites, such as pigments,[31,32] antimicrobial substances,[33] pharmacologically active substances,[34] biosurfactants,[35–37] and aroma compounds,[38,39] which belong to numerous substance classes such as terpenes, terpenoids, polyketides, and derivatives of fatty acids and peptides.[40,41] Due to their broad enzyme portfolio, these organisms are able to decompose persistent biopolymers such as cellulose or lignin. Especially members of the white rot fungi are known to express a broad portfolio of enzymes such as phenol oxidases (laccase) and heme peroxidases (lignin peroxidase, manganese peroxidase, versatile peroxidase, and DyP-type peroxidase) for lignin metabolism.[42–44] Brown rot fungi, on the other hand, do not have a comparable enzyme portfolio, but use the non-enzymatic Fenton reaction to extensively modify lignin. Herein, the oxidation of Fe^{2+}-ions with hydrogen peroxide produces hydroxyl radicals and hydroxyl ions, which modify the lignin structure and allow the enzymatic degradation of (hemi)cellulose. Thus, basidiomycetes are essential to ecosystems as decomposers.[45,46]

Likewise, the species *Cystostereum murrayi* (Fig. 1) belongs to the white rot fungi and is mainly found on deadwood of coniferous trees, although it has been described on deciduous deadwood in North America.[47] The morphologically inconspicuous and rarely occurring species shows a worldwide distribution and can be easily recognized in nature by an intense coconut-like smell emitted by its fruiting bodies.[48] In Germany the fungus belongs to the red-listed species. The fruiting bodies have been described in a few locations of Baden-Wuerttemberg, Bavaria, and Saxony-Anhalt.[49] The few existing

publications on *C. murrayi* mainly deal with its classification, morphology, and occurance.[50–54] Abraham and Hanssen described an unusual benzofuran-ketone with a bisabolane skeleton for the fungus.[55]

Figure 1: Fruiting body of *C. murrayi* on spruce deadwood in the Black Forest National Park (Images: Flavius Popa).

Besides the cultivation of fungi on solid culture media for direct use of the fruiting bodies, the cultivation in liquid media, also known as submerged cultivation, is frequently used. The advantages of this method include, among others, the independence from climatic conditions, a consistent production rate and product quality, a lower risk of contamination, and a shorter growth period.[41,56] The use of submerged mycelium in the food sector has only recently been approved for pea and rice protein fermented with shiitake,[57] as it is classified as novel food under the Regulation (EU) 2015/2283.[58] Other potential applications for the submerged cultivation of basidiomycetes include the production of biomolecules like proteins, carbohydrates such as exopolysaccharides, lipids and, e. g., enzymes, taste- and odor-active compounds, and pharmacologically active compounds.[59–61]

1.2 Flavor compounds

In general, the term “flavor” does not only refer to the olfactory sensation, but rather to the interaction between taste, olfaction, and texture sensations, perceived during food consumption. On the other hand, the expression “aroma” refers to the overall ortho- and retronasal sensation caused by one or multiple volatile substances in a sample.[62] Some of these compounds are able to provide the characteristic sensory identity of a specific aroma and are therefore referred to as character impact compounds.[63] Examples include (*R*)-*p*-menth-1-en-8-thiol in grapefruit,[64] (*E*,*Z*)-2,6-nonadienal in cucumbers,[65] and (*R*)-oct-1-en-3-ol in white-bottom mushrooms.[66,67] However, the characteristic aroma is often derived from the combination of the different key odorants. More than 10,000 volatiles have been identified in

foods yet, whereby only about 230 belong to the key odorants and only a ratio of 3 to 40 of these compounds is relevant for the characteristic olfactory sensation.[68] A general distinction can be made between primary and secondary aroma compounds in terms of their formation.[69] Primary aroma compounds are formed directly in the organism as secondary metabolites, usually by enzymatic reactions from lipids, carbohydrates, or amino acids. In contrast, secondary aromas are formed as a result of microbiological activity (e. g., fermentation of alcoholic beverages), enzymatic activity or thermal reactions.[69] Typical examples of the latter are pyrazines and aldehydes formed thermally during the Maillard reaction and Strecker degradation,[62,69] as well as compounds formed due to enzymatic activity in onions as a result of cell disruption, such as (*Z*)-propanethial *S*-oxide.[70]

1.2.1 Aroma-active fungal volatiles

Fungi produce numerous volatile compounds belonging to several substance classes. Most of these are primary aroma compounds, although secondary aroma compounds are important during processing. The reasons for the formation of volatile substances are manifold and include impacts as repellent or attractant, antimicrobial effects, influences on reproduction, and, e. g., on intra- and inter-species communication.[71–74] Fraatz et al. (2010) classified edible mushrooms into three groups based on their flavor profile: those rich in C8-volatiles, in sulfur-containing volatiles, or in terpenoids.[75]

The first group provides the characteristic “mushroom-like” odor with oct-1-en-3-ol, oct-2-en-1-ol, octan-3-ol, octan-1-ol, oct-1-en-3-one, and octan-3-one as typical representatives.[75] Numerous studies have been published on the formation pathways of these compounds in fungi, but the detailed mechanisms have not been fully elucidated yet.[76] Polyunsaturated fatty acids are used as precursors, which are oxidized enzymatically to form the short-chain volatiles.[77] For oct-1-en-3-ol, the most abundant C8-volatile, two formation hypothesis are frequently discussed in the literature. Tressl et al. (1981) proposed the formation starting from linoleic acid and lipoxygenase oxidation via 13-hydroperoxide (13-HPOD), which is cleaved by a hydroperoxide lyase and reduced by an alcohol oxidoreductase.[78] The second theory by Wurzenberger and Grosch (1982) also postulates a hydroperoxide formation starting from linoleic acid, however, in this case a 10-hydroperoxide (10-HPOD) is suggested, which is subsequently cleaved by a hydroperoxide lyase.[79] Nowadays, the second theory is considered most likely as supplementation experiments using 13-HPOD did not lead to a formation of oct-1-en-3-ol, whereas in contrast, the 10-HPOD was converted.[80] In addition, Assaf et al. (1997) showed that 13-HPOD and oct-1-en-3-ol are formed by independent biosynthetic pathways, although both occurred after supplementation of *Pleurotus pulmonarius* with linoleic acid.[81] However, a corresponding lipoxygenase has not yet been identified in fungi.[76]

Fungi rich in sulfur-containing volatiles include, e. g., *Lentinula edodes*,[82] *Mycetinis alliaceus* (syn. *Marasmius alliaceus*),[83] and *Phallus impudicus*.[84] For *L. edodes*, lenthionine has been identified as the major odorous compound.[82] Besides, also other cyclic and non-cyclic sulfurous aroma compounds such as dimethyl disulfide, dimethyl trisulfide, 1,2,3-trithiolane, and others were found in dried fruiting bodies.[85,86] For the biogenesis of lenthionine and other *S*-containing volatiles, a pathway starting from lentinic acid has been proposed.[87] *M. alliaceus* and *P. impudicus* also produce comparable sulfurous

aroma compounds such as di- and trimethyl disulfide.[83,84] For *M. alliaceus*, numerous other compounds such as 1,2,4-trithiolane, 1,2,4-trithiapentane and dimethyl tetrasulfide have been identified.[83] More recently, submerged cultures of three different *Laetiporus* ssp. have been identified as a source of sulfurous aroma compounds within supplementation experiments using thiamine hydrochloride. Thereby, numerous aroma-active volatiles were identified, including dimethyl disulfide, dimethyl trisulfide, and, in particular, 2-methyl-3-(methylthio)furan, which imparts meaty odor impressions.[88]

The last group is made up by fungi rich in terpenes and terpenoids. While the former are hydrocarbons, terpenoids are formed by functionalization of terpenes.[89] Frequently occurring are alcohols, aldehydes, esters or lactones, and ketones. Terpenoids represent the largest class of natural products with over 80,000 known compounds.[90] Formally, the compounds are derived from isoprene (2-methyl-1,3-butadiene), whose structure was postulated as early as 1884.[91] The linkage of several of these isoprene units leads to terpenes of different chain lengths, which are referred to as hemi (C_5)-, mono- (C_{10}), sesqui- (C_{15}), di- (C_{20}), tri- (C_{30}), tetra- (C_{40}), and polyterpenes $(C_5)_{n,\ n>8}$. This uniform construction principle is also known as the isoprene rule.[92] Mono- and sesquiterpenes are of particular olfactory relevance due to their high volatility.[69] Well-known examples are the limonene stereoisomers, which impart citrus or coniferous-like odors, linalool, with floral or woody scents, and citral, a mixture of the (*E*,*Z*)-isomers geranial and neral, frequently used in the fragrance industry.[93] The biogenesis of this highly diverse substance class, as well as individual representatives, will be discussed in more detail in the following chapter.

In addition to the classification of fungi on the basis of the main aroma compounds, many other volatile compounds of other substance classes are formed by these organisms. For example, aromatic amino acids can be converted to benzaldehyde, 2-phenylethan-1-ol, or *p*-anisaldehyde. The latter compound has been identified for submerged cultures of *Pleurotus sapidus*,[94] but also in fruiting bodies of *Clitocybe odora*,[95] *A. bisporus*, *and B. edulis*,[66] possessing an anise-like odor. Benzaldehyde with a bitter almond-like odor has for example been detected in submerged cultures of *Pleurotus sapidus,*[94] *Bjerkandera adusta,*[96] and in fruiting bodies of *A. bisporus*, *A. campestris*,[66] and other *Pleurotus* ssp. such as *P. ostreatus*[97] and *P. eryngii*.[98] For *p*-anisaldehyde and benzaldehyde as well as cinnamaldehyde and, e. g., 2-phenyl-ethan-1-ol, Lapadatescu et al. (2000) postulated a formation pathway in *B. adusta* starting from L-phenylalanine via a cascade of enzymatic reactions, including an *O*-methyltransferase activity for the formation of *p*-anisaldehyde.[99] Moreover, other aldehydes, alcohols, esters, ketones, lactones, and pyrazines are formed by these organisms.[75] The volatile compounds are also highly dependent on the cultivation type. For instance, aroma analysis of *P. ostreatus* in submerged, surface, and solid support cultures in comparison to the fruiting bodies showed differences in the volatilome as well as in the ratios of the major aroma compounds among each other. While only small amounts of oct-1-en-3-ol were detected in the fruiting bodies, this compound was the main aroma compound in the submerged culture.[100] Submerged cultivation may be particularly suitable for the production of odor-active compounds, as the organisms grow in closed vessels and volatile compounds may be trapped or directly extracted.[59]

1.2.2 Terpenes and terpenoids

For the biosynthesis of terpenes, two different pathways have been described thus far (Fig. 2). In 1967, Lynen published a route nowadays known as acetate-mevalonate or mevalonate pathway.[101] This biosynthetic pathway, used by archaea, some bacteria, and most eukaryotes,[102] is based on the primary linkage of two acetyl-CoA molecules (**1**) to acetoacetyl-CoA (**2**) in a Claisen condensation-like reaction catalyzed by an acetoacetyl-CoA thiolase. Linkage with another acetyl-CoA molecule leads to the formation of 3-hydroxy-3-methylglutaryl-CoA (HMG-CoA, **3**), which is converted by the key enzyme HMG-CoA reductase via the putative intermediate of a hemithioacetal to (*R*)-mevalonic acid (**4**). Two phosphorylation reactions, catalyzed by mevalonate kinase and phosphomevalonate kinase, then form mevalonate pyrophosphate. This is converted to isopentenyl pyrophosphate (IPP, **5**) by mevalonate diphosphate decarboxylase with CO_2 extrusion and ATP consumption. IPP can then be enzymatically converted to dimethylallyl pyrophosphate (DMAPP, **6**) by an isomerase.[101,103] In archea, phosphorylation steps from mevalonate or mevalonate-5-phosphate to IPP differ from the eukaryotic pathway.[104,105] In 1997, an alternative route towards IPP and DMAPP was published by Lichtenthaler et al. starting from glyceraldehyde phosphate (**7**) and pyruvate (**8**).[106] This biosynthetic route, also known as DOXP or MEP pathway, has been described for most bacteria, plants and algae, but not for fungi or mammals.[107] The key intermediate is 1-deoxy-D-xylulose-5-phosphate (**9**), which is converted to 2-methyl-D-erythritol-4-phosphate (**10**) and finally to IPP or DMAPP, which serve as precursors of terpenes and terpenoids.[106]

The precursors IPP and DMAPP are then converted into the corresponding terpenes and terpenoids. The simplest compounds, the hemiterpenes, include, e. g., isoprene (**11**), 3-methylbutanoic acid (**12**) and 3-methylbutan-1-ol (**13**).[108] Head-to-tail linkage of IPP and DMAPP via geranyl diphosphate (GPP) synthase leads to the C_{10}-body GPP (**14**), which can be further converted to monoterpenes.[109] Respective terpene synthases have in fact been described for basidiomycetes. For example, a linalool (**15**) specific synthase has been identified in *Agrocybe pediades*.[110] Similarly, a terpene synthase from *Cyclocybe aegerita* (syn. *Agrocybe aegerita)* produces linalool besides nerolidol (**22**), thus showing also a function as sesquiterpene synthase.[111] In general, monoterpenes can be divided into acyclic, monocyclic and bicyclic compounds.[108] Examples include the stereoisomers of limonene (**16**), dill ether (**17**), *p*-menth-1-en-9-ol (**18**) and, as bicyclic compounds, the lactones known as dihydromenthofurolactones (**19**) and the corresponding C3-unsaturated (**20**) derivatives. All metabolites were detected in submerged cultures of *C. murrayi*. The further addition of a C_5 group to GPP catalyzed by a farnesyl diphosphate (FPP) synthase leads to the formation of FPP (**21**), the precursor of sesquiterpenes.[109] Besides linear, monocyclic, and bicyclic compounds, also tricyclic sesquiterpenes exist in nature.[108] Well known aroma compounds include the above mentioned nerolidol (**22**), as well as nootkatone (**23**) and *ß*-bisabolene (**24**). In addition to the enzyme mentioned above, numerous sesquiterpene synthases have been also identified in Basidiomycota,[112] such as a valencene synthase in *Schizophyllum commune*,[113] Δ-6 protoilludene synthases in *Omphalotus olearius*, and, e. g., sesquiterpene synthases in *Coniophora puteana* producing cubebol and *ß*-copaene.[114] Higher terpenes may be synthesized by further chain elongation.[109]

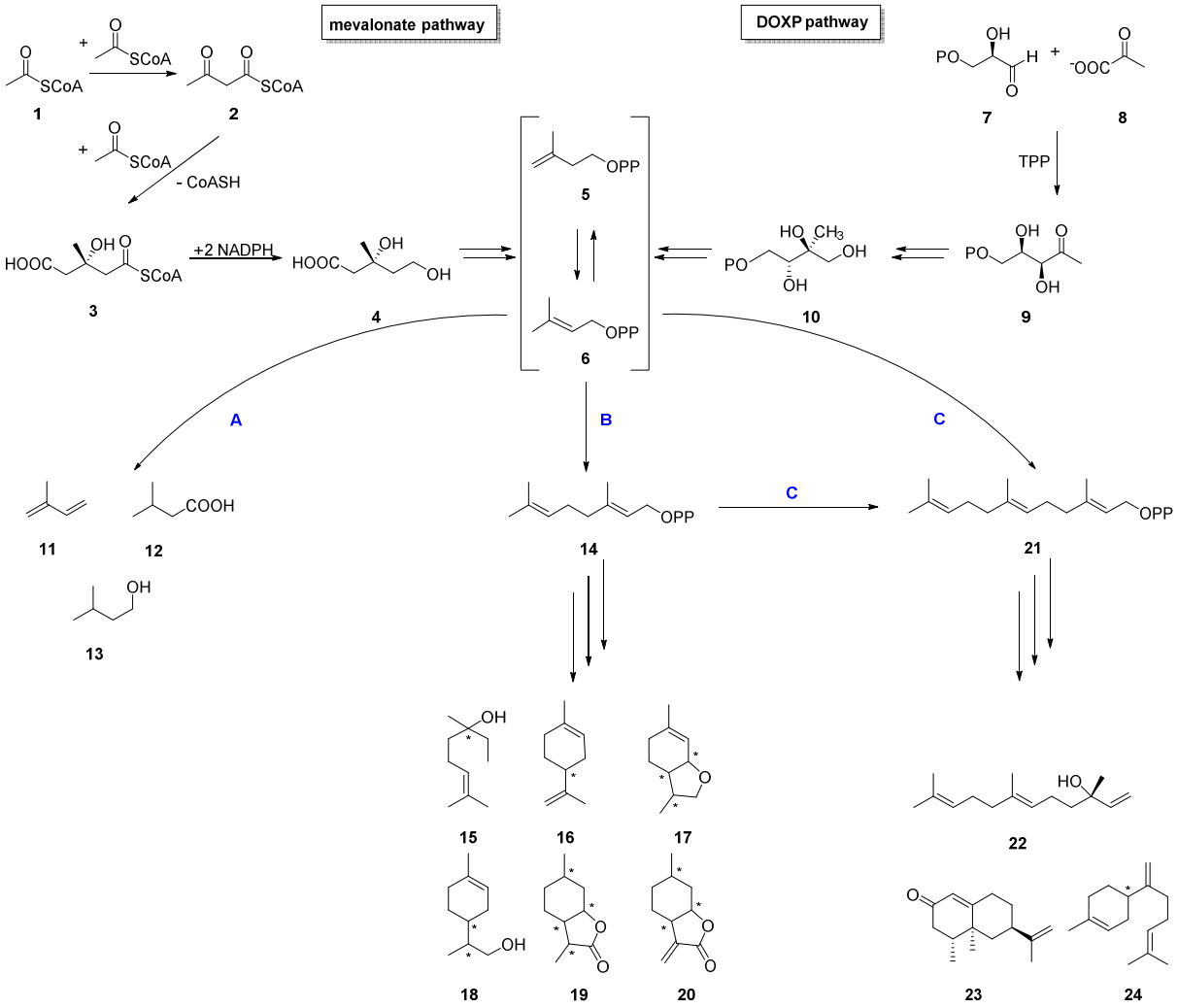

Figure 2: Biosynthetic pathways for terpene formation; left side: Mevalonate pathway starting with the condensation of two acetyl-CoA (**1**) to acetoacetyl-CoA (**2**) via acetoactyl-CoA thiolase and further reaction with acetyl-CoA to 3-hydroxy-3-methylglutaryl-CoA (**3**) via HMG-CoA synthase. This key intermediate is further reduced via HMG-CoA reductase to (*R*)-mevalonic acid (**4**), followed by two phosphorylation steps and decarboxlation via mevalonate kinase, phosphomevalonate kinase, and mevalonate diphosphate decarboxylase to IPP (**5**) and via isopentenyl-pyrophosphate isomerase to DMAPP (**6**); right side: simplified DOXP pathway starting from glyceraldehyde 3-phosphate (**7**) and pyruvate (**8**) to 1-deoxy-D-xylulose-5-phosphate (**9**) and subsequently via 2-methyl-D-erythritol-4-phosphate to IPP and DMAPP. (**A**) Formation of hemiterpenes such as isoprene (**11**), 3-methylbutanoic acid (**12**), and 3-methylbutan-1-ol (**13**); (**B**) formation of geranyl pyrophosphate (**14**) via geranyl diphosphate synthase, and further conversion to monoterpenes such as linalool (**15**), limonene (**16**), dill ether (**17**), *p*-menth-1-en-9-ol (**18**), dihydromenthofurolactone (dml, **19**) and Δ^3-dml (**20**); (**C**) formation of farnesyl diphosphate (**21**) via farnesyl diphosphate synthase, and further conversion to sesquiterpenes such as nerolidol (**22**), nootkatone (**23**), and ß-bisabolene (**24**).

1.2.2.1 Bicyclic benzofuran derivatives

The bicyclic benzofuran derivatives represent a subgroup of monoterpenoids, some of which are of particular interest to the F&F market due to their partly extremely low odor thresholds, interesting odor impressions, and the entry of some representatives in the EU positive list of flavorings.[13] All have a benzofuran skeleton in common, with those derived from 3,6-dimethylbenzofuran in particular being well known as odor active (Fig. 3). In addition to the stereoisomers of the dill ether (**17**) and the (Δ^3)-dml (**19**, **20**) already listed, these include stereoisomers of the wine lactone (**25**), mint lactone (**26**), menthofuran (**27**), and linden ether (**28**).

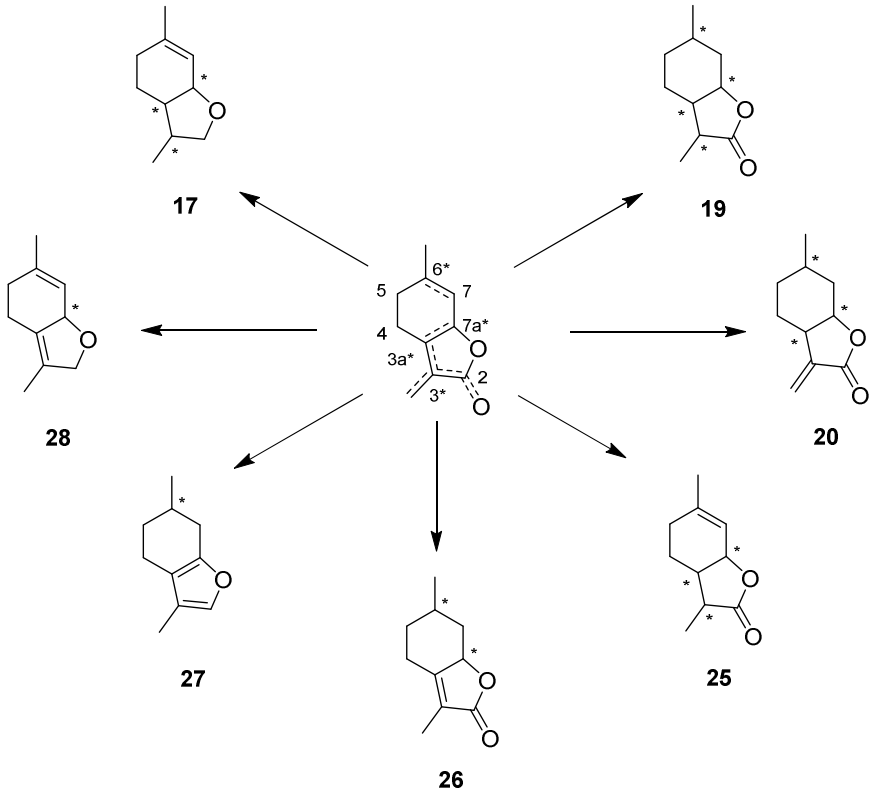

Figure 3: Aroma-active benzofuran derivatives derived from 3,6-dimethylbenzofuran with dill ether (**17**), dml (**19**), Δ^3-dml (**20**) and stereoisomers of the wine lactone (**25**), mint lactone (**26**), menthofuran (**27**), and linden ether (**28**) as representative examples.

The (3*S*,3a*S*,7a*R*)-stereoisomer of **17** has been identified as a key aroma compound in dill herb, possessing the typical dill-like odor.[115,116] Due to three existing stereocenters and therefore eight possible stereoisomers, structural elucidation has been an analytical challenge for over a decade.[116,117] However, stereoisomers with a *trans*-orientation at C3a and C7a are sterically less favorable and thus unlikely within natural pathways.[116] The stereochemistry thereby has a decisive influence on the olfactory impression, which ranges from the characteristic dill-like odor (3*S*,3a*S*,7a*R*), through fainty herbal, unspecific (3*R*,3a*R*,7a*S*), fruity-sweet (3*R*,3a*S*,7a*R*) to herbal, sweet (3*S*,3a*R*,7a*S*).[117] For the biogenesis of this compound in dill herb, supplementation studies of dill leaves suggested a formation pathway via *p*-menth-1-en-9-ol starting from limonene.[118] In *Pleurotus sapidus*, a close relative of the well-known oyster mushroom, a similar formation pathway has been proposed.[119] One stereoisomer of

25 has first been described as a metabolite in koala urine[120] and later the (3*S*,3a*S*,7a*R*)-stereoisomer, also known as wine lactone, in Gewürztraminer wine,[121] possessing a sweetish coconut-like smell and an extremely low odor threshold of 1 x 10^{-5} ng L^{-1} air.[122] In grapes, a formation pathway starting from linalool via oxidation to (*E*)-8-carboxylinalool and the corresponding glucose ester has been suggested. Both, the free acid and the glycoside after yeast hydrolysis, may act as precursors for the wine lactone, formed via cyclization during wine maturation.[123] Two stereoisomers of **25**, as well as two diastereomers of **17**, have in addition been identified within submerged cultures of *P. sapidus*, presumably formed from *p*-menth-1-en-9-ol.[119] Mint lactone (**26**) as well as menthofuran (**27**) occur naturally in *Mentha* ssp. (mint).[124,125] For both compounds, biosynthetic pathways starting from GPP via limonene and pulegone have been proposed and the enzymes have partially been identified.[125–127] Menthofuran is known as a hepatotoxic compound in rats which is also formed as a metabolite during the degradation of pulegone in rat liver.[128] Mint lactone was approved as a flavoring agent under Regulation (EC) 1334/2008, but since the Regulation (EU) 2022/1466 it is no longer listed due to inconclusive toxicological data regarding genotoxic effects.[13,129,130] Linden ether (**28**) was isolated from the blossoms and honey of the lime tree *Tilia cordata*, occurring as an racemic mixture, possessing a flowery and mint like odor.[131,132]

Stereoisomers of **19** were identified in Italo-Mitcham peppermint oil and in fresh peppermint leafs.[133,134] While chemical synthesis routes have been published, other natural sources have rarely been described thus far.[135] The synthesis by enzymatic reaction of isopulegol with hydrogen peroxide catalyzed by lipase B from *Candida antarctica* followed by thermal treatment and acid catalysis was published by Gatfield et al. in 2007.[136] Dihydromenthofurolactones comprise four stereogenic centers and therefore 16 possible stereoisomers, listed in the Appendix of the Regulation (EC) 1334/2008 and therefore approved for their use in food.[13] For the Δ^3-dml (**20**), natural sources have not been described thus far. Buhr (2006) synthesized several stereoisomers of **19** and determined the odor thresholds, referred to the frequently used internal standard (*E*)-dec-2-enal.[122] Although assignment of the stereochemistry was partly contradictory, by far the lowest odor threshold was determined for the (3*S*,3a*S*,6*R*,7a*S*)-stereoisomer (Fig. 4). This stereoisomer was also identified for the submerged cultures of *C. murrayi*. The thresholds of some other stereoisomers differed by several orders of magnitude (up to > 10^6), demonstrating the strong influence of the stereochemistry of chiral aroma compounds on their olfactory properties.

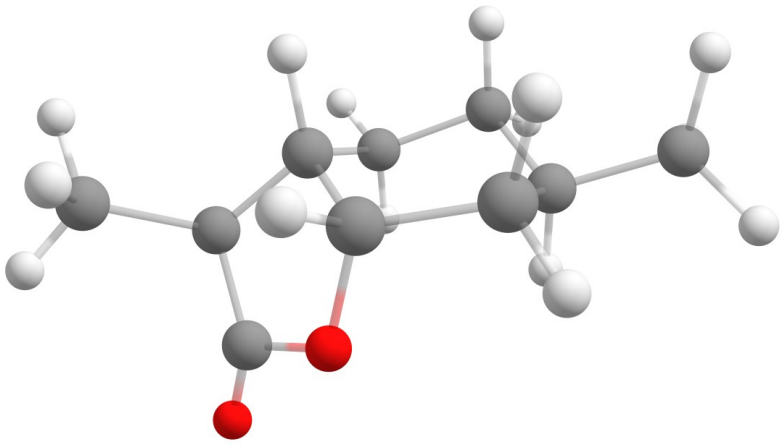

Figure 4: Energetically lowest-lying conformation of (3*S*,3a*S*,6*R*,7a*S*)-dml (dml **a**), computed with Spartan ´20 employing the Merck molecular force field (MMFF) at the Institute of Organic Chemistry (JLU Giessen).

1.3 Aroma analysis

Due to the variety of different flavor compounds and matrices (aqueous, solid, oily), aroma analysis is a challenging task. The concentrations of volatile compounds in foods can vary widely and even trace amounts (ppb) of aroma compounds may be essential for the overall aroma due to low olfactory thresholds, while other compounds present in higher concentrations are less relevant for the overall sensory impression. The classical workflow for the analysis of aroma compounds after the isolation of volatile compounds starts with the differentiation between aroma-active compounds and other volatile compounds by means of aroma dilution analyses using gas chromatography-olfactometry (GC-O). After identification of the perceived volatiles, which may require additional concentration steps, quantification, calculation of aroma values, simulation of the overall aroma and omission experiments are performed.[62,137]

The isolation of volatile aroma compounds is certainly one of the most important and crucial steps in aroma analysis. As mentioned above, possible formation of aroma compounds during extraction, e. g., by enzymatic or chemical reactions, must be taken into account. In addition, the stability of some flavor compounds is rather low and they may be changed under the influence of oxygen, radiation, or heat.[138] A general distinction can be made between methods based on distillation, extraction, or sorption and methods based on the volatility of the analytes. Often a combination of different methods is required in order to identify the key aroma compounds of an unknown sample. In addition, it should be noted that the extraction methods are usually non-exhaustive.[139] One of the most frequently used isolation methods is the liquid-liquid extraction, in which the sample is usually extracted several times with an organic solvent or a mixture of solvents. Due to the large volumes used for extraction, concentration and separation of non-volatile compounds such as lipids or pigments which may interfere within the GC separation is required.[140] One option is the so called solvent assisted flavor evaporation (SAFE), in which volatile compounds are separated from the non-volatile matrix under high vacuum and collected in a liquid nitrogen cooled trap.[141] The obtained extracts are then further concentrated and may be used for aroma extract dilution analysis (AEDA). Hereby, a differentiation between odor-active and other volatiles is obtained by stepwise dilution (usually 1:2 or 1:3) of the original sample with an appropriate solvent and subsequent analysis by means of GC-O until the perceived compounds can no longer be recognized by their characteristic odor.[142] GC-O was first introduced in 1964 by Fuller and coworkers, and uses the human nose besides a GC detector (flame ionization detector or mass spectrometer) for the analysis of volatiles.[143] In addition, AEDA allows for a first estimation of the aroma potency, taking into account the composition of the volatile compounds present in the sample.

Due to the time-consuming nature of liquid-liquid extraction and the need for large amounts of sometimes toxic solvents, numerous solvent-free extraction techniques have been developed and applied for aroma analysis.[144] Moreover, liquid-liquid extraction may discriminate highly volatile substances, either because of polarity or, for example, losses after SAFE due to concentration using a Vigreux column.[145] In 1989, solid phase microextraction (SPME) was developed by Pawliszyn, in which volatile compounds are extracted directly from a liquid sample or from the headspace above a sample on a sorbent coated fiber.[146,147] In addition to numerous sorbent materials, the extraction can be

influenced by the extraction time, salt addition, shaking, stirring, and, e. g., temperature.[148] Using modern GC systems, these methods also allow aroma dilution analysis. The first dilution analysis using this solvent-free extraction technique was published in 2003. Dilution of the extracted aroma compounds is thereby achieved by varying the split ratio at the split/splitless inlet.[149] This methodology has been applied analogously to the use of other solvent-free extraction techniques, including stir bar sorptive extraction (SBSE) and dynamic headspace (DHS) analysis. Unlike SPME, dilution is achieved in a more complex system either by single splitting in a Cold Injection System (CIS) or by means of sequential splitting in a Thermal Desorption Unit (TDU) and the CIS.[119,150,151] Compared to SPME, SBSE offers the advantage of higher capacities, resulting in two to three orders of magnitude higher sensitivity.[139] Currently, two coatings are commercially available, namely polydimethylsiloxane (PDMS) and PDMS/ethylene glycol (EG) copolymer, however also other coatings have been used.[152] The extraction method can either be performed by stirring the coated stir bar directly in the sample (direct immersion SBSE), extraction of the headspace (HS-SBSE) or as a combination using two stir bars (e. g., one stirring in the sample, one placed above in the headspace), called multi-SBSE or Twicester.[153,154] In dynamic headspace analysis, volatile compounds are usually passed through a sorbent material by a carrier gas flow. Analytes are thus continuously removed from equilibrium between sample and headspace and the resulting concentration gradient causes increased release of analytes from the sample.[155] In addition to carbon-based sorbents and PDMS, Tenax (poly(2,6-diphenylphenylene oxide)) is often used.[156] Similarly to SBSE, extraction parameters such as extraction temperature and time, stirring of the sample, flow rate and volume can be varied to suit the sample.[145] The practical advantage of this method is the possibility of fully automating the extraction.

The perceived compounds can then be identified, whereby the following criteria must be fulfilled for an unequivocal identification:

- mass spectra (EI-MS, CI-MS) and retention indices (RI) must be determined on two GC columns of different polarity
- results must be compared with literature data
- for commercially available compounds: mass spectra and RI must be acquired
- for non-commercially available compounds: (1) isolation for nuclear magnetic resonance (NMR) spectroscopy, followed by synthesis of the compound (comparison of NMR spectra); (2) if isolation is not possible, HRMS for structural suggestion, followed by synthesis and NMR analysis.[157]

For chiral compounds, authentic standards of the respective enantiomers are additionally required for an unambiguous assignment.[157] The analysis of these enantiomers is usually carried out using multidimensional gas chromatography (MDGC) systems, whereby the initial separation is performed on an achiral column and the analytes can be selectively transferred to a second chiral column by means of a heart-cut system (GC-GC).[158] For this purpose, a multi Dean's switch system is commonly used, which allows the selective transfer of the GC effluent from the first GC (achiral) to the second GC containing a chiral column.[159,160] The first amino acid derivative-based chiral phases were used by Gil-Av et al. in 1966.[161] Nowadays, many chiral phases used in gas chromatography are based on differently

modified cyclodextrins.[162] The choice of the chiral column is often unpredictable and even if preferences for the separation of certain functional groups on certain phases exist, the selection of the chiral phase remains a matter of trial and error.[163] The chiral separation allows to calculate the purity of a chiral compound. As a measure, the so called enantiomeric excess (ee) is used, however, although the parameter is still frequently used, it is increasingly replaced by the enantiomeric ratio (er).[164]

After quantification, which can be challenging depending on the sample matrix, the determination of aroma activity values (OAV) shall be mentioned briefly at this point. The OAV concept was published in 1957 by Patton and Josephson as the ratio of the concentration of a respective compound in the sample to the odor threshold in this sample matrix.[165] Thus, an OAV >1 indicates a contribution of the respective compound to the overall aroma. However, the concept has been questioned, among other things, due to the fact that odor thresholds are highly variable (interindividually and methodologically) and interactions between different odorants are ignored.[166,167] Nevertheless, the concept is still applied and requires the determination of odor thresholds for the respective compound in the corresponding matrix. In general, two types of odor thresholds are distinguished. The detection threshold refers to the concentration at which an odorant becomes perceivable without the need to describe its characteristic. Contrarily, the recognition threshold is the lowest concentration at which an assessor consistently assigns the same descriptor for the characteristic odor.[168] However, there is often no strict differentiation between the two parameters. Both thresholds are highly dependent on the matrix in which the parameter is determined. Aqueous systems (aqueous sugar or alcoholic solutions) are often used, as the odorants are often dissolved in these matrices (e. g., beverages such as wine). In addition, also oil phases as well as the odor threshold in air are deployed. For the latter, a GC-O approach can be used for the determination, which has the advantage that the substances can be sniffed without interfering impurities.[169] The methodology described for the determination in air, which has served as the basis for most of the odor thresholds published to date, was introduced by Ullrich and Grosch in 1987.[170] The odor threshold is thereby referred to an internal standard of known odor threshold (O_I). The standard should be selected with an odor threshold similar to that of the compound being measured. Using GC-O experiments, a combined dilution series of the internal standard and the compound to be analyzed is examined and the so-called *D*-values (D) are determined. This value corresponds to the dilution (*D*-value = 2^X; in which x is the number of 1:2 dilutions) up to which the characteristic odor was perceived. Using the known concentrations of the internal standard (c_I) and the analyte (c_A), the odor threshold (O_A) can be calculated (Equation 1).[170]

$$O_A = \frac{O_I \cdot c_A \cdot D_I}{c_I \cdot D_A} \quad (1)$$

One issue is that in the past, (*E*)-dec-2-enal was almost exclusively utilized as the internal standard, without taking into account the odor threshold of the substance being analyzed. Additionally, a fixed value of 2.7 ng L^{-1} air was utilized for the internal standards odor threshold, disregarding interindividual differences in perception. This value was calculated from the odor threshold determined in water using Henry's constant.[171,172] It is important to note that odor thresholds are dependent on physiological factors (gender, age, etc.) as well as methodological factors (experimental design, delivery system, etc.) and may therefore vary significantly.[173,174]

1.4 Aroma perception

The first theories about the relationship between structure and olfactory perception were postulated in ancient times. Titus Lucretius Carus (98 to 54 B.C.), for example, hypothesized that pleasant smelling substances have a smooth, round structure, whereas unpleasant substances have a rough surface.[175] Although there is now a much better understanding of the olfactory process, the details are still not fully understood.

The human olfactory recognition takes place in the approximately 2.5 cm^2 large olfactory mucosa (*Regio olfactoria*) located at the back of the nasal cavity below the cribriform plate and is composed of 10 to 25 million olfactory cells as well as supporting and basal cells.[176,177] The olfactory cells are bipolar neurons that have the ability of mitosis and an average lifespan of 60 days before being renewed by the basal cells of the epithelium.[176] At the apical end, the neuron cell extends a dendrite which forms a knob at the epithelial surface and emits several cilia at the tip which serve as a chemoreceptive surface (*Cilia olfactoria*) and contain the olfactory receptors in the mucus layer.[178] The basal pole extends in a thin (0.2 µm) axon.[176] Thousands of these axons merge into a bundle (*Filia olfactoria*) that pass through the cribriform plate of the nasal bone into the olfactory bulb (*Bulbus olfactorius*) of the forebrain and converge with the dendrites of mitral cells. The unit formed by the dendrites of mitral cells and axons of the olfactory cells is called glomerulus.[176,177] Importantly, each neuron expresses only one type of receptor protein in the cilia, and neurons of one receptor type converge in one glomerulus.[179,180] In humans, about 900 olfactory receptor genes are known, of which only about 400 encode functional receptors.[181,182] In addition, the olfactory epithelium contains Bowman's glands, which secrete the mucus that covers the olfactory epithelium.[177] These also include different enzymes, which are essential for the metabolization of odorants before reaching the receptors, within the so called perireceptor events.[183]

Olfactory receptors are G protein-coupled receptors with seven transmembrane domains. In mammals, they are generally divided into two classes, the odorant receptors (ORs) and the trace amine-associated receptors (TAARs).[177] The latter are specifically associated with the perception of amines, however only six TAARs have been described for humans.[184] ORs, on the other hand, are divided into two classes based on sequence homologies: the class I receptors, also known as fish-like receptors due to their initial discovery, respond to polar, water-soluble compounds such as fatty acids, while the much larger class II receptors tend to respond to more hydrophobic compounds.[184,185] Once an odorant reaches a suitable receptor via the respiratory air, docking with this receptor causes a conformational change within the protein.[177] Many aroma compounds are rather hydrophobic molecules, while the mucus, as an aqueous medium, is polar. To increase the solubility of these compounds, the so-called odorant binding proteins are discussed for the transport to the receptors.[177,186] In vertebrates, these small proteins are *ß*-barrels composed of antiparallel *ß*-sheets and belong to the lipocalin superfamily; in insects, they mainly contain *α*-helical domains.[187] Other discussed functions include scavenging of molecules to prevent receptor saturation and of cyto- and genotoxic compounds as a protective mechanism of the nasal mucosa.[186] In insects, knockout of these proteins leads to an impaired pheromone perception.[188,189] While they are essential for insects, their functions in humans are still unclear.

The conformational change of the receptor in the cilia after odorant docking activates an olfactory-specific G-protein (G_{olf}). Thereby, guanosine 5´-diphosphate (GDP) is exchanged for guanosine 5´-triphosphate (GTP), which causes a dissociation of the *β*- and *γ*-units from the *α*-subunit and activates the adenylate cyclase (AC) type III. The latter catalyzes the conversion of adenosine triphosphate (ATP) to cyclic adenosine monophosphate (cAMP), which has a crucial role in signal transduction. The cAMP activates cyclic nucleotide-gated (CNG) channels, causing an influx of Ca^{2+}- and Na^{+}-ions into the cilia and therefore a depolarization. In addition, Ca^{2+}-ion entry activates Ca^{2+}-activated Cl^{-}-channels and causes a Cl^{-}-ion efflux, contributing to the olfactory cell depolarization. This depolarization spreads to the dendrite and the soma of the olfactory cell, generating an action potential (Fig. 5). In general, one activated membrane receptor can activate several G proteins, each of which activates one AC type III, producing about a thousand molecules of cAMP per second.[190–192] After the stimulus, rapid regeneration of the olfactory neurons is required. The increased Ca^{2+} concentration leads to the binding of Ca^{2+}-ions to calmodulin, which in turn binds to the CNG channel, decreasing the affinity for cAMP and thus reducing Ca^{2+} influx into the cell. In addition, calmodulin activates calmodulin kinase II, which phosphorylates AC type III, reducing the formation of cAMP, and a cyclic nucleotide phosphodiesterase, which degrades cAMP.[177] Besides, Ca^{2+} is removed from the cell via Na^{+}/Ca^{2+} exchangers and a Ca^{2+}-ATPase.[190]

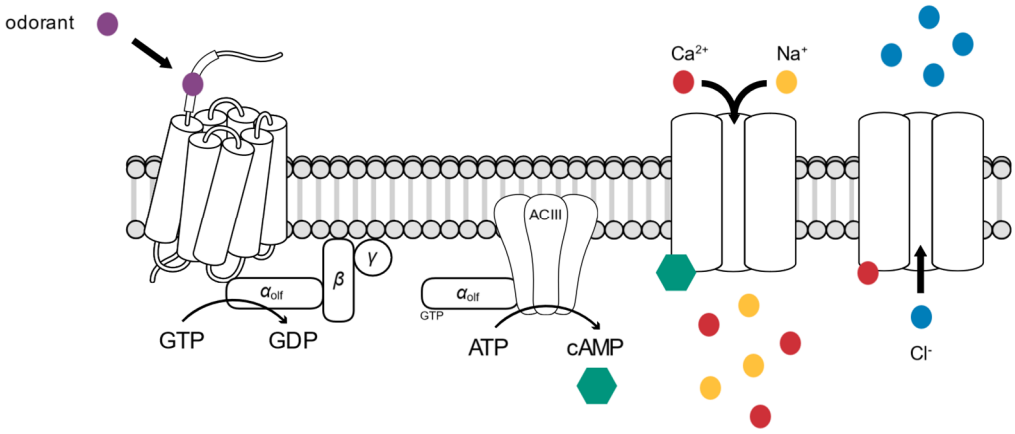

Figure 5: Illustration of the signal transduction cascade of the olfactory system. After odorant binding at the odorant binding receptor, adenylate cyclase III is induced via a α_{olf} subunit of G_{olf} protein and converts ATP to cAMP; cyclic nucleotide-gated (CNG) channels are activated via cAMP, causing Ca^{2+} and Na^{+} influx and depolarization of the olfactory cell; increasing Ca^{2+}-ion concentration activates Ca^{2+}-activated Cl^{-}-channels, causing an increased depolarization due to Cl^{-}-ion efflux. Own figure based on Pifferi et al. (2009).[190]

The signal transduction cascade that follows the activation of a receptor protein is generally the same for each odorant. Thus, the difference in perception and differentiation of different odorants is due to the activation pattern of the receptors. Most odorants are capable of activating multiple receptors, and most receptors respond to multiple compounds. This activation pattern could also explain the concentration-dependent perception of odor impressions for certain odorants, since more receptors are activated at higher concentrations.[177]

1.5 Objective

The present dissertation aimed to investigate the aroma profile of the basidiomycetous fungus *Cystostereum murrayi*, which is known for its coconut-like odor emitted by the fruiting bodies in nature. Therefore, submerged cultivation in different media as well as sensory analyses should be performed in order to define cultivation parameters with respect to the most pleasant and intense coconut-like odor. Based on these results, the identification of key aroma compounds by means of aroma dilution analysis was crucial. As an alternative to the conventional and frequently used aroma extract dilution analysis, an automated solvent-free dilution analysis using dynamic headspace extraction should be established. As the compounds with the highest flavor dilution factors could not be identified by their mass spectra alone, structural elucidation after isolation by means of HRMS and NMR was required. For further structural analysis of the dihydromenthofurolactones on a stereospecific basis, chiral analysis by means of multidimensional gas chromatography after organic synthesis of the probable stereoisomers should be performed.

Besides the dihydromenthofurolactones, the dill ethers were identified as a second class of bicyclic benzofuran derivatives in the submerged culture of the fungus. Structural similarities of these compounds suggested similar biosynthetic pathways, which should be investigated using both labeled and non-labeled potential precursors.

Since one stereoisomer of the dihydromenthofurolactones showed a high flavor dilution factor at a comparatively low concentration, a low odor threshold was supposed. Typically, odor thresholds in air are determined using an internal standard with a significantly higher odor threshold. Thus, a novel method for odor threshold determination without the use of an internal standard should be established and tested using the aforementioned lactone as well as the compound with the lowest odor threshold known to date.

As part of a second project, aroma analysis in combination with transcriptomic analyses should be applied to identify enzymes involved in flavor compound generation such as *p*-anisaldehyde in *Pleurotus sapidus*, a close relative to the oyster mushroom. Subsequently, the identified *O*-methyltransferase should be expressed heterologously in *E. coli*, characterized, and crystallized.

2. References

(1) Ohloff, G. *Riechstoffe und Geruchssinn*; Springer-Verlag: Heidelberg, 1990.

(2) Dima, C.; Dima, S. Essential oils in foods: Extraction, stabilization, and toxicity. *Curr. Opin. Food Sci.* **2015**, *5*, 29–35.

(3) Surburg, H.; Panten, J. *Common fragrance and flavor materials*; Wiley-VCH Verlag: Hoboken, NJ, USA, 2006.

(4) Reimer, K. Über eine neue Bildungsweise aromatischer Aldehyde. *Chem. Ber.* **1876**, *9*, 423–427.

(5) Anastas, P.; Eghbali, N. Green chemistry: Principles and practice. *Chem. Soc. Rev.* **2010**, *39*, 301–312.

(6) Armanino, N.; Charpentier, J.; Flachsmann, F.; Goeke, A.; Liniger, M.; Kraft, P. What's hot, what's not: The trends of the past 20 years in the chemistry of odorants. *Angew. Chem., Int. Ed. Engl.* **2020**, *59*, 16310–16344.

(7) Mattos, L. H. S.; Speziali, M. G. Patent landscape: Technology development behind science in the flavor and fragrances (F&F) area. *World Pat. Inf.* **2017**, *51*, 57–65.

(8) Asioli, D.; Aschemann-Witzel, J.; Caputo, V.; Vecchio, R.; Annunziata, A.; Næs, T.; Varela, P. Making sense of the "clean label" trends: A review of consumer food choice behavior and discussion of industry implications. *Food Res. Int.* **2017**, *99*, 58–71.

(9) Carocho, M.; Barreiro, M. F.; Morales, P.; Ferreira, I. C. F. R. Adding molecules to food, pros and cons: A review on synthetic and natural food additives. *Compr. Rev. Food Sci. Food Saf.* **2014**, *13*, 377–399.

(10) Lee, J.-W.; Trinh, C. T. Towards renewable flavors, fragrances, and beyond. *Curr. Opin. Biotechnol.* **2020**, *61*, 168–180.

(11) Guentert, M. The flavour and fragrance industry - Past, present, and future. In *Flavours and Fragrances: Chemistry, bioprocessing and sustainability*; Berger, R. G., Ed.; Springer-Verlag: Heidelberg, 2007; pp 1–14.

(12) Brenna, E.; Parmeggiani, F. Biotechnological production of flavors. In *Industrial biotechnology*; Wittmann, C., Liao, J. C., Eds.; Wiley-VCH Verlag: Weinheim, Germany, 2017; pp 271–308.

(13) Regulation (EC) No 1334/2008 of the European Parliament and of the Council of 16 December 2008 on flavourings and certain food ingredients with flavouring properties for use in and on foods and amending Council Regulation (EEC) No 1601/91, Regulations (EC) No 2232/96 and (EC) No 110/2008 and Directive 2000/13/EC last amended on 09/26/2022.

(14) Borges, K. B.; Borges, W. d. S.; Durán-Patrón, R.; Pupo, M. T.; Bonato, P. S.; Collado, I. G. Stereoselective biotransformations using fungi as biocatalysts. *Tetrahedron: Asymmetry* **2009**, *20*, 385–397.

(15) Serra, S.; Fuganti, C.; Brenna, E. Biocatalytic preparation of natural flavours and fragrances. *Trends Biotechnol.* **2005**, *23*, 193–198.

(16) Schmidt-Dannert, C. Biocatalytic portfolio of Basidiomycota. *Curr. Opin. Chem. Biol.* **2016**, *31*, 40–49.

(17) Naranjo-Ortiz, M. A.; Gabaldón, T. Fungal evolution: Diversity, taxonomy and phylogeny of the fungi. *Biol. Rev. Cambridge Philos. Soc.* **2019**, *94*, 2101–2137.

(18) He, M.-Q.; Zhao, R.-L.; Hyde, K. D.; Begerow, D.; Kemler, M.; Yurkov, A.; McKenzie, E. H. C.; Raspé, O.; Kakishima, M.; Sánchez-Ramírez, S.*; et al.* Notes, outline and divergence times of Basidiomycota. *Fungal Diversity* **2019**, *99*, 105–367.

(19) Hibbett, D. S.; Binder, M.; Bischoff, J. F.; Blackwell, M.; Cannon, P. F.; Eriksson, O. E.; Huhndorf, S.; James, T.; Kirk, P. M.; Lücking, R.*; et al.* A higher-level phylogenetic classification of the fungi. *Mycol. Res.* **2007**, *111*, 509–547.

(20) de Mattos-Shipley, K. M. J.; Ford, K. L.; Alberti, F.; Banks, A. M.; Bailey, A. M.; Foster, G. D. The good, the bad and the tasty: The many roles of mushrooms. *Stud. Mycol.* **2016**, *85*, 125–157.

(21) Hibbett, D. S. A phylogenetic overview of the *Agaricomycotina*. *Mycologia* **2006**, *98*, 917–925.

(22) Kües, U.; Rühl, M. Mushroom production. In *Wood production, wood technology, and biotechnological impacts*; Kües, U., Ed.; Universitätsverlag Göttingen: Göttingen, 2007.

(23) Royse, D. J.; Baars, J.; Tan, Q. Current overview of mushroom production in the world. In *Edible and medicinal mushrooms*; Diego, C. Z., Pardo-Giménez, A., Eds.; John Wiley & Sons: Chichester, UK, 2017; pp 5–13.

(24) Pelkmans, J. F.; Lugones, L. G.; Wösten, H. A. B. Fruiting body formation in basidiomycetes. In *Growth, Differentiation and Sexuality: A comprehensive treatise on fungi as experimental systems for basic and applied research,* 3rd ed.; Wendland, J., Ed.; Springer International Publishing: Basel, 2016; pp 387–405.

(25) Watkinson, S. C.; Boddy, L.; Money, N. P.; Carlile, M. J. *The fungi*, 3rd ed.; Elsevier: Amsterdam, 2016.

(26) Ramírez, L.; Larraya, L. M.; Pisabarro, A. G. Molecular tools for breeding basidiomycetes. *Int. Microbiol.* **2000**, *3*, 147–152.

(27) Kües, U. Life history and developmental processes in the basidiomycete *Coprinus cinereus*. *Microbiol. Mol. Biol. Rev.* **2000**, *64*, 316–353.

(28) Bürger, F.; Koch, M.; Fraatz, M. A.; Omarini, A. B.; Berger, R. G.; Zorn, H. Production of an anise- and woodruff-like aroma by monokaryotic strains of *Pleurotus sapidus* grown on citrus side streams. *Molecules* **2022**, *27*.

(29) Omarini, A. B.; Plagemann, I.; Schimanski, S.; Krings, U.; Berger, R. G. Crosses between monokaryons of *Pleurotus sapidus* or *Pleurotus florida* show an improved biotransformation of (+)-valencene to (+)-nootkatone. *Bioresour. Technol.* **2014**, *171*, 113–119.

(30) Krahe, N.-K.; Berger, R. G.; Witt, M.; Zorn, H.; Omarini, A. B.; Ersoy, F. Monokaryotic *Pleurotus sapidus* strains with intraspecific variability of an alkene cleaving DyP-type peroxidase activity as a result of gene mutation and differential gene expression. *Int. J. Mol. Sci.* **2021**, *22*.

(31) Gill, M. The biosynthesis of pigments in basidiomycetes. *Aust. J. Chem.* **2001**, *54*, 721.

(32) Velíšek, J.; Cejpek, K. Pigments of higher fungi - A review. *Czech J. Food Sci.* **2011**, *29*, 87–102.

(33) Alves, M. J.; Ferreira, I. C. F. R.; Dias, J.; Teixeira, V.; Martins, A.; Pintado, M. A review on antimicrobial activity of mushroom (basidiomycetes) extracts and isolated compounds. *Planta Med.* **2012**, *78*, 1707–1718.

(34) Vieira Gomes, D. C.; de Alencar, M. V. O. B.; Dos Reis, A. C.; de Lima, R. M. T.; de Oliveira Santos, J. V.; Da Mata, A. M. O. F.; Soares Dias, A. C.; Da Costa, J. S.; de Medeiros, M. d. G. F.; Paz,

M. F. C. J.*; et al.* Antioxidant, anti-inflammatory and cytotoxic/antitumoral bioactives from the phylum Basidiomycota and their possible mechanisms of action. *Biomed. Pharmacother.* **2019**, *112*, 108643.

(35) Abdel-Mawgoud, A. M.; Stephanopoulos, G. Simple glycolipids of microbes: Chemistry, biological activity and metabolic engineering. *Synth. Syst. Biotechnol.* **2018**, *3*, 3–19.

(36) Garay, L. A.; Sitepu, I. R.; Cajka, T.; Xu, J.; Teh, H. E.; German, J. B.; Pan, Z.; Dungan, S. R.; Block, D. E.; Boundy-Mills, K. L. Extracellular fungal polyol lipids: A new class of potential high value lipids. *Biotechnol. Adv.* **2018**, *36*, 397–414.

(37) Da Silva, A. F.; Banat, I. M.; Giachini, A. J.; Robl, D. Fungal biosurfactants, from nature to biotechnological product: Bioprospection, production and potential applications. *Bioprocess Biosyst. Eng.* **2021**, *44*, 2003–2034.

(38) Korpi, A.; Järnberg, J.; Pasanen, A.-L. Microbial volatile organic compounds. *Crit. Rev. Toxicol.* **2009**, *39*, 139–193.

(39) Morath, S. U.; Hung, R.; Bennett, J. W. Fungal volatile organic compounds: A review with emphasis on their biotechnological potential. *Fungal Biol. Rev.* **2012**, *26*, 73–83.

(40) Schüffler, A. Secondary metabolites of basidiomycetes. In *Physiology and Genetics*; Anke, T., Schüffler, A., Eds.; Springer International Publishing: Basel, 2018.

(41) Dudekula, U. T.; Doriya, K.; Devarai, S. K. A critical review on submerged production of mushroom and their bioactive metabolites. *3 Biotech* **2020**, *10*, 337.

(42) Dashtban, M.; Schraft, H.; Syed, T. A.; Qin, W. Fungal biodegradation and enzymatic modification of lignin. *Int. J. Biochem. Mol. Biol.* **2010**, *1*, 36–50.

(43) Sugano, Y.; Muramatsu, R.; Ichiyanagi, A.; Sato, T.; Shoda, M. DyP, a unique dye-decolorizing peroxidase, represents a novel heme peroxidase family: ASP171 replaces the distal histidine of classical peroxidases. *J. Biol. Chem.* **2007**, *282*, 36652–36658.

(44) Sugano, Y.; Yoshida, T. DyP-Type peroxidases: Recent advances and perspectives. *Int. J. Mol. Sci.* **2021**, *22*.

(45) Rytioja, J.; Hildén, K.; Yuzon, J.; Hatakka, A.; de Vries, R. P.; Mäkelä, M. R. Plant-polysaccharide-degrading enzymes from basidiomycetes. *Microbiol. Mol. Biol. Rev.* **2014**, *78*, 614–649.

(46) Arantes, V.; Goodell, B. Current understanding of brown-rot fungal biodegradation mechanisms: A review. In *Deterioration and protection of sustainable biomaterials*; Schultz, T. P., Goodell, B., Nicholas, D. D., Eds.; American Chemical Society: Washington, DC, USA, 2014; pp 3–21.

(47) Sverdrup-Thygeson, A.; Lindenmayer, D. Ecological continuity and assumed indicator fungi in boreal forest: The importance of the landscape matrix. *For. Ecol. Manage.* **2003**, *174*, 353–363.

(48) Ziegenbein, F. C.; Hanssen, H.-P.; König, W. A. Chemical constituents of the essential oils of three wood-rotting fungi. *Flavour Fragr. J.* **2006**, *21*, 813–816.

(49) German Mycological Society. *Cystostereum murrayi* (Berk. & M.A. Curtis) Pouzar. https://www.pilze-deutschland.de/organismen/cystostereum-murrayi-berk-ma-curtis-pouzar-1959 (accessed April 1, 2024).

(50) Binder, M.; Hibbett, D. S.; Larsson, K.-H.; Larsson, E.; Langer, E.; Langer, G. The phylogenetic distribution of resupinate forms across the major clades of mushroom-forming fungi (Homobasidiomycetes). *Syst. Biodivers.* **2005**, *3*, 113–157.

(51) Scholler, M.; Bernauer, T.; Ebel, C.; Miggel, B.; Murmann-Kristen, L.; Schnittler, M. Eine mykologische Bestandsaufnahme des Bannwalds „Wilder See – Hornisgrinde“ (Nordschwarzwald, Baden-Württemberg). *Carolinea* **2013**, *71*, 153–159.

(52) Larsson, K.-H. Re-thinking the classification of corticioid fungi. *Mycol. Res.* **2007**, *111*, 1040–1063.

(53) Prasher, I. B. *Wood-rotting non-gilled Agaricomycetes of Himalayas*; Springer Netherlands: Dordrecht, 2015.

(54) Edman, M.; Gustafsson, M. Wood-disk traps provide a robust method for studying spore dispersal of wood-decaying basidiomycetes. *Mycologia* **2003**, *95*, 553.

(55) Kramer, R.; Abraham, W.-R. Volatile sesquiterpenes from fungi: What are they good for? *Phytochem. Rev.* **2012**, *11*, 15–37.

(56) Tang, Y.-J.; Zhu, L.-W.; Li, H.-M.; Li, D.-S. Submerged culture of mushrooms in bioreactors – Challenges, current state-of-the-art, and future prospects. *Food Technol. Biotechnol.* **2007**, *45*, 221–229.

(57) Comission Implementing Regulation (EU) 2023/6 of 3 January 2023 authorising the placing on the market of pea and rice protein fermented by *Lentinula edodes* (Shiitake mushroom) mycelia as a novel food and amending Implementing Regulation (EU) 2017/2470.

(58) Regulation (EU) 2015/2283 of the European Parliament and of the Council of 25 November 2015 on novel foods, amending Regulation (EU) No 1169/2011 of the European Parliament and of the Council and repealing Regulation (EC) No 258/97 of the European Parliament and of the Council and Commission Regulation (EC) No 1852/2001.

(59) Bakratsas, G.; Polydera, A.; Katapodis, P.; Stamatis, H. Recent trends in submerged cultivation of mushrooms and their application as a source of nutraceuticals and food additives. *Future Foods* **2021**, *4*, 100086.

(60) Berger, R. G.; Ersoy, F. Improved foods using enzymes from basidiomycetes. *Processes* **2022**, *10*, 726.

(61) Jaros, D.; Köbsch, J.; Rohm, H. Exopolysaccharides from Basidiomycota: Formation, isolation and techno-functional properties. *Eng. Life Sci.* **2018**, *18*, 743–752.

(62) Belitz, H.-D.; Grosch, W.; Schieberle, P. *Food Chemistry*; Springer: Berlin, Heidelberg, 2009.

(63) Robert J. McGorrin. Character-impact flavor and off-flavor compounds in foods. In *Flavor, fragrance, and odor analysis,* 2nd ed.; Marsili, R., Ed.; CRC Press: Boca Raton, USA, 2016; pp 207–262.

(64) Demole, E.; Enggist, P.; Ohloff, G. 1-*p*-Menthene-8-thiol: A powerful flavor impact constituent of grapefruit juice (*Citrus parodisi* MACFAYDEN). *Helv. Chim. Acta* **1982**, *65*, 1785–1794.

(65) Schieberle, P.; Ofner, S.; Grosch, W. Evaluation of potent odorants in cucumbers (*Cucumis sativus*) and muskmelons (*Cucumis melo*) by aroma extract dilution analysis. *J. Food Sci.* **1990**, *55*, 193–195.

(66) Buchbauer, G.; Jirovetz, L.; Wasicky, M.; Nikiforov, A. Zum Aroma von Speisepilzen. *Z. Lebensm.-Unters. Forsch.* **1993**, *197*, 429–433.

(67) Cronin, D. A.; Ward, M. K. The characterisation of some mushroom volatiles. *J. Sci. Food Agric.* **1971**, *22*, 477–479.

(68) Dunkel, A.; Steinhaus, M.; Kotthoff, M.; Nowak, B.; Krautwurst, D.; Schieberle, P.; Hofmann, T. Nature's chemical signatures in human olfaction: A foodborne perspective for future biotechnology. *Angew. Chem., Int. Ed. Engl.* **2014**, *53*, 7124–7143.

(69) Jeleń, H. Specificity of food odorants. In *Food Flavors*; Jelen, H., Ed.; Chemical & Functional Properties of Food Components; CRC Press: Boca Raton, USA, 2011; pp 1–18.

(70) Keusgen, M. Volatile compounds of the genus *Allium* L. (Onions). In *Deterioration and protection of sustainable biomaterials*; Schultz, T. P., Goodell, B., Nicholas, D. D., Eds.; American Chemical Society: Washington, DC, USA, 2014; pp 183–214.

(71) Hung, R.; Lee, S.; Bennett, J. W. Fungal volatile organic compounds and their role in ecosystems. *Appl. Microbiol. Biotechnol.* **2015**, *99*, 3395–3405.

(72) Dickschat, J. S. Fungal volatiles - A survey from edible mushrooms to moulds. *Nat. Prod. Rep.* **2017**, *34*, 310–328.

(73) Li, N.; Alfiky, A.; Vaughan, M. M.; Kang, S. Stop and smell the fungi: Fungal volatile metabolites are overlooked signals involved in fungal interaction with plants. *Fungal Biol. Rev.* **2016**, *30*, 134–144.

(74) Chitarra, G. S.; Abee, T.; Rombouts, F. M.; Posthumus, M. A.; Dijksterhuis, J. Germination *Penicillium paneum* conidia is regulated by 1-octen-3-ol, a volatile self-inhibitor. *Appl. Environ. Microbiol.* **2004**, *70*, 2823–2829.

(75) Fraatz, M. A.; Zorn, H. Fungal flavours. In *The Mycota: Industrial applications*; Hofrichter, M., Ed.; Springer Berlin Heidelberg: Berlin, Heidelberg, 2011; pp 249–268.

(76) Combet, E.; Eastwood, D. C.; Burton, K. S.; Henderson, J. Eight-carbon volatiles in mushrooms and fungi: Properties, analysis, and biosynthesis. *Mycoscience* **2006**, *47*, 317–326.

(77) Pennerman, K. K.; Yin, G.; Bennett, J. W. Eight-carbon volatiles: Prominent fungal and plant interaction compounds. *J. Exp. Bot.* **2022**, *73*, 487–497.

(78) Tressl, R.; Bahri, D.; Engel, K.-H. Lipid oxidation in fruits and vegetables. In *Deterioration and protection of sustainable biomaterials*; Schultz, T. P., Goodell, B., Nicholas, D. D., Eds.; American Chemical Society: Washington, DC, USA, 2014; pp 213–232.

(79) Wurzenberger, M.; Grosch, W. The enzymic oxidative breakdown of linoleic acid in mushrooms (*Psalliota bispora*). *Z. Lebensm.-Unters. Forsch.* **1982**, *175*, 186–190.

(80) Wurzenberger, M.; Grosch, W. The formation of 1-octen-3-ol from the 10-hydroperoxide isomer of linoleic acid by a hydroperoxide lyase in mushrooms (*Psalliota bispora*). *Biochim. Biophys. Acta, Lipids Lipid Metab.* **1984**, *794*, 25–30.

(81) Assaf, S.; Hadar, Y.; Dosoretz, C. G. 1-Octen-3-ol and 13-hydroperoxylinoleate are products of distinct pathways in the oxidative breakdown of linoleic acid by *Pleurotus pulmonarius*. *Enzyme Microb. Technol.* **1997**, *21*, 484–490.

(82) Morita, K.; Kobayashi, S. Isolation, structure, and synthesis of lenthionine and its analogs. *Chem. Pharm. Bull.* **1967**, *15*, 988–993.

(83) Rapior, S.; Breheret, S.; Talou, T.; Bessière, J.-M. Volatile flavor constituents of fresh *Marasmius alliaceus* (Garlic Marasmius). *J. Agric. Food Chem.* **1997**, *45*, 820–825.

(84) Borg-Karlson, A.-K.; O. Englund, F.; Unelius, C. Dimethyl oligosulphides, major volatiles released from *Sauromatum guttatum* and *Phallus impudicus*. *Phytochemistry* **1994**, *35*, 321–323.

(85) Chen, C.-C.; Ho, C.-T. Identification of sulfurous compounds of Shiitake mushroom (*Lentinus edodes* Sing.). *J. Agric. Food Chem.* **1986**, *34*, 830–833.

(86) Wu, C.-M.; Wang, Z. Volatile compounds in fresh and processed Shiitake mushrooms (*Lentinus edodes* Sing.). *Food Sci. Technol. Res.* **2000**, *6*, 166–170.

(87) Chen, C.-C.; Liu, S.-E.; Wu, C.-M.; Ho, C.-T. Enzymic formation of volatile compounds in Shiitake mushroom (*Lentinus edodes* Sing.). In *Deterioration and protection of sustainable biomaterials*; Schultz, T. P., Goodell, B., Nicholas, D. D., Eds.; American Chemical Society: Washington, DC, USA, 2014; pp 176–183.

(88) Yalman, S.; Trapp, T.; Vetter, C.; Popa, F.; Fraatz, M. A.; Zorn, H. Formation of a meat-like flavor by submerged cultivated *Laetiporus montanus*. *J. Agric. Food Chem.* **2023**, *71*, 8083–8092.

(89) Wagner, K.-H.; Elmadfa, I. Biological relevance of terpenoids. Overview focusing on mono-, di- and tetraterpenes. *Ann. Nutr. Metab.* **2003**, *47*, 95–106.

(90) Burkhardt, I.; Kreuzenbeck, N. B.; Beemelmanns, C.; Dickschat, J. S. Mechanistic characterization of three sesquiterpene synthases from the termite-associated fungus *Termitomyces*. *Org. Biomol. Chem.* **2019**, *17*, 3348–3355.

(91) Tilden, W. A. XLVI. - On the decomposition of terpenes by heat. *J. Chem. Soc., Trans.* **1884**, *45*, 410–420.

(92) Ruzicka, L. The isoprene rule and the biogenesis of terpenic compounds. *Experientia* **1953**, *9*, 357–367.

(93) Breitmaier, E. *Terpene*; Vieweg+Teubner Verlag: Wiesbaden, 1999.

(94) Trapp, T.; Zajul, M.; Ahlborn, J.; Stephan, A.; Zorn, H.; Fraatz, M. A. Submerged cultivation of *Pleurotus sapidus* with molasses: Aroma dilution analyses by means of solid phase microextraction and stir bar sorptive extraction. *J. Agric. Food Chem.* **2018**, *66*, 2393–2402.

(95) Rapior, S.; Breheret, S.; Talou, T.; Pélissier, Y.; Bessière, J.-M. The anise-like odor of *Clitocybe odora*, *Lentinellus cochleatus* and *Agaricus essettei*. *Mycologia* **2002**, *94*, 373–376.

(96) Berger, R. G.; Neuhäuser, K.; Drawert, F. Characterization of the odour principles of some basidiomycetes: *Bjerkandera adusta*, *Poria aurea*, *Tyromyces sambuceus*. *Flavour Fragr. J.* **1986**, *1*, 181–185.

(97) Nyegue, M.; Zollo, P.-H. A.; Bessière, J.-M.; Rapior, S. Volatile components of fresh *Pleurotus ostreatus* and *Termitomyces shimperi* from Cameroon. *J. Essent.Oil Bear. Plants* **2003**, *6*, 153–160.

(98) Mau, J.-L.; Lin, Y.-P.; Chen, P.-T.; Wu, Y.-H.; Peng, J.-T. Flavor compounds in king oyster mushrooms *Pleurotus eryngii*. *J. Agric. Food Chem.* **1998**, *46*, 4587–4591.

(99) Lapadatescu, C.; Giniès, C.; Le Quéré, J. L.; Bonnarme, P. Novel scheme for biosynthesis of aryl metabolites from L-phenylalanine in the fungus *Bjerkandera adusta*. *Appl. Environ. Microbiol.* **2000**, *66*, 1517–1522.

(100) Kabbaj, W.; Breheret, S.; Guimberteau, J.; Talou, T.; Olivier, J. M.; Bensoussan, M.; Sobal, M.; Roussos, S. Comparison of volatile compound production in fruit body and in mycelium of *Pleurotus ostreatus* identified by submerged and solid-state cultures. *Appl. Biochem. Biotechnol.* **2002**, *102-103*, 463–469.

(101) Lynen, F. Biosynthetic pathways from acetate to natural products. *Pure Appl. Chem.* **1967**, *14*, 137–167.

(102) Lombard, J.; Moreira, D. Origins and early evolution of the mevalonate pathway of isoprenoid biosynthesis in the three domains of life. *Mol. Biol. Evol.* **2011**, *28*, 87–99.

(103) Miziorko, H. M. Enzymes of the mevalonate pathway of isoprenoid biosynthesis. *Arch. Biochem. Biophys.* **2011**, *505*, 131–143.

(104) Dellas, N.; Thomas, S. T.; Manning, G.; Noel, J. P. Discovery of a metabolic alternative to the classical mevalonate pathway. *eLife* **2013**, *2*, e00672.

(105) Vinokur, J. M.; Korman, T. P.; Cao, Z.; Bowie, J. U. Evidence of a novel mevalonate pathway in archaea. *Biochemistry* **2014**, *53*, 4161–4168.

(106) Lichtenthaler, H. K.; Schwender, J.; Disch, A.; Rohmer, M. Biosynthesis of isoprenoids in higher plant chloroplasts proceeds via a mevalonate-independent pathway. *FEBS Lett.* **1997**, *400*, 271–274.

(107) Frank, A.; Groll, M. The methylerythritol phosphate pathway to isoprenoids. *Chem. Rev.* **2017**, *117*, 5675–5703.

(108) Ludwiczuk, A.; Skalicka-Woźniak, K.; Georgiev, M. I. Terpenoids. In *Pharmacognosy,* 1st ed.; Badal, S., Delgoda, R., Eds.; Elsevier: Amsterdam, 2017; pp 233–266.

(109) Oldfield, E.; Lin, F.-Y. Terpene biosynthesis: Modularity rules. *Angew. Chem., Int. Ed. Engl.* **2012**, *51*, 1124–1137.

(110) Zhang, C.; Chen, X.; Lee, R. T. C.; T, R.; Maurer-Stroh, S.; Rühl, M. Bioinformatics-aided identification, characterization and applications of mushroom linalool synthases. *Commun. Biol.* **2021**, *4*, 223.

(111) Zhang, C.; Seow, V. Y.; Chen, X.; Too, H.-P. Multidimensional heuristic process for high-yield production of astaxanthin and fragrance molecules in *Escherichia coli*. *Nat. Commun.* **2018**, *9*, 1858.

(112) Gressler, M.; Löhr, N. A.; Schäfer, T.; Lawrinowitz, S.; Seibold, P. S.; Hoffmeister, D. Mind the mushroom: Natural product biosynthetic genes and enzymes of Basidiomycota. *Nat. Prod. Rep.* **2021**, *38*, 702–722.

(113) Scholtmeijer, K.; Cankar, K.; Beekwilder, J.; Wösten, H. A. B.; Lugones, L. G.; Bosch, D. Production of (+)-valencene in the mushroom-forming fungus *S. commune*. *Appl. Microbiol. Biotechnol.* **2014**, *98*, 5059–5068.

(114) Mischko, W.; Hirte, M.; Fuchs, M.; Mehlmer, N.; Brück, T. B. Identification of sesquiterpene synthases from the Basidiomycota *Coniophora puteana* for the efficient and highly selective *β*-copaene and cubebol production in *E. coli*. *Microb. Cell Fact.* **2018**, *17*, 164.

(115) Blank, I.; Grosch, W. Evaluation of potent odorants in dill seed and dill herb (*Anethum graveolens* L.) by aroma extract dilution analysis. *J. Food Sci.* **1991**, *56*, 63–67.

(116) Brunke, E.-J.; Hammerschmidt, F.-J.; Koester, F.-H.; Mair, P. Constituents of dill (*Anethum graveolens* L.) with sensory importance. *J. Essent. Oil Res.* **1991**, *3*, 257–267.

(117) Reichert, S.; Wüst, M.; Beck, T.; Mosandl, A. Stereoisomeric flavor compounds LXXXI: Dill ether and its cis-stereoisomers: Synthesis and enantioselective analysis. *J. High Resolut. Chromatogr.* **1998**, *21*, 185–188.

(118) Reichert, S.; Fischer, D.; Asche, S.; Mosandl, A. Stable isotope labelling in biosynthetic studies of dill ether, using enantioselective multidimensional gas chromatography, online coupled with isotope ratio mass spectrometry. *Flavour Fragrance J.* **2000**, *15*, 303–308.

(119) Trapp, T.; Kirchner, T.; Birk, F.; Fraatz, M. A.; Zorn, H. Biosynthesis of stereoisomers of dill ether and wine lactone by *Pleurotus sapidus*. *J. Agric. Food Chem.* **2019**, *67*, 13400–13411.

(120) Southwell, I. A. Essential oil metabolism in the koala III: Novel urinary monoterpenoid lactones. *Tetrahedron Lett.* **1975**, *16*, 1885–1888.

(121) Guth, H. Determination of the configuration of wine lactone. *Helv. Chim. Acta* **1996**, *79*, 1559–1571.

(122) Buhr, K. Untersuchungen zu Struktur-Geruchsbeziehungen von Lactonen. Dissertation, Bergische Universität Wuppertal, Wuppertal, 2006.

(123) Ilc, T.; Halter, D.; Miesch, L.; Lauvoisard, F.; Kriegshauser, L.; Ilg, A.; Baltenweck, R.; Hugueney, P.; Werck-Reichhart, D.; Duchêne, E.*; et al.* A grapevine cytochrome P450 generates the precursor of wine lactone, a key odorant in wine. *New Phytol.* **2017**, *213*, 264–274.

(124) Wüst, M.; Mosandl, A. Important chiral monoterpenoid ethers in flavours and essential oils - enantioselective analysis and biogenesis. *Z. Lebensm.-Unters. Forsch.* **1999**, *209*, 3–11.

(125) Akhila, A.; Srivastava, R.; Rani, K.; Thakur, R. S. Biosynthesis of (−)-mintlactone and (+)-isomintlactone in *Mentha piperita*. *Phytochemistry* **1991**, *30*, 485–489.

(126) Bertea, C. M.; Schalk, M.; Karp, F.; Maffei, M.; Croteau, R. Demonstration that menthofuran synthase of mint (*Mentha*) is a cytochrome P450 monooxygenase: Cloning, functional expression, and characterization of the responsible gene. *Arch. Biochem. Biophys.* **2001**, *390*, 279–286.

(127) Fuchs, L. K.; Holland, A. H.; Ludlow, R. A.; Coates, R. J.; Armstrong, H.; Pickett, J. A.; Harwood, J. L.; Scofield, S. Genetic manipulation of biosynthetic pathways in mint. *Front. Plant Sci.* **2022**, *13*, 928178.

(128) Khojasteh, S. C.; Oishi, S.; Nelson, S. D. Metabolism and toxicity of menthofuran in rat liver slices and in rats. *Chem. Res. Toxicol.* **2010**, *23*, 1824–1832.

(129) Thakkar, Y.; Moustakas, H.; Api, A. M.; Smith, B.; Williams, G.; Greim, H.; Eisenbrand, G.; Dekant, W. Assessment of the genotoxic potential of mintlactone. *Food Chem. Toxicol.* **2022**, *159*, 112659.

(130) Commission Regulation (EU) 2022/1466 of 5 September 2022 amending Annex I to Regulation (EC) No 1334/2008 of the European Parliament and of the Council as regards the removal of certain flavouring substances from the Union list.

(131) Blank, I.; Fischer, K.-H.; Grosch, W. Intensive neutral odourants of linden honey: Differences from honeys of other botanical origin. *Z. Lebensm.-Unters. Forsch.* **1989**, *189*, 426–433.

(132) Blank, I.; Grosch, W.; Eisenreich, W.; Bacher, A.; Firl, J. Determination of the chemical structure of linden ether. *Helv. Chim. Acta* **1990**, *73*, 1250–1257.

(133) Näf, R.; Velluz, A. Phenols and lactones in Italo-Mitcham peppermint oil *Mentha* × *piperita* L. *Flavour Fragr. J.* **1998**, *13*, 203–208.

(134) Shigeto, A.; Wada, A.; Kumazawa, K. Identification of the novel odor active compounds "*p*-menthane lactones" responsible for the characteristic aroma of fresh peppermint leaf. *Biosci., Biotechnol., Biochem.* **2020**, *84*, 421–427.

(135) Gaudin, J.-M. Synthesis and organoleptic properties of *p*-menthane lactones. *Tetrahedron* **2000**, *56*, 4769–4776.

(136) Gatfield, I.; Hilmer, J.-M.; Betram, H.-J. Conversion of some unsaturated cyclic ethers to lactones catalyzed by Lipase B from *Candida antarctica*. *Perfum. flavor.* **2007**, *32*, 28–31.

(137) Grosch, W. Evaluation of the key odorants of foods by dilution experiments, aroma models and omission. *Chem. Senses* **2001**, *26*, 533–545.

(138) Augusto, F.; Leite e Lopes, A.; Zini, C. A. Sampling and sample preparation for analysis of aromas and fragrances. *TrAC, Trends Anal. Chem.* **2003**, *22*, 160–169.

(139) Wells, M. J. M. Principles of extraction and the extraction of semivolatile organics from liquids. In *Sample preparation techniques in analytical chemistry*; Mitra, S., Ed.; John Wiley & Sons: Hoboken, NJ, USA, 2003; pp 37–138.

(140) Sánchez-Palomo, E.; Alañón, M. E.; Díaz-Maroto, M. C.; González-Viñas, M. A.; Pérez-Coello, M. S. Comparison of extraction methods for volatile compounds of Muscat grape juice. *Talanta* **2009**, *79*, 871–876.

(141) Engel, W.; Bahr, W.; Schieberle, P. Solvent assisted flavour evaporation - A new and versatile technique for the careful and direct isolation of aroma compounds from complex food matrices. *Z. Lebensm.-Unters. Forsch.* **1999**, *209*, 237–241.

(142) Grosch, W. Detection of potent odorants in foods by aroma extract dilution analysis. *Trends Food Sci. Technol.* **1993**, *4*, 68–73.

(143) Fuller, G. H.; Steltenkamp, R.; Tisserand, G. A. The gas chromatograph with human sensor: Perfumer model. *Ann. N. Y. Acad. Sci.* **1964**, *116*, 711–724.

(144) Vas, G.; Vékey, K. Solid-phase microextraction: A powerful sample preparation tool prior to mass spectrometric analysis. *J. Mass Spectrom.* **2004**, *39*, 233–254.

(145) Da Costa, N. C.; Eri, S. Identification of aroma chemicals. In *Chemistry and technology of flavors and fragrances*; Rowe, D. J., Ed.; Blackwell Publishing Ltd: Oxford, UK, 2004; pp 12–34.

(146) Belardi, R. P.; Pawliszyn, J. B. The application of chemically modified fused silica fibers in the extraction of organics from water matrix samples and their rapid transfer to capillary columns. *Water Qual. Res. J.* **1989**, *24*, 179–191.

(147) Arthur, C. L.; Pawliszyn, J. Solid phase microextraction with thermal desorption using fused silica optical fibers. *Anal. Chem.* **1990**, *62*, 2145–2148.

(148) Pawliszyn, J. Solid phase microextraction. *Adv. Exp. Med. Biol.* **2001**, *488*, 73–87.

(149) Hwan Kim, T.; Lee, S. M.; Kim, Y.-S.; Kim, K. H.; Oh, S.; Lee, H. J. Aroma dilution method using GC injector split ratio for volatile compounds extracted by headspace solid phase microextraction. *Food Chem.* **2003**, *83*, 151–158.

(150) Trapp, T.; Jäger, D. A.; Fraatz, M. A.; Zorn, H. Development and validation of a novel method for aroma dilution analysis by means of stir bar sorptive extraction. *Z. Lebensm.-Unters. Forsch.* **2018**, *244*, 949–957.

(151) Brescia, F. F.; Pitelas, W.; Yalman, S.; Popa, F.; Hausmann, H. G.; Wende, R. C.; Fraatz, M. A.; Zorn, H. Formation of diastereomeric dihydromenthofurolactones by *Cystostereum murrayi* and aroma dilution analysis based on dynamic headspace extraction. *J. Agric. Food Chem.* **2021**, *69*, 5997–6004.

(152) Hasan, C. K.; Ghiasvand, A.; Lewis, T. W.; Nesterenko, P. N.; Paull, B. Recent advances in stir-bar sorptive extraction: Coatings, technical improvements, and applications. *Anal. Chim. Acta* **2020**, *1139*, 222–240.

(153) Ochiai, N.; Sasamoto, K.; Ieda, T.; David, F.; Sandra, P. Multi-stir bar sorptive extraction for analysis of odor compounds in aqueous samples. *J. Chromatogr. A* **2013**, *1315*, 70–79.

(154) David, F.; Ochiai, N.; Sandra, P. Two decades of stir bar sorptive extraction: A retrospective and future outlook. *TrAC, Trends Anal. Chem.* **2019**, *112*, 102–111.

(155) Slack, G. C.; Snow, N. H.; Kou, D. Extraction of volatile organic compounds from solids and liquids. In *Sample preparation techniques in analytical chemistry*; Mitra, S., Ed.; John Wiley & Sons: Hoboken, NJ, USA, 2003; pp 183–225.

(156) Bazemore, R. Sample preparation. In *Practical analysis of flavor and fragrance materials*; Goodner, K., Rouseff, R., Eds.; John Wiley & Sons: Hoboken, 2011; pp 23–44.

(157) Molyneux, R. J.; Schieberle, P. Compound identification: A Journal of Agricultural and Food Chemistry perspective. *J. Agric. Food Chem.* **2007**, *55*, 4625–4629.

(158) Marriott, P. J.; Chin, S.-T.; Maikhunthod, B.; Schmarr, H.-G.; Bieri, S. Multidimensional gas chromatography. *TrAC, Trends Anal. Chem.* **2012**, *34*, 1–21.

(159) Schomburg, G.; Husamanm, H.; Hübinger, E.; König, W. A. Multidimensional capillary gas chromatography-enantiomeric separations of selected cuts using a chiral second column. *J. High Resol. Chromatogr.* **1984**, *7*, 404–410.

(160) Sharif, K. M.; Chin, S.-T.; Kulsing, C.; Marriott, P. J. The microfluidic Deans switch: 50 Years of progress, innovation and application. *TrAC, Trends Anal. Chem.* **2016**, *82*, 35–54.

(161) Gil-Av, E.; Feibush, B.; Charles-Sigler, R. Separation of enantiomers by gas liquid chromatography with an optically active stationary phase. *Tetrahedron Lett.* **1966**, *7*, 1009–1015.

(162) Betzenbichler, G.; Huber, L.; Kräh, S.; Morkos, M.-L. K.; Siegle, A. F.; Trapp, O. Chiral stationary phases and applications in gas chromatography. *Chirality* **2022**, *34*, 732–759.

(163) Schurig, V. Chiral separations using gas chromatography. *TrAC, Trends Anal. Chem.* **2002**, *21*, 647–661.

(164) Gawley, R. E. Do the terms "% ee" and "% de" make sense as expressions of stereoisomer composition or stereoselectivity? *J. Org. Chem.* **2006**, *71*, 2411–2416.

(165) Patton, S.; Josephson, D. V. A method for determining significance of volatile flavor compounds in foods. *J. Food Sci.* **1957**, *22*, 316–318.

(166) Ferreira, V.; de La Fuente, A.; Sáenz-Navajas, M. P. Wine aroma vectors and sensory attributes. In *Managing wine quality*; Andrew Reynolds, Ed.; Elsevier: Amsterdam, 2022; pp 3–39.

(167) Mosquera, M. E. G.; Jiménez, G.; Tabernero, V.; Vinueza-Vaca, J.; García-Estrada, C.; Kosalková, K.; Sola-Landa, A.; Monje, B.; Acosta, C.; Alonso, R.*; et al.* Terpenes and terpenoids: Building blocks to produce biopolymers. *Sustainable Chem.* **2021**, *2*, 467–492.

(168) International Organization for Standardization. *Sensory analysis - Vocabulary;* ISO 5492:2008. https://www.iso.org/standard/38051.html (accessed February 16, 2024).

(169) Buttery, R. G. Flavor chemistry and odor thresholds. In *Flavor chemistry*; Teranishi, R., Wick, E. L., Hornstein, I., Eds.; Springer US: Boston, 1999; pp 353–365.

(170) Ullrich, F.; Grosch, W. Identification of the most intense volatile flavour compounds formed during autoxidation of linoleic acid. *Z. Lebensm.-Unters. Forsch.* **1987**, *184*, 277–282.

(171) Teranishi, R.; Buttery, R. G.; Guadagni, D. G. Odor quality and chemical structure in fruit and vegetable flavors. *Ann. N. Y. Acad. Sci.* **1974**, *237*, 209–216.

(172) Boelens, M. H.; van Gemert, L. J. Physicochemical parameters related to organoleptic properties of favour components. In *Developments in food flavours*; Birch, G. G., Lindley, M. G., Eds.; Elsevier Applied Science: London, 1986; pp 23–49.

(173) Stevens, J. C.; Cain, W. S.; Burke, R. J. Variability of olfactory thresholds. *Chem. Senses* **1988**, *13*, 643–653.

(174) Audouin, V.; Bonnet, F.; Vickers, Z. M.; Reineccius, G. A. Limitations in the use of odor activity values to determine important odorants in foods. In *Deterioration and protection of sustainable biomaterials*; Schultz, T. P., Goodell, B., Nicholas, D. D., Eds.; American Chemical Society: Washington, DC, USA, 2014; pp 156–171.

(175) Büchner, K. *De rerum natura: Welt aus Atomen*; P. Reclam: Stuttgart, 1986.

(176) Rehner, G.; Daniel, H. *Biochemie der Ernährung*, 3rd ed.; Springer: Heidelberg, 2010.

(177) Trimmer, C.; Mainland, J. D. The olfactory system. In *Conn's Translational Neuroscience*; Conn, M., Ed.; Elsevier: Amsterdam, 2017; pp 363–377.

(178) Mori, K.; Yoshihara, Y. Molecular recognition and olfactory processing in the mammalian olfactory system. *Prog. Neurobiol.* **1995**, *45*, 585–619.

(179) Malnic, B.; Hirono, J.; Sato, T.; Buck, L. B. Combinatorial receptor codes for odors. *Cell* **1999**, *96*, 713–723.

(180) Bystrova, M. F.; Kolesnikov, S. S. The “one neuron–one receptor” rule in the physiology and genetics of olfaction. *Neurosci. Behav. Physiol.* **2021**, *51*, 1008–1017.

(181) Mainland, J. D.; Li, Y. R.; Zhou, T.; Liu, W. L. L.; Matsunami, H. Human olfactory receptor responses to odorants. *Sci. Data* **2015**, *2*, 150002.

(182) Young, J. M.; Trask, B. J. The sense of smell: Genomics of vertebrate odorant receptors. *Hum. Mol. Genet.* **2002**, *11*, 1153–1160.

(183) Pelosi, P. Perireceptor events in olfaction. *J. Neurobiol.* **1996**, *30*, 3–19.

(184) Fleischer, J.; Breer, H.; Strotmann, J. Mammalian olfactory receptors. *Front. Cell. Neurosci.* **2009**, *3*, 9.

(185) Billesbølle, C. B.; de March, C. A.; van der Velden, W. J. C.; Ma, N.; Tewari, J.; Del Torrent, C. L.; Li, L.; Faust, B.; Vaidehi, N.; Matsunami, H.*; et al.* Structural basis of odorant recognition by a human odorant receptor. *Nature* **2023**, *615*, 742–749.

(186) Tegoni, M.; Pelosi, P.; Vincent, F.; Spinelli, S.; Campanacci, V.; Grolli, S.; Ramoni, R.; Cambillau, C. Mammalian odorant binding proteins. *Biochim. Biophys. Acta* **2000**, *1482*, 229–240.

(187) Pelosi, P.; Knoll, W. Odorant-binding proteins of mammals. *Biol. Rev. Cambridge Philos. Soc.* **2022**, *97*, 20–44.

(188) Rihani, K.; Ferveur, J.-F.; Briand, L. The 40-year mystery of insect odorant-binding proteins. *Biomolecules* **2021**, *11*.

(189) Venthur, H.; Zhou, J.-J. Odorant receptors and odorant-binding proteins as insect pest control targets: A comparative analysis. *Front. Physiol.* **2018**, *9*, 1163.

(190) Pifferi, S.; Menini, A.; Kurahashi, T. Signal transduction in vertebrate olfactory cilia. In *The neurobiology of olfaction*; Menini, A., Ed.; Frontiers in Neuroscience; CRC Press: Boca Raton, USA, 2009; pp 203–224.

(191) Menini, A.; Lagostena, L.; Boccaccio, A. Olfaction: From odorant molecules to the olfactory cortex. *News Physiol. Sci.* **2004**, *19*, 101–104.

(192) Firestein, S. How the olfactory system makes sense of scents. *Nature* **2001**, *413*, 211–218.

3. **Chapter:** Aroma Profile of *Cystostereum murrayi*

Formation of diastereomeric dihydromenthofurolactones by *Cystostereum murrayi* and aroma dilution analysis based on dynamic headspace extraction

Brescia, F. F.; Pitelas, W.; Yalman, S.; Popa, F.; Hausmann, H. G.; Wende, R. C.; Fraatz, M. A.; Zorn, H.

J. Agr. Food Chem. **2021**, *69* (21), 5997–6004.

https://doi.org/10.1021/acs.jafc.1c01478

JOURNAL OF AGRICULTURAL AND FOOD CHEMISTRY

pubs.acs.org/JAFC Article

Formation of Diastereomeric Dihydromenthofurolactones by *Cystostereum murrayi* and Aroma Dilution Analysis Based on Dynamic Headspace Extraction

Fabio F. Brescia, Wassilios Pitelas, Suzan Yalman, Flavius Popa, Heike G. Hausmann, Raffael C. Wende, Marco A. Fraatz, and Holger Zorn*

Cite This: *J. Agric. Food Chem.* 2021, 69, 5997−6004 Read Online

ACCESS | Metrics & More | Article Recommendations | Supporting Information

ABSTRACT: Submerged cultures of the basidiomycota *Cystostereum murrayi* emit an intensive coconut-like, sweetish, and buttery smell. For identification of the key aroma compounds, an aroma dilution analysis using dynamic headspace was performed by adjusting the split ratio of the GC inlet system. Flavor dilution (FD) factors varied from 2^2 up to $\geq 2^{18}$, whereby the largest class of compounds represented terpenoids, including two rare stereoisomers of 3,6-dimethyl-2,3,3a,4,5,7a-hexahydrobenzofuran (dill ether, ee $\geq$ 99.9). By means of nuclear magnetic resonance spectroscopy, the substances with the highest FD factors (2^9, 2^{12}, and 2^{18}) were identified as diastereomers of 3,6-dimethyl-3a,4,5,6,7,7a-hexayhydro-3*H*-1-benzofuran-2-one (dihydromenthofurolactone) and as its corresponding C3-unsaturated lactone. The latter two compounds have not been described for *Cystostereum murrayi* or for any other basidiomycota previously. Supplementation studies using 2-^{13}C-D-glucose indicated that these lactones as well as the two stereoisomers of dill ether and other terpenoids were formed de novo by the fungus.

KEYWORDS: *Cystostereum murrayi, submerged cultivation, dynamic headspace, aroma dilution analysis, flavoring substances, Black Forest National Park*

INTRODUCTION

Due to an increasing consumer interest in natural food ingredients, the demand for natural flavorings is globally rising.[1] To meet this demand, new approaches for the production of natural flavor compounds need to be developed. In recent years, basidiomycota have emerged as a promising source for natural flavorings. Over 30,000 species are currently known within this phylum, while the major part has not been investigated with respect to their flavor production potential.[2] For the growth of basidiomycota, submerged cultivation is widely used as this method represents an environmentally friendly, efficient, inexpensive, and well-controllable process in which agricultural side-streams may be used as substrates.[3]

Examples for aroma production by basidiomycota in submerged culture include, e.g., *Pleurotus sapidus* (PSA) and *Lentinula edodes*.[4,5] The fungus *Cystostereum murrayi* (CMU) may be especially interesting for aroma production, since its fruiting bodies are associated with an intense coconut-like odor.[6] However, aroma profiles of fruiting bodies or submerged cultures of CMU have not been studied yet. CMU was first described by Berkeley and Curtis in 1868 as *Thelephora murrai* from New England, USA, and later renamed and newly combined into the genus *Cystostereum* in 1959 by Pouzar.[7,8] The basidiomycota is classified as a type species of the genus *Cystostereum* belonging to the order *Agaricales*. The species forms crustlike, perennial fruiting bodies growing on coniferous deadwood, causing a white-rot and degrading lignin. Remarkably, in North America, CMU is reported from deadwood of deciduous trees.[9] The fungus shows a worldwide occurrence with main distribution in boreal-montane forests in the northern hemisphere. It is a red-listed species in many European countries and proposed as indicator of old forests with a long habitat continuity since the fungus prefers this environment.[10,11] In Germany, it is only known to be present in a few locations in Baden-Württemberg and Bavaria.[12] The collection used within this study (KR-M-0053174) originates from the former long-term protected forest "Wilder See", which is unmanaged now for more than 100 years. Since 2014, it belongs to the core zone of the Black Forest National Park. While aroma compounds or an aroma profile of submerged cultivated CMU have not been reported yet, an unusual benzofuran ketone has been described for CMU.[13]

The aims of this study were to analyze the aroma profile of submerged cultivated CMU and to identify the aroma compounds responsible for the coconut-like odor. For this, an aroma dilution analysis (ADA) using a dynamic headspace (DHS) was applied. To the best of our knowledge, this extraction method has not been used for an ADA so far. Furthermore, the major biosynthetic pathways of the identified key aroma compounds were elucidated using ^{13}C-labeled D-glucose as a potential precursor. The identified dihydromen-

Received: March 12, 2021
Revised: May 6, 2021
Accepted: May 6, 2021
Published: May 19, 2021

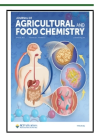

https://doi.org/10.1021/acs.jafc.1c01478
J. Agric. Food Chem. 2021, 69, 5997−6004

thofurolactones formed by CMU represent highly potent flavoring substances, listed on the EU positive list of flavorings, and are therefore of special interest for the flavor industry. The results of this study demonstrate the great potential for human purposes harbored in rare species.

MATERIALS AND METHODS

Chemicals. All chemicals for the cultivation of CMU and PSA on agar plates and in submerged culture were purchased from AppliChem (Darmstadt, Germany), Carl Roth (Karlsruhe, Germany), Sigma-Aldrich (Taufkirchen, Germany), and Th. Geyer (Hamburg, Germany). Diethyl ether (99.5%) was supplied by BCH Bruehl-Chemikalien Handel (Bruehl, Germany) and *n*-pentane (99%) from Th. Geyer. *n*-Hexane (97%) was purchased from Honeywell (Seelze, Germany). Isopropyl alcohol (99.8%) was obtained from Carl Roth. Chloroform-*d* [99.8 atom% D, with 0.03 vol % tertramethylsilane (TMS), stabilized with Ag], chloroform-*d* [99.8 atom% D, anhydrous], 2-^{13}C-D-glucose, mint lactone (99%), linalool (97%), and oct-1-en-3-one (96%) were obtained from Sigma-Aldrich. 3-Methylbutanoic acid (98%) was supplied by Alfa Aesar (Kandel, Germany), 2-phenylethan-1-ol (99%) by Acros Organics (Fair Lawn, USA), and 4-acetyl-1-methylcyclohexene (95%) by Chempur (Karlsruhe, Germany). Helium (5.0) as well as hydrogen (5.0) were purchased from Praxair (Düsseldorf, Germany) and nitrogen (5.0) from Air Liquide (Düsseldorf, Germany). All purity specifications represent the respective minimum.

Fungi. Fruiting bodies of CMU (Figure 1) were collected from spruce deadwood in the Black Forest National Park (48.56994°, 8.23752°). A cubic piece of the fruiting body was fixed to the lid of a *Petri* dish containing malt yeast peptone (MYP) agar [7 g malt extract, 0.5 g yeast extract, 1 g soy peptone, and 15 g agar per liter of ultrapure water] using vaseline. After mycelium growth was observed, a 0.5 cm × 0.5 cm overgrown agar piece was transferred to MYP agar and cultivated at 24 °C in darkness until 80% of the agar was covered with mycelium. Finally, a 0.5 cm × 0.5 cm overgrown agar piece was transferred to malt extract agar (20 g malt extract and 15 g agar per liter of ultrapure water) and kept as agar stock culture. The species was determined by its ecological, morphological, and molecular (ITS-region) characteristics and confirmed as *Cystostereum murrayi* (DSM no. 112590). *Pleurotus sapidus* (DSM no. 8266) was obtained from the German Collection of Microorganisms and Cell Cultures (Brunswick, Germany) and kept on malt extract (ME) agar as stock cultures.

Figure 1. Fruiting body of *Cystostreum murrayi* in the Black forest National Park on coniferous deadwood (Image: Flavius Popa).

Cultivation. For the submerged cultivation of CMU, a standard nutrition solution (SNS) according to Fraatz et al.[14] was used, containing L-asparagine monohydrate (4.5 g), potassium dihydrogen phosphate (1.5 g), magnesium sulfate monohydrate (0.5 g), yeast extract (3.0 g), trace element solution (1 mL; $CuSO_4 \cdot 5\ H_2O$ (5 mg L^{-1}), EDTA (400 mg L^{-1}), $FeCl_3 \cdot 6\ H_2O$ (80 mg L^{-1}), $MnSO_4 \cdot H_2O$ (30 mg L^{-1}), and $ZnSO_4 \cdot 7\ H_2O$ (90 mg L^{-1})), and D-glucose monohydrate (30 g) (pH 6.0; respective compound per liter of ultrapure water) was separately autoclaved. For elucidation of the biochemical pathways, a modified SNS solution (SNS$^+$) was used in which 50% of D-glucose was substituted by 2-^{13}C-D-glucose.

For precultures, a 0.5 cm × 0.5 cm piece of an 80% overgrown ME agar stock culture was transferred to an Erlenmeyer flask containing the respective autoclaved medium (40% filling volume of the flask, v/v) and homogenized at 10,000 rpm for 30 s by means of an Ultra-Turrax T25 homogenizer (IKA, Staufen, Germany). Cultivation of precultures was carried out at 24 °C in darkness for 22 days on a rotary shaker (Orbitron, Infors, Einsbach, Germany) at 150 rpm (25 mm shaking diameter). For the inoculation of main cultures, two precultures were homogenized (Ultra-Turrax; 10,000 rpm, 30 s), pooled, and added to the main culture (ratio 1:10, v/v) containing the same autoclaved medium as used for the preculture. Cultivation was carried out under the same conditions as for the precultures for 11 days (ADA) or 21 days. PSA was cultivated in a malt extract peptone (MEP) medium as reported previously.[15]

Preparation of Samples for Sensory Analysis, ADA, and Semiquantitative Analysis. For ADA, sensory analysis, and semiquantitation, the culture medium was separated from the mycelium of CMU by centrifugation (3000*g*, 10 min, and 4 °C). Afterward, 2.5 mL of the supernatant was transferred to autoclaved headspace vials (20 mL) under sterile conditions, sealed with a silicon/PTFE screw cap, and stored at −20 °C until further use.

Sensory Analysis. Sensory analysis of the CMU culture supernatant was performed with a trained panel (n = 8). Main culture supernatants from days 1 to 21 were harvested every second day as described above from the same main culture and analyzed by orthonasal smelling. The samples were ranked according to their sweetish and coconut-like aroma.

Dynamic Headspace Extraction and ADA. For ADA, dynamic headspace (DHS) was used as extraction technique. Culture supernatants stored at −20 °C in headspace vials (20 mL) were thawed for 20 min at 22 °C. Afterward, DHS extraction was accomplished by means of a GERSTEL DHS module (GERSTEL, Mülheim an der Ruhr, Germany) connected to a MultiPurpose Sampler robotic (MPS robotic; GERSTEL). The samples were incubated in the DHS module for 10 min at 30 °C and 500 rpm agitator speed. For extraction, the analytes (30 °C sample temperature) were purged with 750 mL of nitrogen at a flow rate of 50 mL min^{-1} and trapped at 30 °C on an adsorbent tube packed with TenaxTA. The transfer line temperature of the DHS module was kept at 150 °C. An additional dry purge step of the adsorbent tubes was performed with 500 mL of nitrogen at a flow rate of 100 mL min^{-1} and an adsorbent tube temperature of 30 °C. Adsorbent tubes were subsequently desorbed in a Thermal Desorption Unit 2 (TDU; GERSTEL) and cryofocused in a Cold Injection System 4 (CIS) (GERSTEL) equipped with a deactivated glass wool liner in a solvent-vent mode. The TDU temperature was kept for 0.5 min at 40 °C, then raised at 120 °C min^{-1} to 250 °C, and held for 12 min. For cryofocusing, CIS was held for 0.5 min at −70 °C and raised at 12 °C s^{-1} to 250 °C (5 min hold time). For aroma dilution analysis, split ratios in TDU and CIS were varied, as reported previously.[4,16]

Gas Chromatography−Mass Spectrometry−Olfactometry (GC−MS−O) Analysis. For gas chromatographic analysis, an Agilent 7890B gas chromatograph connected to an Agilent 5977B mass spectrometer (Agilent Technologies, Waldbronn, Germany) was used. The system was equipped with a TDU and a CIS (GERSTEL;

https://doi.org/10.1021/acs.jafc.1c01478
J. Agric. Food Chem. 2021, 69, 5997−6004

parameters cf. dynamic headspace extraction and aroma dilution analysis). As a polar column, an Agilent VF-WAXms [30 m × 0.25 mm; 0.25 μm film thickness; temperature program, 40 °C (3 min), heating to 240 °C (12 min) with 5 °C min^{-1}; carrier gas, helium (1.56 mL min^{-1}, constant flow)] was used. Chromatographic separation on a nonpolar column was carried out on an Agilent DB-5 ms column [30 m × 0.25 mm; 0.25 μm film thickness; temperature program, 40 °C (3 min), heating to 320 °C (12 min) with 5 °C min^{-1}; carrier gas, helium (1.56 mL min^{-1}, constant flow)]. After the GC column, the carrier gas flow was split 1:1 by means of a μFlowManager Splitter (GERSTEL) into the mass spectrometer [transfer line temperature, 250 °C; electron ionization energy, 70 eV; ion source temperature, 230 °C; quadrupole temperature, 150 °C; scan range, m/z 33−300] and to a GERSTEL Olfactory Detection Port 3 (ODP) [transfer line temperature, 300 °C; mixing chamber temperature, 200 °C; mixing chamber gas, nitrogen].

Compound Identification. For identification of perceived odor-active compounds in the culture supernatant of CMU, the obtained mass spectra and the retention indices (RI) calculated according to van den Dool and Kratz[17] on two columns of different polarities were compared to the published data and the National Institute of Standards and Technology (NIST) 2011 MS library. Commercially available standards were used for further identification, if possible.

Isolation of Aroma Compounds by Liquid−Liquid Extraction, Purification, and Identification. For odor-active compounds that could not be identified by the procedures described above, the supernatant of the main culture (21 days) was extracted by means of liquid−liquid extraction (ratio 9:4, v/v) using distilled *n*-pentane/diethyl ether (1:1, v/v). Extraction was carried out in a shaking flask on a magnetic stirrer for 30 min at 250 rpm. After extraction, the mixture was kept for 30 min in an ultrasonic bath. The phases were separated and the extraction procedure was repeated twice with the aqueous phase. The combined organic phases were dried over anhydrous sodium sulfate and concentrated using a Vigreux column (water bath temperature, 43 °C) to a final volume of about 2 mL. The extract was subsequently purified by means of preparative HPLC. Therefore, a YL9110S HPLC system (Young Lin, Anyang, South Korea) with a quaternary pump [flow rate 15 mL min^{-1}; isocratic *n*-hexane and isopropyl alcohol, 99.6/0.4, v/v], equipped with a polar Macherey Nagel Nucleodur 100−5 column (guard column 10 × 16 mm, preparative column 250 × 21 mm) (Düren, Germany) was used. Detection was accomplished by an YL9120S ultraviolet/visible (UV/VIS) detector (Young Lin; detection wavelength of 230 and 265 nm) and fractionation by a CHF 112SC fraction collector (Advantec, Dublin, CA, USA). After preparative separation, further purification was performed by means of column chromatography (silica gel 60) with distilled *n*-pentane/diethyl ether (90:10, v/v) as an eluent. The structures of the aroma compounds were elucidated by means of GC−MS, electrospray ionization time of flight−mass spectrometry (ESI−TOF−MS) and nuclear magnetic resonance (NMR).

Accurate masses were determined by means of a Bruker Daltonics MicrOTOF (Bremen, Germany) using direct infusion (82 μL h^{-1}) after dilution of the isolated aroma compounds in methanol. ESI in a positive mode (spray voltage, 4500 V; dry heater, 180 °C; dry gas, 4 L min^{-1}; nebulizer, 0.4 bar) was used for ionization. The mass detector was operated in a scan mode (scan range, m/z 50−1200) and calibrated using a sodium formate solution. Data analysis was carried out by means of Bruker Daltonics DataAnalysis 3.4 software.

For NMR experiments (^{1}H NMR, ^{13}C NMR, DEPT 135, ^{1}H, ^{1}H correlation spectroscopy (COSY), heteronuclear single-quantum correlation (HSQC), heteronuclear multiple-bond correlation (HMBC), and Nuclear Overhauser Effect spectroscopy (NOESY)) with $CDCl_3$ as solvent, a Bruker Avance III 600 MHz (Rheinstetten, Germany) was used.

Extraction of Reference Compounds. Extraction of dried dill leaves (10 g) and linden blossom honey (295 g) was carried out using PTFE beakers. Dill leaves were extracted twice using 200 mL *n*-pentane/diethyl ether (1:1, v/v) on a magnetic stirrer at 250 rpm for 45 min. After separation of the extracted dill leaves, the extract was concentrated using a Vigreux column (water bath temperature, 43 °C) and purified by means of column chromatography (silica gel 60) with distilled *n*-pentane/diethyl ether (90:10, v/v) as the eluent. Linden honey was dissolved in 500 mL sodium chloride solution (200 g L^{-1}) and extracted using 200 mL *n*-pentane/diethyl ether (1:1, v/v) as described before. Extraction was repeated twice and the combined organic phases were dried over anhydrous sodium sulfate. After separation of sodium sulfate by filtration, the extract was concentrated using a Vigreux column (water bath temperature, 43 °C) to a final volume of about 2 mL. Supernatants of PSA (fourth day of main culture) were extracted as described above for CMU and concentrated to a final volume of approximately 2 mL by means of a Vigreux column.

Enantioselective Multidimensional GC−MS (Enantio−MDGC−MS). Enantioselective analyses were carried out by means of an MDGC system consisting of two Shimadzu GC-2010 Plus gas chromatographs (GC 1 and GC 2) (Shimadzu Europa, Duisburg, Germany), connected via a Multi Deans Switch (MDS) for the selective transfer of analytes from the achiral (GC 1) to the chiral (GC 2) column. GC 1 was equipped with a Shimadzu AOC-20i autosampler, a polar column [Agilent VF-WAXms; 30 m × 0.25 mm; 0.25 μm film thickness; temperature program, 40 °C (3 min), heating to 220 °C (9 min) with 10 °C min^{-1}; carrier gas, helium (191.2 kPa, constant pressure); linear velocity, 25 cm s^{-1}], a split/splitless inlet [250 °C; split ratio range, 2:1−40:1; injection volume, 1 μL], a flame ionization detector (FID) [250 °C; H_2, 40 mL min^{-1}; air flow, 400 mL min^{-1}; N_2 make up gas, 30 mL min^{-1}], and the MDS (switching pressure, 116.7 kPa). Transfer line temperature between GC 1 and GC 2 was set to 200 °C. The second GC was equipped with a chiral column [Macherey Nagel; Hydrodex ß-TBDac; 25 m × 0.25 mm; temperature program, 40 °C (0.25 min), heating to 65 °C (30 min) with 20 °C min^{-1}, heating to 85 °C (20 min) with 5 °C min^{-1}; linear velocity, 45 cm s^{-1}] and a Shimadzu QP2010 Ultra mass spectrometer [transfer line temperature, 250 °C; electron ionization energy, 70 eV; ion source temperature, 200 °C; quadrupole temperature, 150 °C; scan range, m/z 33−300]. Data analysis was performed using Shimadzu GCMSsolution version 2.72 and for mass spectra comparison NIST 2011 MS library was used.

Semiquantitative Analysis. For semiquantitative determination of selected aroma compounds, 2.5 mL of the CMU culture supernatant (culture day 11) was extracted using 2.0 mL distilled *n*-pentane/diethyl ether (1:1.12, v/v) using a rotary incubator (Stuart, Stone, UK) at 40 rpm for 10 min. Prior to extraction, 100 μL of an internal standard solution (mint lactone, 0.59 mg mL^{-1}) dissolved in distilled *n*-pentane/diethyl ether (1:1.12, v/v) was added to the supernatant. The organic layer was separated by centrifugation (3000*g*, 10 min, and 4 °C), dried over anhydrous sodium sulfate, and analyzed by GC−MS.

Statistics. ADA was performed with three persons (two males and one female, ages between 24 and 26 years). Given FD factors represent the respective median. Semiquantitative determination of the selected aroma compounds was performed in triplicate.

■ RESULTS AND DISCUSSION

Submerged Cultivation and Sensory Analysis of CMU. To identify the aroma compounds responsible for the coconut-like aroma of CMU, the fungus was cultivated submerged. During the cultivation in SNS medium, an intense coco aroma was perceived. The cultivation of CMU in MEP medium resulted in a comparable aroma but with a lower intensity. For the determination of the culture day on which the fungus produced the most intense coconut-like odor, a sensory panel evaluated the supernatant by orthonasal smelling. The overall aroma was described as sweetish, coconut-like, and buttery. Based on these results, culture day 11 was chosen for ADA.

ADA and Identification of Key Aroma Compounds. Aroma extract dilution analysis (AEDA) using liquid extracts is a well-known technique that has been widely used in aroma

https://doi.org/10.1021/acs.jafc.1c01478
J. Agric. Food Chem. 2021, 69, 5997−6004

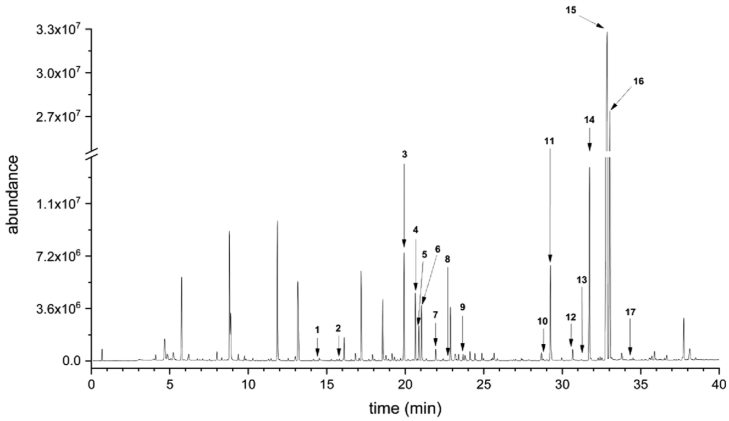

Figure 2. GC−MS chromatogram (VF-WAXms) from the DHS extraction of the CMU culture supernatant on culture day 11 (split ratio 4:1).

Table 1. Flavor Dilution (FD) Factors of Perceived Aroma Compounds in the Culture Supernatant of CMU by Means of DHS Extraction

		RI_{polar} VF-WAXms		$RI_{nonpolar}$ DB-5MS				
no.	compound	sample	standard	sample	standard	perceived odor impression	FD factor	identification[a]
1	oct-1-en-3-one	1307	1304	989	977	mushroom	128	MS, RI, STD
2	ni[b]	1357				floral	4	
3	3,6-dimethyl-2,3,3a,4,5,7a-hexahydrobenzofuran (dill ether)[c]	1522	1512	1190	1187	tarragon, herbaceous, floral	4	MS, RI
4	linalool	1551	1551	1102	1103	floral, sweetish	64	MS, RI, STD
5	4-acetyl-1-methylcyclohexene	1560	1558	1144	1134	sweetish, coconut	8	MS, RI, STD
6	3,9-epoxy-*p*-mentha-1,8(10)-diene[d]	1569	1561	1193	1189	floral	32	MS, RI
7	3,6-dimethyl-2,3,3a,4,5,7a-hexahydrobenzofuran (dill ether)[c]	1603	1598	1235	1233	earthy, cabbage	32	MS, RI
8	ni	1640		1209		cress	4	
9	3-methylbutanoic acid	1680	1673	858	849	cheesy, pungent	32	MS, RI, STD
10	2-phenylethan-1-ol	1920	1912	1118	1109	floral, rose	16	MS, RI, STD
11	*p*-menth-1-en-9-ol[e]	1942	1934	1302	1298	sweetish, coconut	64	MS, RI, STD
12	ni	2015				sweetish, cream, coconut	128	
13	ni	2037				sweetish, honey	16	
14	3,6-dimethyl-3a,4,5,6,7,7a-hexayhydro-3*H*-1-benzofuran-2-one	2067		1399		coconut, sweetish	≥262,144	MS, NMR, HRMS
15	3,6-dimethyl-3a,4,5,6,7,7a-hexayhydro-3*H*-1-benzofuran-2-one	2125		1433		coumarin, floral	512	MS, NMR, HRMS
16	3-methylene-6-methyl-hexahydro-benzofuran-2(3*H*)-one	2134		1412		coconut	4096	MS, NMR, HRMS
17	ni	2209				herbaceous, sotolon-like	8	

[a]Identification by comparison of the measured MS spectra with the NIST database (MS), comparison of the calculated retention indices with the published data on a polar and a nonpolar column (RI), comparison of retention indices and MS spectra with authentic standards (STD), and by means of NMR and HRMS after isolation of the respective compound. [b]ni, not identified. [c]For the identification, an extract of linden blossom honey was used. [d]No standard commercially available, RI published.[4] [e]The standard was synthesized; NMR data have been published.[15]

analysis. Hereby, the original extract is diluted stepwise in an appropriate solvent and analyzed by means of GC−O.[18] The highest dilution factor at which a compound can still be perceived is indicated as the flavor dilution (FD) factor.[19] Because AEDA cannot be used for solvent-free extraction techniques, such as solid phase microextraction (SPME) and stir bar sorptive extraction (SBSE), the so-called ADA has been developed. The use of solvent-free extraction methods such as HS-SPME[5] and SBSE[4,16] for the implementation of ADA has already been reported. The dilution of the sample was thereby achieved by variation of the split ratio in the injection system of the GC. In the current study this approach was successfully transferred to solvent-free dynamic headspace extraction and applied to culture supernatants of CMU (Figure 2).

Starting with a split ratio of 4:1, a total of 17 odor-active compounds were perceived in the sample that were not present in the medium blank. FD factors varied from FD = 4 up to FD ≥ 262,144. The determination of higher FD factors (>262,144) was not possible due to limited split capacities in the TDU and the CIS (maximum split ratio of 512 each). Compound identification was achieved by the comparison of the obtained mass spectra and the calculated RI measured on

https://doi.org/10.1021/acs.jafc.1c01478
J. Agric. Food Chem. 2021, 69, 5997−6004

two columns of different polarities with the literature and, if available, with authentic standards. The perceived odor impressions were compared to those described in the literature (Table 1).

Among the identified compounds in the submerged culture was the aliphatic carbonyl oct-1-en-3-one (**1**, FD 128) and the carboxylic acid 3-methylbutanoic acid (**9**, FD 32). Oct-1-en-3-one is known as a typical C8 hydrocarbon with a mushroom-like odor which is formed due to enzymatic oxidation of fatty acids[20] and has been described for several basidiomycota.[4,21−23] The unpleasant smelling substance 3-methylbutanoic acid is known as a degradation product of leucine in plants and can also be formed by different bacteria, yeasts, and mushrooms.[22,23]

As an aromatic compound, the floral and rose-scented 2-phenylethan-1-ol was identified (**10**, FD 16). The substance can be biosynthesized starting from phenylalanine via the Ehrlich and cinnamate pathways as described for different yeasts and bacteria.[24,25] Furthermore, the formation of the compound has been reported for numerous white-rot fungi, such as *Bjerkandera adusta*, *Phlebia radiata*, and *Trametes suaveolens*, most probably as a degradation product of the lignin metabolism.[26−28]

The majority of the identified odor-active compounds comprised terpenoids. One of those was the acyclic monoterpenoid linalool (**4**, FD 64), which possesses a floral odor. Linalool occurs naturally in over 200 different plant species, e.g., in herbs such as basil, coriander, marjoram, and laurel.[29] Nevertheless, the formation of linalool has also been reported for several fungi.[5,30] The sweetish and coconut-like odor of **5** (FD 8) was assigned to the unusual C9 hydrocarbon 4-acetyl-1-methylcyclohexene. As a degradation product of limonene, the compound is mainly produced chemically during ozonolysis.[31] However, the biosynthesis has been previously described for PSA grown in submerged culture.[4] To the best of our knowledge, in addition to this no further occurrence in basidiomycota has been reported so far.

By comparison of the obtained mass spectra and the calculated RI with the literature data, the floral odor perceived for **6** (FD 32) was assigned to 3,9-epoxy-*p*-mentha-1,8(10)-diene. Wardencki et al. described the odor of this compound as fruity, herbal, and dill-like whereas Trapp et al. reported it to be anisic and tarragon-like. However, no absolute stereochemistry was given by the respective authors.[4,32] The sweetish and coconut-like odor emitted by **11** (FD 64) was assigned to *p*-menth-1-en-9-ol. The compound has been described previously by Trapp et al. in the submerged cultures of PSA and has been identified as a potential precursor in the *de novo* biosynthesis of wine lactone and dill ethers.[4,15] Interestingly, the latter substances were also detected in the cultures of CMU (**3**, FD 4 and **7**, FD 32). Further studies on the biogenesis of these compounds by fungi have, to the best of our knowledge, not been reported yet.

Due to the three stereogenic centers of the dill ethers, eight stereoisomers can theoretically be formed (Figure 3). However, the stereoisomers with a *trans*-connection in the tetrahydrofuran ring system are unlikely to be biosynthesized via natural pathways due to the resulting ring strain.[33] The odor impressions of the four *cis*-stereoisomers vary from a characteristic dill-like odor (**3a**) to rather herbal, flowery, tarragon-like, sweet, and minty odors (**3b**, **7c**, and **7d**).[4,34] Natural sources for dill ethers are dill for enantiopure **3a** and different honey varieties for all four *cis*-isomers.[35−37] Based on

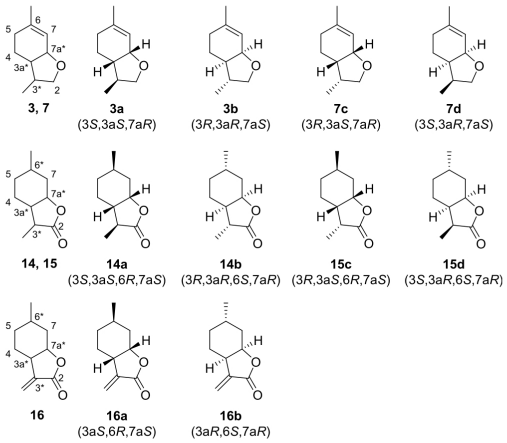

Figure 3. Structures of 3,6-dimethyl-2,3,3a,4,5,7a-hexahydrobenzofuran (**3**, **7**; dill ethers), 3,6-dimethyl-3a,4,5,6,7,7a-hexayhydro-3*H*-1-benzofuran-2-one (**14**, **15**), and the corresponding unsaturated lactone 3-methylene-6-methyl-hexahydro-benzofuran-2(3*H*)-one (**16**).

this occurrence, *n*-pentane/diethyl ether extracts of these natural sources were used as references for the analysis via MDGC. In addition, an organic extract of submerged cultivated PSA was used for enantioselective analysis (cf. Supporting Information, Figure S1). The chromatographic data indicated that CMU produced the stereoisomers **3b** and **7d** comparable to PSA, both with an enantiomeric excess (ee) of ≥99.9. This fact and also the occurrence of *p*-menth-1-en-9-ol indicated that the biosynthesis of the dill ethers may follow the same biosynthetic route as in PSA.

However, the substances with the highest FD factors (**14**, **15**, and **16**) could not be identified by comparison of the mass spectra with the NIST database. Interestingly, compounds **14** and **15** showed comparable mass spectra which indicated structural similarities. After liquid−liquid extraction and purification by means of preparative HPLC and column chromatography, the structures of substances **14** and **15** were elucidated by NMR spectroscopy as two different stereoisomers of 3,6-dimethyl-3a,4,5,6,7,7a-hexayhydro-3*H*-1-benzofuran-2-one (cf. Supporting Information S2). In contrast, compound **16** was identified as the corresponding C(3) unsaturated lactone (Figure 3). These substances showed high structural similarities compared to the dill ethers and wine lactones formed by PSA in submerged culture and only differed in the missing double bond between C(6) and C(7). Due to this fact, **14** and **15** have four stereogenic centers, which results in a total of 16 possible stereoisomers. Assuming again that the isomers with a *trans*-connection are unlikely to be formed via natural pathways,[33] eight different *cis*-stereoisomers could theoretically be formed. Indeed, employing 2D-NMR experiments confirmed the *cis*-connection of **14**/**15** and **16**. However, the absolute configuration of the lactones could not be determined by NMR spectroscopy. Gas chromatographic analysis of **15** using five different chiral stationary phase columns (Hydrodex ß-TBDac, γ-TBDac, γ-DiMOM, ß-6TBDM, and ß-PM) showed only one signal and no separation (data not shown), which suggested that only one stereoisomer

https://doi.org/10.1021/acs.jafc.1c01478
J. Agric. Food Chem. 2021, 69, 5997−6004

was present. Due to the stereospecific formation of dill ethers by CMU and PSA and the selective production of the wine lactones by PSA, a stereospecific biosynthesis of the lactones **14**/**15** and **16** seems to be likely. Compound **16** could act as a direct precursor for **14** and **15**, as the corresponding enantiomers of the saturated lactones only differ in the configuration of the methyl group at C(3). The presence of a reductase which is capable of catalyzing a respective reaction in a basidiomycota has recently been reported.[38]

Natural sources of **14**, **15**, and **16** are rarely described in the literature. For example, different stereoisomers of the saturated lactones were identified in Italo-Mitcham peppermint oil.[39,40] In contrast, several routes have been reported for the chemical synthesis, especially of the saturated lactones.[41−45] Gaudin synthesized eight of the 16 possible stereoisomers of the saturated lactones and evaluated the odor properties of these compounds.[41] For **14a**, the odor was described as coumarinic, lactonic, and weak and for **15c** as coumarinic, fatty, and weak. The perceived odor impressions were partly comparable to those described by Gaudin; however, no absolute stereochemistry was determined within this study.

Semiquantitative Analysis. The three compounds with the highest FD (**14**−**16**) were semiquantitatively analyzed after the addition of an internal standard (mint lactone) using a liquid−liquid microextraction. As all three compounds are not commercially available, a structurally similar lactone was used for semiquantitation. Compound **15**, which had the largest peak area in the DHS chromatogram, was detected with a concentration of approx. 86 mg L^{-1}. The concentrations determined for the lactones **14** (8 mg L^{-1}) and **16** (22 mg L^{-1}) were significantly lower, which was in accordance with the observed peak areas in the DHS chromatogram. As the culture media were not optimized for the growth of this fungus and aroma production, these concentrations are surprisingly high. Also, in comparison to the concentrations of dill ethers and wine lactones formed by PSA during submerged cultivation in SNS medium (<150 μg L^{-1}), the concentrations of the lactones **14**−**16** were significantly higher. The determined high FD factors could therefore be a result of the high concentrations in the supernatant. However, the FD for **14** was ≥512-fold higher than that of **15**, while the concentration was about 11-fold lower. This indicates that lactone **14** has a significantly lower odor threshold than lactone **15**. Odor thresholds of **14** and **15** in air have been reported by Buhr.[46] The thresholds varied from >100 ng L^{-1} to 7 × 10^{-6} ng L^{-1}. However, the assignment of the absolute stereochemistry in that previous study was partly incorrect and the GC−MS data differed from those reported in the literature and those determined in this study. Nevertheless, the odor threshold reported for the two isomers of **14** (1 × 10^{-6} ng L^{-1} for **14a** and >100 ng L^{-1} for **14b**) were lower compared to those of **15** (7.5 ng L^{-1} for **15c** and >100 ng L^{-1} for **15d**), which correlated well with the data of this study.

Supplementation Studies with 2-^{13}C-Glucose. In order to elucidate whether the lactones **14**−**16** and the dill ethers are formed de novo starting from D-glucose, the culture medium was supplemented with 2-^{13}C-D-glucose (SNS^{+}). The mass spectra of the respective lactones and dill ethers all showed mass shifts of m/z +1, +2, and +3. For example, the mass spectrum of lactone **14** derived from nonlabeled glucose showed a base peak of m/z 95. Compared to the base peak, the relative intensity of m/z 96 was 22%, m/z 97 was 3%, and m/z 98 was lower than 1%. After supplementation with 50% labeled glucose, the relative intensity of m/z 96 accounted for 74%, m/z 97 for 25%, and m/z 98 for 6% of the m/z 95 base peak. It has to be mentioned that the relative abundances of the fragment ions m/z 96, 97, and 98 are mainly due to fragment ions and only represent to a minor extend the ^{13}C pattern. Except for oct-1-en-3-one, 3-methylbutanoic acid, and 2-phenylethan-1-ol, these mass shifts were observed for all other identified compounds (cf. Supporting Information, Figure S3). This indicated that the compounds were formed *de novo* in the course of the acetate-mevalonate pathway. Starting from one molecule of 2-^{13}C-D-glucose, one molecule each of labeled and nonlabeled acetyl-CoA is formed as a result of glycolysis. Three molecules of acetyl-CoA are then transformed to one molecule of isopentenyl pyrophosphate (IPP), whereby one molecule of CO_2 is split off. Thus, two ^{13}C labels are theoretically possible within one IPP-molecule und therefore up to four ^{13}C labels in monoterpenes.[47]

■ ASSOCIATED CONTENT

Supporting Information

The Supporting Information is available free of charge at https://pubs.acs.org/doi/10.1021/acs.jafc.1c01478.

S1: Chiral separation of dill ethers stereoisomers;

S2: ^{13}C and ^{1}H NMR spectra, NMR, GC−MS, and HRMS data of lactones **14**, **15**, and **16**;

S3: GC−MS data of the identified aroma compounds within labeling studies using 2-^{13}C-D-glucose and references; and

S4: ITS sequence of *Cystostereum murrayi* (PDF)

■ AUTHOR INFORMATION

Corresponding Author

Holger Zorn − *Institute of Food Chemistry and Food Biotechnology, Justus Liebig University Giessen, Giessen 35392, Germany; Fraunhofer Institute for Molecular Biology and Applied Ecology, Giessen 35392, Germany;* orcid.org/0000-0002-8383-8196; Phone: +49. (0).641.99.349-00; Email: holger.zorn@uni-giessen.de

Authors

Fabio F. Brescia − *Institute of Food Chemistry and Food Biotechnology, Justus Liebig University Giessen, Giessen 35392, Germany*

Wassilios Pitelas − *Institute of Food Chemistry and Food Biotechnology, Justus Liebig University Giessen, Giessen 35392, Germany*

Suzan Yalman − *Institute of Food Chemistry and Food Biotechnology, Justus Liebig University Giessen, Giessen 35392, Germany*

Flavius Popa − *Black Forest National Park, Seebach 77889, Germany*

Heike G. Hausmann − *Institute of Organic Chemistry, Justus Liebig University Giessen, Giessen 35392, Germany*

Raffael C. Wende − *Institute of Organic Chemistry, Justus Liebig University Giessen, Giessen 35392, Germany;* orcid.org/0000-0002-2242-4723

Marco A. Fraatz − *Institute of Food Chemistry and Food Biotechnology, Justus Liebig University Giessen, Giessen 35392, Germany;* orcid.org/0000-0002-5028-9653

Complete contact information is available at: https://pubs.acs.org/10.1021/acs.jafc.1c01478

https://doi.org/10.1021/acs.jafc.1c01478
J. Agric. Food Chem. 2021, 69, 5997−6004

Notes

The authors declare no competing financial interest.

■ ACKNOWLEDGMENTS

This project has partially been financed with funds of LOEWE – Landes-Offensive zur Entwicklung Wissenschaftlich-ökonomischer Exzellenz-AromaPlus (State Offensive for the Development of Scientific and Economic Excellence). Special thanks go to Dr. Markus Scholler from the Natural History Museum Karlsruhe and the project group "A mycological inventory of the Bannwald Wilder See – Hornisgrinde" for the contribution of the fungus and the culture of *Cystostereum murrayi*.

■ ABBREVIATIONS USED

ADA, aroma dilution analysis; CIS, cold injection system; CMU, *Cystostereum murrayi*; DHS, dynamic headspace; ee, enantiomeric excess; FD, flavor dilution; ME, malt extract; MYP, malt yeast peptone; O, olfactometry/olfactometric; ODP, olfactory detection port; PSA, *Pleurotus sapidus*; RI, retention index/indices; SNS, standard nutrition solution; TDU, thermal desorption unit.

■ REFERENCES

(1) Paula Dionísio, A.; Molina, G.; Souza de Carvalho, D.; dos Santos, R.; Bicas, J. L.; Pastore, G. M. Natural flavourings from biotechnology for foods and beverages. In *Natural food additives, ingredients and flavourings*; Baines, D., Seal, R., Eds. Woodhead Publishing Limited: Oxford, Philadelphia, 2012; 233; 231–259.

(2) Gressler, M.; Löhr, N. A.; Schäfer, T.; Lawrinowitz, S.; Seibold, P. S.; Hoffmeister, D. Mind the mushroom: natural product biosynthetic genes and enzymes of Basidiomycota. *Nat. Prod. Rep.* **2021**, *38*, 702–722.

(3) Lomascolo, A.; Stentelaire, C.; Asther, M.; Lesage-Meessen, L. Basidiomycetes as new biotechnological tools to generate natural aromatic flavours for the food industry. *Trends Biotechnol.* **1999**, *17*, 282–289.

(4) Trapp, T.; Zajul, M.; Ahlborn, J.; Stephan, A.; Zorn, H.; Fraatz, M. A. Submerged cultivation of *Pleurotus sapidus* with molasses: Aroma dilution analyses by means of solid phase microextraction and stir bar sorptive extraction. *J. Agric. Food Chem.* **2018**, *66*, 2393–2402.

(5) Zhang, Y.; Fraatz, M. A.; Horlamus, F.; Quitmann, H.; Zorn, H. Identification of potent odorants in a novel nonalcoholic beverage produced by fermentation of wort with shiitake (*Lentinula edodes*). *J. Agric. Food Chem.* **2014**, *62*, 4195–4203.

(6) Ziegenbein, F. C.; Hanssen, H.-P.; König, W. A. Chemical constituents of the essential oils of three wood-rotting fungi. *Flavour Fragr. J.* **2006**, *21*, 813–816.

(7) Berkeley, M. J.; Curtis, M. A. Fungi cubenses (*Hymenomycetes*). *Bot. J. Linn. Soc.* **1868**, *10*, 321–341.

(8) Pouzar, Z. New genera of higher fungi III. *Česká Mykologie* **1959**, *13*, 10–19.

(9) Eriksson, J.; Ryvarden, L. *The Corticiaceae of North Europe: Volume 3: Coronicium - Hyphoderma*; Fungiflora: Oslo, 1975.

(10) Bernicchia, A.; Savino, E.; Pérez Gorjon, S. Aphyllophoraceous wood-inhabiting fungi on Pinus spp. in Italy. *Mycotaxon* **2007**, *101*, 185–188.

(11) Dämon, W.; Krisai-Greilhuber, I. *Die Pilze Österreichs*; Österreichische Mykologische Gesellschaft: Wien, 2017.

(12) http://www.pilze-deutschland.de/organismen/cystostereum-murrayi-berk-ma-curtis-pouzar-1959 (accessed Dez 14, 2020).

(13) Kramer, R.; Abraham, W.-R. Volatile sesquiterpenes from fungi: what are they good for? *Phytochem. Rev.* **2012**, *11*, 15–37.

(14) Fraatz, M. A.; Naeve, S.; Hausherr, V.; Zorn, H.; Blank, L. M. A minimal growth medium for the basidiomycete *Pleurotus sapidus* for metabolic flux analysis. *Fungal Biol. Biotechnol.* **2014**, *1*, 1–8.

(15) Trapp, T.; Kirchner, T.; Birk, F.; Fraatz, M. A.; Zorn, H. Biosynthesis of stereoisomers of dill ether and wine lactone by *Pleurotus sapidus*. *J. Agric. Food Chem.* **2019**, *67*, 13400–13411.

(16) Trapp, T.; Jäger, D. A.; Fraatz, M. A.; Zorn, H. Development and validation of a novel method for aroma dilution analysis by means of stir bar sorptive extraction. *Eur. Food Res. Technol.* **2018**, *244*, 949–957.

(17) van den Dool, H.; Kratz, P. D. A generalization of the retention index system including linear temperature programmed gas-liquid partition chromatography. *J. Chromatogr. A* **1963**, *11*, 463–471.

(18) Ullrich, F.; Grosch, W. Identification of the most intense volatile flavour compounds formed during autoxidation of linoleic acid. *Z. Lebensm. Unters. Forsch.* **1987**, *184*, 277–282.

(19) Schieberle, P.; Grosch, W. Evaluation of the flavour of wheat and rye bread crusts by aroma extract dilution analysis. *Z. Lebensm. Unters. Forsch.* **1987**, *185*, 111–113.

(20) Tasaki, Y.; Kobayashi, D.; Sato, R.; Hayashi, S.; Joh, T. Variations in 1-octen-3-ol and lipoxygenase gene expression in the oyster mushroom *Pleurotus ostreatus* according to fruiting body development, tissue specificity, maturity, and postharvest storage. *Mycoscience* **2019**, *60*, 170–176.

(21) Zhang, H.; Pu, D.; Sun, B.; Ren, F.; Zhang, Y.; Chen, H. Characterization and comparison of key aroma compounds in raw and dry porcini mushroom (*Boletus edulis*) by aroma extract dilution analysis, quantitation and aroma recombination experiments. *Food Chem.* **2018**, *258*, 260–268.

(22) Kleofas, V.; Popa, F.; Fraatz, M. A.; Rühl, M.; Kost, G.; Zorn, H. Aroma profile of the anise-like odour mushroom *Cortinarius odorifer*. *Flavour Fragr. J.* **2015**, *30*, 381–386.

(23) Wu, S.; Zorn, H.; Krings, U.; Berger, R. G. Characteristic volatiles from young and aged fruiting bodies of wild *Polyporus sulfureus* (Bull.:Fr.) Fr. *J. Agric. Food Chem.* **2005**, *53*, 4524–4528.

(24) Etschmann, M.; Bluemke, W.; Sell, D.; Schrader, J. Biotechnological production of 2-phenylethanol. *Appl. Microbiol. Biotechnol.* **2002**, *59*, 1–8.

(25) Lomascolo, A.; Lesage-Meessen, L.; Haon, M.; Navarro, D.; Antona, C.; Faulds, C.; Marcel, A. Evaluation of the potential of *Aspergillus niger* species for the bioconversion of L-phenylalanine into 2-phenylethanol. *World J. Microbiol. Biotechnol.* **2001**, *17*, 99–102.

(26) Gross, B.; Gallois, A.; Spinnler, H.-E.; Langlois, D. Volatile compounds produced by the ligninolytic fungus *Phlebia radiata* Fr. (Basidiomycetes) and influence of the strain specificity on the odorous profile. *J. Biotechnol.* **1989**, *10*, 303–308.

(27) Lapadatescu, C.; Feron, G.; Vergoignan, C.; Djian, A.; Durand, A.; Bonnarme, P. Influence of cell immobilization on the production of benzaldehyde and benzyl alcohol by the white-rot fungi *Bjerkandera adusta*, *Ischnoderma benzoinum* and *Dichomitus squalens*. *Appl. Microbiol. Biotechnol.* **1997**, *47*, 708–714.

(28) Lomascolo, A.; Asther, M.; Navarro, D.; Antona, C.; Delattre, M.; Lesage-Meessen, L. Shifting the biotransformation pathways of L-phenylalanine into benzaldehyde by *Trametes suaveolens* CBS 334.85 using HP20 resin. *Lett. Appl. Microbiol.* **2001**, *32*, 262–267.

(29) Aprotosoaie, A. C.; Hăncianu, M.; Costache, I.-I.; Miron, A. Linalool: a review on a key odorant molecule with valuable biological properties. *Flavour Fragr. J.* **2014**, *29*, 193–219.

(30) Zhang, Y.; Fraatz, M. A.; Müller, J.; Schmitz, H.-J.; Birk, F.; Schrenk, D.; Zorn, H. Aroma characterization and safety assessment of a beverage fermented by *Trametes versicolor*. *J. Agric. Food Chem.* **2015**, *63*, 6915–6921.

(31) Donahue, N. M.; Tischuk, J. E.; Marquis, B. J.; Huff Hartz, K. E. Secondary organic aerosol from limona ketone: insights into terpene ozonolysis via synthesis of key intermediates. *Phys. Chem. Chem. Phys.* **2007**, *9*, 2991–2998.

(32) Wardencki, W.; Chmiel, T.; Dymerski, T.; Biernacka, P.; Plutowska, B. Application of gas chromatography, mass spectrometry and olfactometry for quality assessment of selected food products. *Ecol. Chem. Eng. S* **2009**, *16*, 287–300.

https://doi.org/10.1021/acs.jafc.1c01478
J. Agric. Food Chem. 2021, 69, 5997–6004

(33) Reichert, S.; Mosandl, A. Stereoisomeric flavor compounds LXXXII dill ether and its stereoisomers: Synthesis and enantioselective analysis. *J. High Resol. Chromatogr.* **1999**, *22*, 631−634.
(34) Reichert, S.; Wüst, M.; Beck, T.; Mosandl, A. Stereoisomeric flavor compounds LXXXI: Dill ether and its *cis*-stereoisomers: Synthesis and enantioselective analysis. *J. High Resol. Chromatogr.* **1998**, *21*, 185−188.
(35) Blank, I.; Grosch, W. Evaluation of potent odorants in dill seed and dill herb (*Anethum graveolens* L.) by aroma extract dilution analysis. *J. Food Sci.* **1991**, *56*, 63−67.
(36) Blank, I.; Fischer, K.-H.; Grosch, W. Intensive neutral odourants of linden honey differences from honeys of other botanical origin. *Z. Lebensm. Unters. Forsch.* **1989**, *189*, 426−433.
(37) Alissandrakis, E.; Tarantilis, P. A.; Harizanis, P. C.; Polissiou, M. Aroma investigation of unifloral Greek citrus honey using solid-phase microextraction coupled to gas chromatographic-mass spectrometric analysis. *Food Chem.* **2007**, *100*, 396−404.
(38) Karrer, D.; Gand, M.; Rühl, M. Expanding the biocatalytic toolbox with a new type of ene/yne-reductasefrom *Cyclocybe aegerita*. *ChemCatChem* **2021**, *13*, 2191−2199.
(39) Näf, R.; Velluz, A. Phenols and lactones in Italo-Mitcham peppermint oil *Mentha* × *piperita* L. *Flavour Fragr. J.* **1998**, *13*, 203−208.
(40) Takahashi, K.; Someya, T.; Muraki, S.; Yoshida, T. A new keto-alcohol, (−)-mintlactone, (+)-*iso*-mintlactone and minor components in peppermint oil. *Agric. Biol. Chem.* **1980**, *44*, 1535−1543.
(41) Gaudin, J.-M. Synthesis and organoleptic properties of *p*-menthane lactones. *Tetrahedron* **2000**, *56*, 4769−4776.
(42) Chavan, S. P.; Zubaidha, P. K.; Dhondge, V. D. A short and efficient synthesis of (−)-mintlactone and (+)-isomintlactone. *Tetrahedron* **1993**, *49*, 6429−6436.
(43) Carda, M.; Marco, J. A. Total synthesis of the monoterpenes (−)-mintlactone and (+)-isomintlactone. *Tetrahedron* **1992**, *48*, 9789−9800.
(44) Serra, S.; Nobile, I. Chemoenzymatic preparation of the *p*-menth-1,5-dien-9-ol stereoisomers and their use in the enantiospecific synthesis of natural *p*-menthane monoterpenes. *Tetrahedron: Asymmetry* **2011**, *22*, 1455−1463.
(45) Friedrich, D.; Bohlmann, F. Total synthesis of various elemanolides. *Tetrahedron* **1988**, *44*, 1369−1392.
(46) Buhr, K. *Untersuchung zu Struktur-Wirkungsbeziehungen von Lactonen*. Dissertation, Bergische Universität Wuppertal, Wuppertal, 2006.
(47) Eichinger, D.; Bacher, A.; Zenk, M. H.; Eisenreich, W. Analysis of metabolic pathways via quantitative prediction of isotope labeling patterns: a retrobiosynthetic ^{13}C NMR study on the monoterpene loganin. *Phytochemistry* **1999**, *51*, 223−236.

https://doi.org/10.1021/acs.jafc.1c01478
J. Agric. Food Chem. 2021, 69, 5997−6004

4. **Chapter:** Chiral analysis and biosynthetic studies on benzofuran derivatives

Structure elucidation of aroma-active bicyclic benzofuran derivatives formed by *Cystostereum murrayi*

Brescia, F. F.; Koch, M.; Wende, R. C.; Schreiner, P. R.; Zorn, H.; Fraatz, M. A.

J. Agr. Food Chem. **2023**, *71* (20), 7744–7751.

https://doi.org/10.1021/acs.jafc.3c01807

JOURNAL OF AGRICULTURAL AND FOOD CHEMISTRY

pubs.acs.org/JAFC Article

Structure Elucidation of Aroma-Active Bicyclic Benzofuran Derivatives Formed by *Cystostereum murrayi*

Published as part of the Journal of Agricultural and Food Chemistry virtual special issue "BIOFLAVOUR 2022 - Biotechnology of Flavours, Fragrances, and Functional Ingredients".

Fabio F. Brescia, Maximilian Koch, Raffael C. Wende, Peter R. Schreiner, Holger Zorn, and Marco A. Fraatz*

Cite This: *J. Agric. Food Chem.* 2023, 71, 7744–7751 Read Online

ACCESS | Metrics & More | Article Recommendations | Supporting Information

ABSTRACT: Among the monoterpenoid aroma compounds formed by the basidiomycete *Cystostereum murrayi* are highly potent bicyclic benzofuran derivatives. In addition to the dill ethers previously described in a few fungi, two stereoisomers of the rare 3,6-dimethyl-3a,4,5,6,7,7a-hexahydro-3*H*-1-benzofuran-2-one (**1a** and **2c**), also known as dihydromenthofurolactones, and a C3-unsaturated analogue (**3a**) are formed by *C. murrayi*. The analysis of synthesized reference standards of the lactones allowed an unambiguous assignment of the stereoisomers formed by the fungus. Despite a similar structure, two key differences in the stereochemistry of the lactones and dill ethers emerged. The analysis of submerged cultures further revealed the formation of additional, so far unknown, fungal terpenoids, including limonen-10-ol (**7**) and the corresponding aldehyde limonen-10-al (**8**). Analysis of chiral terpenoids as well as supplementation studies, including stable isotope-labeled compounds, indicated independent biogenesis pathways for dill ethers and lactones.

KEYWORDS: *chirality, Cystostereum murrayi, dihydromenthofurolactones, dill ether, flavoring substances*

INTRODUCTION

Terpenes represent one of the largest groups of naturally occurring substances, with thousands of known compounds to date.[1,2] In fungi, terpenes are biosynthesized *via* the precursors dimethylallyl diphosphate and isopentenyl diphosphate, the products of the so-called acetate mevalonate pathway.[3] The linkage of several units of these precursors followed by further reactions, such as cyclization and rearrangement, results in an enormous diversity of substances.[4] Of particular relevance as aroma compounds are monoterpenes, derived from two C_5-units, sesquiterpenes, which are composed of three C_5-units, as well as the respective terpenoids.[5] In addition to numerous well-known compounds, such as linalool, menthol, or carvone, bicyclic 3,6-dimethylbenzofuran derivatives represent a highly interesting subgroup of terpenoids due to their interesting odor impressions and, in some cases, exceptionally low odor thresholds.[6−9]

Dill ethers represent a prominent group of benzofuran derivatives, which have been known for many years as key aroma compounds of the eponymous herbs.[10] Structure elucidation of the eight possible stereoisomers resulting from three stereogenic centers, has been an analytical challenge.[11] A second subgroup is formed by the stereoisomers of the so-called wine lactone, first discovered in the urine of koalas in 1975.[12] Later, the 3*S*,3a*S*,7a*R*-isomer was described in Gewürztraminer wine, and it possessed an extremely low odor threshold.[6] Linden ether, described in linden honey with floral and mint-like odors,[13,14] as well as menthofurolactones, which occur in mint species,[15] are also assigned to the class of bicyclic benzofuran derivatives. Besides, the so-called dihydromenthofurolactones as well as their C3-unsaturated derivates (Δ^3-dml) have recently been described in submerged cultures of the basidiomycete *Cystostereum murrayi*.[8] The fungus was isolated from spruce deadwood (48.56994°, 8.23752°) in the Black Forest National Park and cultured as a wild-type species. The identified diastereoisomers thereby imparted coconut-, coumarin-, and floral-like odors. Apart from mint oil and fresh mint leaves, further natural sources have not been described for the latter compounds.[16,17] Due to the presence of four and three stereogenic centers, respectively, an unambiguous structural elucidation has not yet been achieved for naturally occurring isomers.

The aim of this study was to elucidate the absolute stereochemistry of the dihydromenthofurolactones formed by *C. murrayi* and potential precursors by enantioselective multidimensional gas chromatography (MDGC) in conjunction with authentic standards. Therefore, several terpenoids, including two stereoisomers of Δ^3-dml, were synthesized. In order to clarify the biosynthetic routes toward the benzofuran derivatives, supplementation studies with labeled (deuterium and ^{13}C) and unlabeled terpenoids were performed.

Received: March 21, 2023
Revised: April 27, 2023
Accepted: May 1, 2023
Published: May 12, 2023

https://doi.org/10.1021/acs.jafc.3c01807
J. Agric. Food Chem. 2023, 71, 7744−7751

MATERIALS AND METHODS

Chemicals. Chemicals for the cultivation of *C. murrayi* were purchased from AppliChem (Darmstadt, Germany), Carl Roth (Karlsruhe, Germany), Sigma-Aldrich (Taufkirchen, Germany), and Th. Geyer (Hamburg, Germany). Diethyl ether (99.5%), purchased from BCH Bruehl-Chemikalien Handel (Bruehl, Germany), and *n*-pentane (99%), from Th. Geyer, for liquid−liquid extraction, were distilled prior to use. Chloroform-*d* (99.8%) for NMR experiments, $^{13}C_6$-D-glucose (99%), as well as mint lactone (99%) and (*R*)-linalool (95%) were supplied by Sigma-Aldrich. (*R*)-Limonene (97%) and (*S*)-limonene (97%) were obtained from Alfa Aesar (Kandel, Germany). (*R*/*S*)-linalool (97%) and ethanol (99%) were purchased from Acros Chemicals B.V.B.A (Geel, Belgium). Labeled *rac*-^{13}C-D_2-limonene was supplied by aromaLab GmbH (Martinsried, Germany). Helium (5.0) and hydrogen (5.0) were purchased from Praxair (Düsseldorf, Germany) and nitrogen (5.0) from Air Liquide (Düsseldorf, Germany). Chemicals used for synthesis and their purities are listed in Supporting Information S1. All purity specifications represent the respective minimum.

Synthesis. Synthetic procedures for lactones (**3**), (*R*/*S*)-limonen-10-ol (**7**), and (*R*/*S*)-limonen-10-al (**8**) are described in detail in Supporting Information S1. In general, lactones were synthesized starting from (+)- or (−)-isopulegol, whereas limonene derivatives were synthesized starting from (*R*)- or (*S*)-limonene. NMR analyses of the synthesized products (^{1}H NMR and ^{13}C NMR) were performed in $CDCl_3$ as a solvent on Bruker Avance II 400 MHz or Avance III 400 MHz HD (Rheinstetten, Germany) spectrometers.

Cultivation. *Cystostereum murrayi* (DSM no. 112590) was cultivated on malt extract agar plates and submerged in pre- and main-cultures in Erlenmeyer flasks (40% filling volume) as described previously.[8] Standard nutrition solution (SNS) according to Fraatz *et al.*[18] was used as liquid culture medium. For slant agar cultivation, sterile headspace vials (20 mL) were filled with 4 mL of autoclaved SNS agar (containing 15 g L^{-1} agar in ultrapure water) and placed in slant racks (30°) for solidification. For inoculation, a cylindrical piece (6.25 mm in diameter) of 80% overgrown malt extract stock culture was transferred to the slant agar and cultivated at 24 °C in darkness. Labeling studies were performed using $^{13}C_6$-D-glucose instead of D-glucose (SNS^+).

Supplementation Studies. Supplementation studies were performed in submerged cultures or slant agar. For the supplementation in liquid SNS, main-cultures of *C. murrayi* were inoculated on the 5th culture day under sterile conditions with (*R*)-limonene, (*S*)-limonene, ^{13}C-D_2-limonene, (*R*)-linalool, (4*R*,8*RS*)-*p*-menth-1-en-9-ol, (4*S*,8*RS*)-*p*-menth-1-en-9-ol, (*R*)- and (*S*)-limonen-10-ol, as well as (*S*)-limonen-10-al with a final concentration of 1 mM (referred to the main-culture volume of 220 mL). All supplements were dissolved in 1 mL of ethanol prior to supplementation. Biological controls were cultivated in parallel with the addition of 1 mL of ethanol. Cultivation was continued for 6 d (a total cultivation time of 11 d) after supplementation, and the cultures were subsequently extracted. Slant agar cultures containing SNS^+ were cultivated for 14 d.

Stir Bar Sorptive Extraction, Dynamic Headspace Extraction, and Solid Phase Microextraction. Main cultures were centrifuged at 3000*g* for 10 min (4 °C) on the 11th culture day in order to separate the mycelium from the supernatant. Afterward, 2.5 mL of the supernatant was transferred to sterile headspace vials (20 mL), sealed with silicone/polytetrafluoroethylene (PTFE) screw caps, and stored at −20 °C. Prior to stir bar sorptive extraction (SBSE) using 10 mm Twister stir bars (0.5 mm PDMS coating; GERSTEL, Mülheim an der Ruhr, Germany), the samples were thawed at 4 °C, and 100 μL internal standard solution (mint lactone, 2.45 mg mL^{-1}) dissolved in ultrapure water was added. SBSE extraction was conducted for 30 min and 1000 rpm at 4 °C. Afterward, the stir bars were rinsed with ultrapure water, dried with lint-free tissues, and used for analysis.

Slant agar cultures were extracted by means of a dynamic headspace using a GERSTEL DHS module (GERSTEL) connected to a MultiPurposeSampler robotic (MPS2 robotic; GERSTEL). The samples were extracted at 25 °C with 500 mL of nitrogen at a flow rate of 50 mL min^{-1} and trapped at 30 °C on an adsorbent tube packed with Tenax TA (150 °C transfer line temperature of the DHS module). Additionally, a dry purge step of the adsorbent tubes was performed using 200 mL of nitrogen at a flow rate of 100 mL min^{-1} and an adsorbent tube temperature of 30 °C. The parameters for the thermal desorption unit and the cold injection system were the same as reported previously.[8] For chiral analysis of slant agar cultures after headspace solid phase microextraction (HS-SPME), a divinylbenzene/carboxen/polydimethylsiloxane (DVB/CAR/PDMS; 65 μm, 1 cm length) fiber (Supelco, Steinheim, Germany) was used. Cultures were extracted for 30 min at 24 °C.

Liquid−Liquid Extraction for Chiral Analysis. After separation of the mycelium by centrifugation (*cf.* SBSE, dynamic headspace extraction, and solid phase microextraction), culture supernatants were extracted with an equivalent volume of distilled *n*-pentane/diethyl ether (1:1.12, v/v). Extraction was performed in shaking flasks on a magnetic stirrer for 30 min at 750 rpm. After extraction, the organic layer was separated by centrifugation (3000*g*, 10 min, 4 °C) in PTFE cups. The organic layer was separated, and the extraction procedure was repeated twice with the aqueous phase. The combined organic phases were dried over anhydrous sodium sulfate, concentrated at 43 °C water bath temperature using a Vigreux column to a final volume of about 1.5 mL, and stored at −20 °C until further use.

Gas Chromatography−Mass Spectrometry Analysis. For gas chromatographic analysis, an Agilent 8890 gas chromatograph connected to an Agilent 7010B GC/TQ mass spectrometer (Agilent Technologies, Waldbronn, Germany) and equipped with a thermal desorption unit 2 (GERSTEL) and a cold injection system 4 (GERSTEL) was used. Chromatographic separation on a polar column was performed on an Agilent VF-WAXms [30 m × 0.25 mm; 0.25 μm film thickness; temperature program, 40 °C (3 min), heating with 5 °C min^{-1} to 240 °C (12 min); carrier gas, helium (1.56 mL min^{-1}, constant flow)]. After the column, the carrier gas flow was split 1:1 by means of a μFlowManager Splitter (GERSTEL) between the mass spectrometer [transfer line temperature, 250 °C; electron ionization energy, 70 eV; ion source temperature, 230 °C; quadrupole temperatures, 150 °C; scan range, *m*/*z* 33−300; collision cell quench gas, helium (2.25 mL min^{-1}); collision cell collision gas, nitrogen (1.5 mL min^{-1})] and a GERSTEL Olfactory Detection Port 4 (ODP) [transfer line temperature, 300 °C; mixing chamber temperature, 200 °C; mixing chamber gas, nitrogen], although no sniffing experiments were carried out in this study.

Enantioselective Multidimensional GC−MS. Chiral compounds were analyzed using an enantioselective multidimensional GC−MS (enantio-MDGC−MS) system consisting of two Shimadzu (Shimadzu Europa, Duisburg, Germany) GC-2010 Plus gas chromatographs (GC 1 and GC 2), connected *via* a multi dean switch (MDS) for the selective transfer of analytes from the achiral (GC 1) to the chiral (GC 2) column. Parameters for the first GC system were published previously.[8] For chiral separations, depending on the analyte, a Hydrodex β-TBDAc column (Macherey Nagel, Düren, Germany; 25 m × 0.25 mm; linear velocity, 45 cm s^{-1}) or a CHIRALDEX B-DM column (Sigma-Aldrich; 30 m × 0.25 mm; film thickness, 0.12 μm; linear velocity, 45 cm s^{-1}) were used in the second GC. Temperature programs are listed in the Supporting Information S2 (Table S1) for the respective analytes. The column of the second GC was connected to a Shimadzu QP2010 Ultra mass spectrometer [transfer line temperature, 250 °C; electron ionization energy, 70 eV; ion source temperature, 200 °C; quadrupole temperature, 150 °C; scan range, *m*/*z* 33−300]. Data analysis was performed using Shimadzu GCMSsolution version 2.72, and a NIST 2011 MS library was used for mass spectrum comparison.

Compound Identification. Identification of compounds not described previously was accomplished *via* a comparison of retention indices, calculated according to van Den Dool and Kratz,[19] as well as mass spectra with synthesized reference standards. Standards of lactones **1** and **2** were provided by Nils H. Schebb, University of Wuppertal (Wuppertal, Germany).[20] The synthesis of diaster-

https://doi.org/10.1021/acs.jafc.3c01807
J. Agric. Food Chem. 2023, 71, 7744−7751

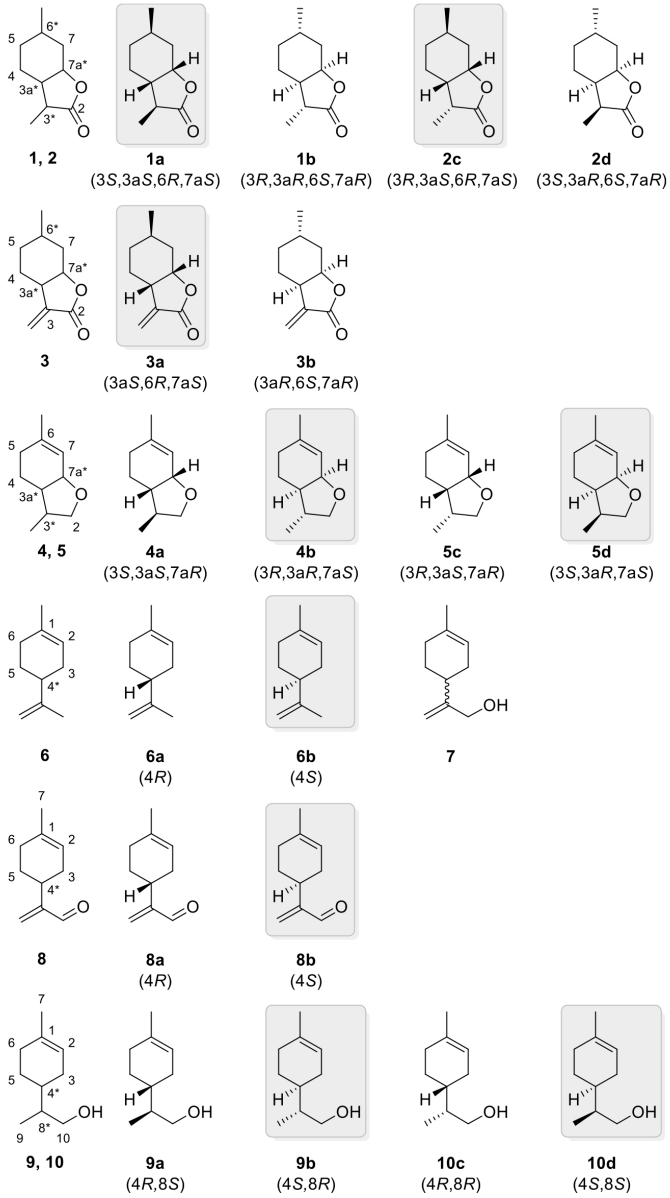

Figure 1. Structures of dihydromenthofurolactones (**1**, **2**), the corresponding C3-unsaturated lactone (**3**), dill ethers (**4**, **5**), limonene (**6**), and limonen-10-ol (**7**) as well as limonen-10-al (**8**), and the *p*-menth-1-en-9-ol stereoisomers (**9**, **10**). Absolute configurations of gray shaded stereoisomers have been identified for *C. murrayi*.

eoisomers of *p*-menth-1-en-9-ol including analytical data was published previously.[7]

RESULTS AND DISCUSSION

***De Novo* Synthesis of Chiral Terpenoids.** Previously published work revealed the formation of numerous terpenoids by the basidiomycete *C. murrayi* when grown in submerged cultures.[8] In addition to well-known substances such as linalool, the fungus also produces rare chiral substances such as dill ethers, and in particular, the so-called dihydromenthofurolactones (dml, **1**, **2**) and the C3-unsaturated analogue (Δ^3-dml, **3**) (Figure 1). Due to the complex stereochemistry resulting from four (dml) and three (Δ^3-dml) stereogenic centers, respectively, and the unavailability of authentic

https://doi.org/10.1021/acs.jafc.3c01807
J. Agric. Food Chem. 2023, 71, 7744−7751

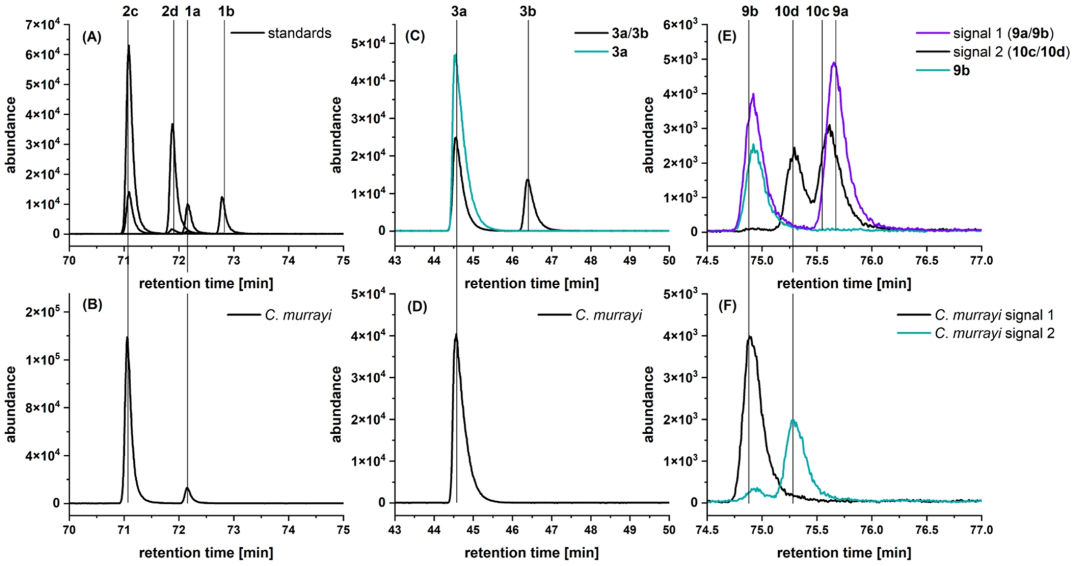

Figure 2. Chiral separation of lactones **1**, **2** (m/z 95), and **3** (m/z 94) as well as of *p*-menth-1-en-9-ol (**9**, **10**; m/z 94) by enantio-MDGC−MS; (A) standards of lactones **1** and **2** derived from hydrogenation of wine lactone stereoisomers;[20] (C) synthetic standards of lactones **3**; (E) synthetic standards of *p*-menth-1-en-9-ol stereoisomers as well as chemo-enzymatically obtained stereoisomer **9b**; (B,D,F*) *n*-pentane/diethyl ether extracts of the *C. murrayi* supernatant in SNS; * two separate MDGC runs were necessary because the signals did not elute with baseline separation.

standards, the absolute configuration of these fungal aroma molecules could not be elucidated conclusively so far. Out of the 16 existing stereoisomers of the dml and the eight Δ^3-dml, four saturated and two unsaturated lactones were considered to be formed by the fungus, as NMR experiments allowed a structural elucidation at the diastereomeric level. The structural similarity of dill ethers (**4**, **5**) and (Δ^3-)dml (**1**, **2**, **3**) suggests related biosynthetic pathways; however, determination of the absolute stereochemistry is mandatory. In addition, an aroma dilution analysis[8] (ADA) revealed perceivable substances, which could not be identified by comparison of the obtained mass spectra with the NIST database but may be relevant for the biogenesis of the benzofuran derivatives.

For the determination of the absolute configuration of the two saturated lactones (**1**, **2**), the provided reference standards were used.[20] As no commercial standards were available for Δ^3-dml (**3**), the two possible unsaturated stereoisomers (**3a**, **3b**) were synthesized (*cf.* Supporting Information S1). The chiral analysis of these standards in comparison to *n*-pentane/diethyl ether extracts of *C. murrayi* supernatants by MDGC revealed that one enantiopure isomer [enantiomeric ratio (er) = >99.9:0.1] each was formed by the fungus: **1a**, **2c**, and **3a** (Figure 2). Importantly, the two identified saturated lactones **1a** and **2c** thereby only differ in the orientation of the methyl-group at C3a*, at which the lactone **3a** contains a double-bond. Compared to the dill ethers **4b** and **5d** formed by the fungus,[8] the orientations of the stereogenic centers at C3a* and C7a* were inverse to those for **1a** and **2c**, suggesting that their biogenesis may not be linked as previously assumed. To the best of our knowledge, **1a** and **2c** have not been identified in other natural sources so far.

The cultivation of *C. murrayi* on agar slants in the presence of $^{13}C_6$-D-glucose confirmed the *de novo* formation of several terpenoids, including dml (**1**, **2**), Δ^3-dml (**3**), the two dill ethers (**4**, **5**), *p*-menth-1-en-9-ol (**9**, **10**), and linalool. In addition, the analysis of both, the $^{13}C_6$-D-glucose supplemented as well as unlabeled reference cultures revealed the formation of limonene (**6**) in the fungus' volatilome (*cf.* Supporting Information S3, Figure S7). For the biogenesis of the dill ethers (**4b**, **5d**) by *Pleurotus sapidus*, Trapp *et al.* propose a pathway *via* two diastereomers of *p*-menth-1-en-9-ol (**9**, **10**), starting from limonene (**6**).[7] With respect to the stereochemistry of the dill ethers (**4b**, **5d**) identified in *C. murrayi*, (*S*)-limonene (**6b**) seemed most likely to be the precursor, whereas the configuration of the (Δ^3-)dml (**1a**, **2c**, **3a**) should be accessible from (*R*)-limonene (**6a**). The chiral analysis of limonene formed by the fungus cultivated in slant agar *via* SPME−MDGC indeed revealed the formation of **6b** (*cf.* Supporting Information S4, Figure S10), which was in accordance with the findings for *P. sapidus*.[7] The absence of **6a** supports the hypothesis of an independent biogenesis of **1a**, **2c**, and **3a** on one side and of **4b** and **5d** on the other.

Limonen-10-ol (**7**) and limonen-10-al (**8**) were also identified in the culture supernatant of *C. murrayi*. For their identification, the respective compounds were synthesized starting from limonene (**6**) (*cf.* Supporting Information S1). While the signal intensity for **7** was too low, the peak intensity of the corresponding aldehyde **8** allowed chiral analysis in order to determine whether the compound may be relevant for the formation of the benzofuran derivatives. Both enantiomers (**8a**, **8b**) were synthesized and separated by enantio-MDGC. The analysis of an extract of *C. murrayi* revealed that the (*S*)-stereoisomer **8b** was present (*cf.* Supporting Information S5, Figure S11). Thus, the stereochemistry matched that of the dill ethers (**4b**, **5d**) and of limonene (**6b**) while being inverse to that of the lactones (**1a**, **2c**, **3a**). Moreover, the retention index as well as the mass spectrum of **8b** corresponded to a perceived

https://doi.org/10.1021/acs.jafc.3c01807
J. Agric. Food Chem. 2023, 71, 7744−7751

compound that was not identified during the ADA of *C. murrayi*.[8] Alcohol **7** occurs naturally in plants, fermented beverages, as well as honey but has, to the best of our knowledge, not been described in basidiomycota so far.[21−23] The same applies to aldehyde **8**, which has been described in essential oils of *Dracocephalum*.[24]

As described previously, the analysis of organic extracts from the supernatant of *C. murrayi* as well as agar slants revealed the formation of *p*-menth-1-en-9-ols (**9**, **10**). However, the evaluation of the chromatograms revealed two co-eluting compounds with similar mass spectra (*cf.* Supporting Information S6, Figure S12). As two stereogenic centers are present in the structure, the findings suggested that two diastereomers were formed by the fungus. Using synthetic standards containing diastereomeric **9a** and **10c** as well as **9b** and **10d**, respectively, the formation of two diastereomers could be confirmed. In order to evaluate whether **9** and/or **10** could act as a precursor for the dill ether as previously described by Trapp *et al.*,[7] chiral analyses were performed. For the initial assignment of the enantiomeric pairs on the achiral stationary phase, **9b** was chemo-enzymatically prepared by the reduction of aldehyde **8a** using *Saccharomyces cerevisiae*, as described in the literature.[25] Thus, the enantiomeric pair **9a**/**9b** could be assigned to the first eluting peak on a polar VF-WAXms column (*cf.* Supporting Information S6, Figure S12). In a subsequent chiral analysis on a CHIRALDEX B-DM column co-elution of the diastereoisomers **9a** and **10c** made a separate transfer of the two diastereomeric compounds from the achiral column necessary. Analysis of the *p*-menth-1-en-9-ol signals showed that only the stereoisomers **9b** and **10d** were formed by the fungus (Figure 2). The observed stereochemistry corresponded to the dill ethers **4b** and **5d** formed by the fungus and was again inverse compared to the tetrahydrofuran-ring system of **1a**, **2c**, and **3a**. In addition, the ratios of the signal intensities of **9b** and **10d** correlated well with those of the dill ethers **4b** and **5d**, as **9b** and **4b** represented the more abundant signals, respectively. Moreover, these findings are in agreement with the results published for *P. sapidus*[7] and again support the assumption of different biosynthetic pathways for (Δ^3-)dml and dill ethers.

Supplementation Studies. Based on the proposed biosynthetic pathways for the dill ethers described in the literature and structural analogues,[7,26] supplementation studies with different terpenes and terpenoids were conducted. Besides the two limonene enantiomers (**6a**, **6b**) and the four *p*-menth-1-en-9-ol stereoisomers (**9a** and **10c**, **9b** and **10d**), the influence of (*R*)- and (*S*)-limonen-10-ol (**7**) as well as (*S*)-limonen-10-al (**8b**) and (*R*)-linalool on the formation of the dill ethers and lactones was investigated.

For the dill ethers, supplementation of the two limonene enantiomers resulted in concentrations comparable to those of the reference cultures (Figure 3). Chiral analysis revealed a minor formation of dill ether **5c** using (*R*)-limonene (**6a**) or (*S*)-limonene (**6b**) (Figure 4). Similar results were reported by Trapp *et al.*.[7] However, in contrast to the previously published increase in the dill ether concentration after supplementation, this effect was not observed for *C. murrayi*. The formation of **5c** might just be a result of impurities due to the accompanying (*R*)-enantiomer in commercially available (*S*)-limonene (*cf.* Supporting Information S4, Figure S10). To further confirm the transformation of limonene to the dill ethers, *rac*-^{13}C-D$_2$-limonene was supplemented to submerged cultures of the fungus. For the dill ethers **4** and **5**, as well as for the *p*-menth-1-en-9-ol (**9**), isotopic shifts were detected for the respective signals (*cf.* Supporting Information S7, Figures S14−S16). Thus, their formation starting from limonene is possible. However, especially the more abundant dill ether **4** showed only minor conversion, whereas the dill ether **5** was more strongly influenced [*e.g.*, ratio of *m*/*z* 137 (main peak) to *m*/*z* 140 (labeled) for dill ether **4** 2.4% and for dill ether **5** 23.3%]. For the previously described aldehyde **8**, no shifts were detected. Compared to the cultures supplemented with *rac*-limonene, the ^{13}C-D$_2$-limonene cultures showed isotopic shifts in the mass spectra of, e.g., isomers of neodihydrocarveol (*cf.* Supporting Information S7, Figure S13), indicating the ability of *C. murrayi* to perform oxyfunctionalization of terpenes, as described in other fungi.[27−29]

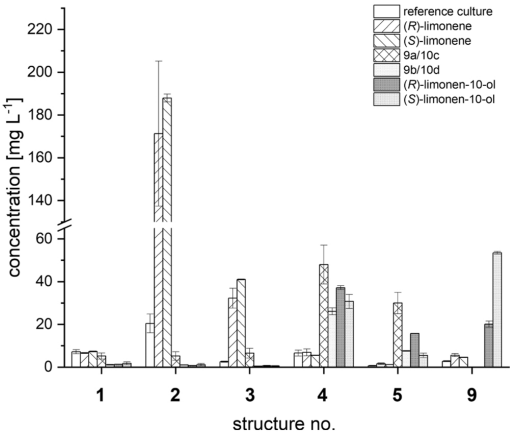

Figure 3. Supplementation studies of *C. murrayi* in SNS with semi-quantitative concentrations (referred to the internal standard mint lactone) of the respective terpenoids analyzed by SBSE−GC−MS. Shown are the respective concentrations of the compounds listed on the abscissa (structures according to Figure 1) depending on the supplement used (*cf.* legend). Reference cultures were cultivated with the addition of ethanol without further supplements.

In contrast, a strong influence on the stereochemistry and the concentration of the dill ethers in supplementation studies using the *p*-menth-1-en-9-ol stereoisomers was noticed (Figures 3 and 4). While the stereochemistry was only slightly influenced using diastereomeric **9b** and **10d** (resulting in an er of 95:5 for **4b** and 88:12 for **5d**), supplementation of **9a** and **10c** resulted in higher values for **4a** (er = 97:3) and **5c** (er = 99:1). Comparable results were obtained with (*S*)-limonen-10-ol (**4b** er = 89:11, **5d** er = 75:25) and (*R*)-limonen-10-ol (**4a** er = 97:3, **5c** er = 97:3). Also herein, supplementation influenced the stereochemistry as well as the concentrations (Figures 3 and 4). As the stereochemistry of the identified aldehyde **8b** correlates with that of dill ether, this compound was supplemented to submerged cultures in order to evaluate whether the concentrations of **4b** and **5d** are influenced. Thereby, the semi-quantitated concentrations of dill ether increased 15- (**4b**) and 8-fold (**5d**), respectively. In addition, the effect on the stereochemistry (*cf.* Supporting Information S8, Figure S17) of dill ethers **3b** and **5d** was comparable to the *p*-menth-1-en-9-ol supplementation. Linalool showed no influence on the stereochemistry of the formed dill ethers.

https://doi.org/10.1021/acs.jafc.3c01807
J. Agric. Food Chem. 2023, 71, 7744−7751

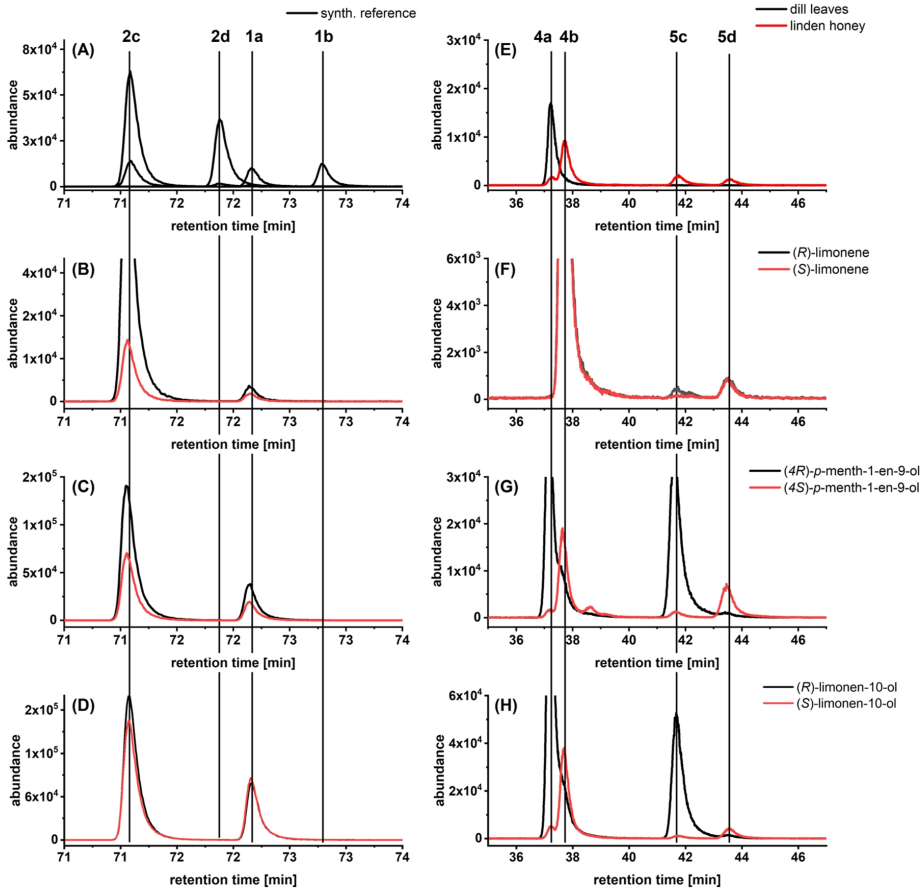

Figure 4. Chiral analysis of lactones **1** and **2** (m/z 95, A–D) and dill ethers **4** and **5** (m/z 137; E–H) by enantio-MDGC–MS in supplementation experiments in submerged culture; (A) synthetic standards of **1** and **2**; (E) natural references for dill ethers; (B,F) supplementation of (*R*)- and (*S*)-limonene; (C,G) supplementation of (4*R*)- and (4*S*)-*p*-menth-1-en-9-ol; and (D,H) supplementation of (*R*)- and (*S*)-limonen-10-ol.

The results of the supplementation studies can be summarized far more easily for (Δ^3-)dml. No influence was observed on the stereochemistry, regardless of which of the above-mentioned terpenes or terpenoids was used for supplementation (Figure 4). Although the concentrations of the lactones increased especially after supplementation of (*R*)- and (*S*)-limonene (Figure 3), no mass shifts were observed using ^{13}C-D$_2$-limonene, indicating a stress-induced effect. Furthermore, these results further strengthen the assumption of non-linked biogenesis.

Our results strongly suggest different biosynthesis pathways for the lactones and dill ethers for the fungus *C. murrayi*. Common to both is a *de novo* formation starting from glucose, as supported by the supplementation experiments with ^{13}C$_6$-D-glucose. However, subsequent metabolites that occur as intermediates differ. Thus, the lactones and dill ethers display inverted stereochemistries of the tetrahydrofuran-ring. The dill ethers might be formed from limonen-10-al (**8**) *via* limonen-10-ol (**7**) or directly from *p*-menth-1-en-9-ols (**9b**, **10d**). For aldehyde **8**, limonene may potentially act as a precursor; however, no isotopic labels were detected employing ^{13}C-D$_2$-limonene. Therefore, the biotransformation of limonene could be a side pathway of dill ether formation but not necessarily the *de novo* pathway. For lactones **1a**, **2c**, and **3a**, except for the *de novo* formation, intermediate metabolites yet remain unknown. However, the same terpenoid precursors as for the dill ethers could be excluded. Finally, interesting yet unreported stereoisomers of the lactones as fungal secondary metabolites were identified, and a linked formation of the three lactones seems very likely due to the comparable stereochemistry.

■ ASSOCIATED CONTENT

Supporting Information

The Supporting Information is available free of charge at https://pubs.acs.org/doi/10.1021/acs.jafc.3c01807.

Synthetic procedure for lactones **3a** and **3b**, limonen-10-ol (**7**), and limonen-10-al (**8**); chromatographic conditions for chiral separation using MDGC; GC–MS data of identified aroma compounds within labeling

https://doi.org/10.1021/acs.jafc.3c01807
J. Agric. Food Chem. 2023, 71, 7744–7751

studies using $^{13}C_6$-D-glucose; chiral separation of limonene stereoisomers; chiral separation of limonen-10-al stereoisomers; assignment of *p*-menth-1-en-9-ol stereoisomers; GC−MS data of selected aroma compounds within labeling studies using ^{13}C-D_2-limonene; and effect of (*S*)-limonen-10-al supplementation on dill ether formation (PDF)

AUTHOR INFORMATION

Corresponding Author

Marco A. Fraatz − *Institute of Food Chemistry and Food Biotechnology, Justus Liebig University Giessen, 35392 Giessen, Germany;* orcid.org/0000-0002-5028-9653; Phone: +49 (0) 641 99 349-02; Email: marco.fraatz@lcb.chemie.uni-giessen.de

Authors

Fabio F. Brescia − *Institute of Food Chemistry and Food Biotechnology, Justus Liebig University Giessen, 35392 Giessen, Germany*

Maximilian Koch − *Institute of Food Chemistry and Food Biotechnology, Justus Liebig University Giessen, 35392 Giessen, Germany*

Raffael C. Wende − *Institute of Organic Chemistry, Justus Liebig University Giessen, 35392 Giessen, Germany;* orcid.org/0000-0002-2242-4723

Peter R. Schreiner − *Institute of Organic Chemistry, Justus Liebig University Giessen, 35392 Giessen, Germany;* orcid.org/0000-0002-3608-5515

Holger Zorn − *Institute of Food Chemistry and Food Biotechnology, Justus Liebig University Giessen, 35392 Giessen, Germany; Fraunhofer Institute for Molecular Biology and Applied Ecology, 35392 Giessen, Germany;* orcid.org/0000-0002-8383-8196

Complete contact information is available at: https://pubs.acs.org/10.1021/acs.jafc.3c01807

Funding

Part of the analytical equipment used was funded by the Deutsche Forschungsgemeinschaft (DFG, German Research Foundation)—463380894.

Notes

The authors declare no competing financial interest.

ACKNOWLEDGMENTS

Special thanks go to Dr. Flavius Popa from the Black Forest National Park for the donation of the fungus.

ABBREVIATIONS USED

ADA, aroma dilution analysis; CIS, cold injection system; DHS, dynamic headspace; er, enantiomeric ratio; FD, flavor dilution; ME, malt extract; O, olfactometry/olfactometric; ODP, olfactory detection port; RI, retention index/indices; SNS, standard nutrition solution; TDU, thermal desorption unit

REFERENCES

(1) Burkhardt, I.; Kreuzenbeck, N. B.; Beemelmanns, C.; Dickschat, J. S. Mechanistic characterization of three sesquiterpene synthases from the termite-associated fungus *Termitomyces*. *Org. Biomol. Chem.* **2019**, *17*, 3348−3355.

(2) Wagner, K.-H.; Elmadfa, I. Biological relevance of terpenoids. Overview focusing on mono-di- and tetraterpenes. *Ann. Nutr. Metab.* **2003**, *47*, 95−106.

(3) Schmidt-Dannert, C. Biosynthesis of terpenoid natural products in fungi. *Adv. Biochem. Eng./Biotechnol.* **2014**, *148*, 19−61.

(4) Sacchettini, J. C.; Poulter, C. D. Creating isoprenoid diversity. *Science* **1997**, *277*, 1788−1789.

(5) Sales, A.; Paulino, B. N.; Pastore, G. M.; Bicas, J. L. Biogeneration of aroma compounds. *Curr. Opin. Food Sci.* **2018**, *19*, 77−84.

(6) Guth, H. Determination of the configuration of wine lactone. *Helv. Chim. Acta* **1996**, *79*, 1559−1571.

(7) Trapp, T.; Kirchner, T.; Birk, F.; Fraatz, M. A.; Zorn, H. Biosynthesis of stereoisomers of dill ether and wine lactone by *Pleurotus sapidus*. *J. Agric. Food Chem.* **2019**, *67*, 13400−13411.

(8) Brescia, F. F.; Pitelas, W.; Yalman, S.; Popa, F.; Hausmann, H. G.; Wende, R. C.; Fraatz, M. A.; Zorn, H. Formation of diastereomeric dihydromenthofurolactones by *Cystostereum murrayi* and aroma dilution analysis based on dynamic headspace extraction. *J. Agric. Food Chem.* **2021**, *69*, 5997−6004.

(9) Winterhalter, P.; Bonnländer, B. Aroma-active benzofuran derivatives: Analysis, sensory properties, and pathways of formation. In *Aroma Active Compounds in Foods*; Takeoka, G. R., Güntert, M., Engel, K.-H., Eds.; ACS Symposium Series; American Chemical Society: Washington, DC, 2001; pp 21−32.

(10) Blank, I.; Grosch, W. Evaluation of potent odorants in dill seed and dill herb (*Anethum graveolens* L.) by aroma extract dilution analysis. *J. Food Sci.* **1991**, *56*, 63−67.

(11) Brunke, E.-J.; Hammerschmidt, F.-J.; Koester, F.-H.; Mair, P. Constituents of dill (*Anethum graveolens* L.) with sensory importance. *J. Essent. Oil Res.* **1991**, *3*, 257−267.

(12) Southwell, I. A. Essential oil metabolism in the koala iii novel urinary monoterpenoid lactones. *Tetrahedron Lett.* **1975**, *16*, 1885−1888.

(13) Wüst, M.; Mosandl, A. Important chiral monoterpenoid ethers in flavours and essential oils—enantioselective analysis and biogenesis. *Eur. Food Res. Technol.* **1999**, *209*, 3−11.

(14) Blank, I.; Fischer, K.-H.; Grosch, W. Intensive neutral odourants of linden honey—Differences from honeys of other botanical origin. *Z. Lebensm.-Unters. Forsch.* **1989**, *189*, 426−433.

(15) Frérot, E.; Bagnoud, A.; Vuilleumier, C. Menthofurolactone: A new p-menthane lactone in *Mentha piperita* L.: Analysis, synthesis and olfactory properties. *Flavour Fragrance J.* **2002**, *17*, 218−226.

(16) Näf, R.; Velluz, A. Phenols and lactones in Italo-Mitcham peppermint oil *Mentha* × *piperita* L. *Flavour Fragrance J.* **1998**, *13*, 203−208.

(17) Shigeto, A.; Wada, A.; Kumazawa, K. Identification of the novel odor active compounds "*p*-menthane lactones" responsible for the characteristic aroma of fresh peppermint leaf. *Biosci., Biotechnol., Biochem.* **2020**, *84*, 421−427.

(18) Fraatz, M. A.; Naeve, S.; Hausherr, V.; Zorn, H.; Blank, L. M. A minimal growth medium for the basidiomycete *Pleurotus sapidus* for metabolic flux analysis. *Fungal Biol. Biotechnol.* **2014**, *1*, 9.

(19) van Den Dool, H.; Dec. Kratz, P. A generalization of the retention index system including linear temperature programmed gas-liquid partition chromatography. *J. Chromatogr.* **1963**, *11*, 463−471.

(20) Buhr, K. Untersuchungen zu Struktur-Geruchsbeziehungen von Lactonen. Ph.D. Dissertation, Bergische Universität Wuppertal, 2006.

(21) Alissandrakis, E.; Tarantilis, P. A.; Harizanis, P. C.; Polissiou, M. Aroma investigation of unifloral Greek citrus honey using solid-phase microextraction coupled to gas chromatographic−mass spectrometric analysis. *Food Chem.* **2007**, *100*, 396−404.

(22) Roux, M. L.; Cronje, J. C.; Burger, B. V.; Joubert, E. Characterization of volatiles and aroma-active compounds in honeybush (*Cyclopia subternata*) by GC-MS and GC-O analysis. *J. Agric. Food Chem.* **2012**, *60*, 2657−2664.

(23) Tomiyama, K.; Aoki, H.; Oikawa, T.; Sakurai, K.; Kasahara, Y.; Kawakami, Y. Characteristic volatile components of Japanese sour

citrus fruits: Yuzu, Sudachi and Kabosu. *Flavour Fragrance J.* **2012**, *27*, 341−355.
(24) Özek, G.; Tabanca, N.; Radwan, M. M.; Shatar, S.; Altantsetseg, A.; Baatar, D.; Başer, K. H.; Becnel, J. J.; Özek, T. Preparative capillary GC for characterization of five *Dracocephalum* essential oils from Mongolia, and their mosquito larvicidal activity. *Nat. Prod. Commun.* **2016**, *11*, 1934578X1601101.
(25) Serra, S.; Fuganti, C.; Gatti, F. G. A chemoenzymatic, preparative synthesis of the isomeric forms of *p*-menth-1-en-9-ol: Application to the synthesis of the isomeric forms of the cooling agent 1-hydroxy-2,9-cineole. *Eur. J. Org. Chem.* **2008**, *2008*, 1031−1037.
(26) Reichert, S.; Fischer, D.; Asche, S.; Mosandl, A. Stable isotope labelling in biosynthetic studies of dill ether, using enantioselective multidimensional gas chromatography, online coupled with isotope ratio mass spectrometry. *Flavour Fragrance J.* **2000**, *15*, 303−308.
(27) Onken, J.; Berger, R. G. Effects of *R*-(+)-limonene on submerged cultures of the terpene transforming basidiomycete *Pleurotus sapidus*. *J. Biotechnol.* **1999**, *69*, 163−168.
(28) Fraatz, M. A.; Berger, R. G.; Zorn, H. Nootkatone—a biotechnological challenge. *Appl. Microbiol. Biotechnol.* **2009**, *83*, 35−41.
(29) Bicas, J. L.; Dionísio, A. P.; Pastore, G. M. Bio-oxidation of terpenes: an approach for the flavor industry. *Chem. Rev.* **2009**, *109*, 4518−4531.

5. **Chapter:** Novel method for odor threshold determination in air

Determining ultra-low organic molecular odor thresholds in air helps identify the most potent fungal aroma compound

Brescia, F. F.; Passinger, J.; Wende, R. C.; Schreiner, P. R.; Zorn, H.; Fraatz, M. A.

J. Agr. Food Chem. **2024**, *72* (13), 7511–7516.

https://doi.org/10.1021/acs.jafc.3c08438

JOURNAL OF AGRICULTURAL AND FOOD CHEMISTRY

pubs.acs.org/JAFC Article

Determining Ultra-Low Organic Molecular Odor Thresholds in Air Helps Identify the Most Potent Fungal Aroma Compound

Published as part of Journal of Agricultural and Food Chemistry virtual special issue "13th Wartburg Symposium on Flavor Chemistry and Biology".

Fabio F. Brescia, Jan Passinger, Raffael C. Wende, Peter R. Schreiner, Holger Zorn, and Marco A. Fraatz*

Cite This: https://doi.org/10.1021/acs.jafc.3c08438 Read Online

ACCESS | Metrics & More | Article Recommendations | Supporting Information

ABSTRACT: The determination of odor threshold values can be performed in various matrices, including air, and serves as a parameter to compare the potencies of odorous compounds. Typically, the odor thresholds in air are determined by gas chromatography−olfactory (GC−O) and referenced to an internal standard, most often (*E*)-dec-2-enal. Herein, a direct gas chromatography-flame ionization detector-olfactory analysis method for the determination of odor thresholds in air is reported. As model substrates for this novel approach, naturally occurring substances (*R*)-1-*p*-menthene-8-thiol as well as (3*S*,3a*S*,6*R*,7a*S*)-3,6-dimethyl-3a,4,5,6,7,7a-hexahydro-3*H*-1-benzofuran-2-one were used. The latter compound was synthesized from (−)-isopulegol and exhibited an extremely low odor recognition threshold of 1.9×10^{-6} ng L^{-1} air, the lowest value reported for a fungal aroma compound thus far.

KEYWORDS: *gas chromatography, natural products, olfaction, perception, smell*

INTRODUCTION

Of the many thousands of known aroma compounds, those perceivable in (ultra)trace concentrations stand out. As a measure of the potency of such substances, the so-called odor threshold is used with a qualifying term. The detection threshold refers to the concentration at which an odor becomes perceivable, yet without the need to identify the sensation. The odor recognition threshold is the lowest concentration at which the characteristic odor is each time assigned with the same descriptor by the assessor.[1] However, a sharp distinction is not always made between these two types of odor thresholds in the literature. The odor thresholds are crucial for the calculation of odor activity values following aroma dilution analyses and the subsequent quantitation, providing information on whether an odorant contributes to the overall impression of the sample.[2] Potent aroma compounds thereby may also represent off-flavors, like 2,4,6-trichloroanisole in wine,[3] or pollutants in the industrial production of chemicals.[4] Perceptibility herein always depends on whether the concentration of the flavor in the respective matrix is above its odor threshold.

The odor thresholds depend on the affinity of the compounds to the odorant receptors and from a structural point of view on the chemical composition, the presence of stereogenic centers, the molecular mass, and the polarity.[5] The latter, in particular, is relevant in terms of aroma release from solid or liquid matrices with different polarities. This also explains why the determination of odor thresholds is performed on different matrices. Water is frequently used as a solvent for threshold determinations, as it is often the medium in which the compounds are dissolved in food. In contrast to other solvents, such as alcoholic solutions or lipids, the use of water does not emit background odors that could impede the perception. For determination, the compound of interest is typically dissolved in water, placed in a suitable container, and after equilibration, different dilutions are sniffed. Yet, there are some critical aspects to consider when determining odor thresholds in water. The method itself was not standardized for a long time, and using published data from that period may have led to unreliable results. In recent years, however, the methodology for determining odor thresholds in water has been systematically addressed and standardized.[6,7] Furthermore, the determination may be influenced by odorous impurities, either from the water used or from the substance itself, as well as by the limited solubility of nonpolar substances.

Alternatively, odor thresholds can be determined in air, which offers the advantage of being independent of matrix effects. First reports of this approach date back to the late 19th century, when Fischer and Penzoldt used lecture halls for the odor threshold determination of a chlorophenol and a thiol.[8] A similar method was applied by Leonardos et al. for industrial air pollutants using a test room of defined volume.[4] Only a few years later, a completely different approach was published, in which the odor threshold in air was indirectly determined via

Received: November 13, 2023
Revised: February 20, 2024
Accepted: March 8, 2024

https://doi.org/10.1021/acs.jafc.3c08438
J. Agric. Food Chem. XXXX, XXX, XXX−XXX

the odor threshold in water using a previously determined distribution coefficient, known as the Henry constant.[9−11] This method was used by Teranishi et al.[12] to determine the odor threshold of (*E*)-dec-2-enal (**1**) to be 2.7 ng L^{-1} (air). As instrumentation progressed, Ullrich and Grosch established a method for odor threshold determination, which relies on high-resolution gas chromatography−olfactometry (HRGC−O) and the use of an internal standard with a known odor threshold chosen depending on the respective analyte.[13] The substance of interest is diluted stepwise together with the internal standard, and the resulting dilutions are sniffed via GC−O until the compound can no longer be perceived. The highest dilution factor at which the respective compound can still be perceived (known as the *D*-value) as well as the concentrations of the substance and internal standard, together with the odor threshold of the internal standard, can then be used to calculate the odor threshold of the compound of interest.[13] This method is now established as a common procedure and finds widespread use. Hexanal was initially used as internal standard, but was replaced by (*E*)-non-2-enal[14,15] and later by (*E*)-dec-2-enal (**1**).[16] In the following decades, almost exclusively the latter compound was used to determine odor thresholds. However, it was not taken into account whether the analyzed compounds share a similar odor threshold, although this was explicitly demanded by Ullrich and Grosch.[13] An additional problem is that a fixed odor threshold is used for **1**, irrespective of individual perception differences.

The aim of this work was to develop a more robust approach for odor threshold determination by direct GC−O analysis without the need for an internal standard. In addition to the use of an on-column inlet, the split ratio of the μFlowManager (GERSTEL) between the flame ionization detector (FID) and the olfactory detection port (ODP) was determined as a function of the retention index. As a result, a new method for the calculation of odor threshold values was established.

MATERIALS AND METHODS

Chemicals. Chemicals used for synthesis as well as their purities are listed in Supporting Information S1. (*E*)-dec-2-enal was purchased from Sigma-Aldrich (Taufkirchen, Germany), ethyl acetate (99.8%) was from Th. Geyer (Hamburg, Germany), and the *n*-alkane standard solution (C_7−C_{30} homologues) was obtained from Supelco, Inc. (Bellefonte, US). Hydrogen (5.0) was purchased from Praxair (Düsseldorf, Germany) whereas nitrogen (5.0) was obtained from Air Liquide (Düsseldorf, Germany). All purity specifications represent the respective minimum.

Gas chromatography−Flame Ionization Detector−Olfactometry (GC−FID−O) Analysis. For gas chromatographic analyses, an Agilent 7890A gas chromatograph (Agilent Technologies, Waldbronn, Germany) equipped with an Agilent 7693 injection tower, a cool on-column inlet (inlet temperature, 40 °C), and a flame ionization detector (FID) was used. Chromatographic separations were performed using a polar Agilent VF-WAXms column (30 m × 0.32 mm; 0.25 μm film thickness; temperature program, 40 °C (3 min), heating to 240 °C (7 min) with 5 °C min^{-1}; carrier gas, hydrogen (2.2 mL min^{-1}, constant flow)). After the GC column, the carrier gas flow was split 1:1 by means of a μFlowManager splitter between the FID (temperature, 250 °C; hydrogen flow, 40 mL min^{-1}; air flow, 400 mL min^{-1}; makeup flow (N_2), 25 mL min^{-1}) and an Olfactory Detection Port 3 (GERSTEL GmbH & Co. KG, Mülheim a. d. Ruhr, Germany; transfer line temperature, 250 °C; mixing chamber temperature, 150 °C; mixing chamber gas, nitrogen). Lengths of ODP and FID transfer capillaries (deactivated; 0.15 mm i.d.) were calculated using GERSTEL ODP Column Calculator 1.3.1.0. For chiral analysis, two sequentially connected Macherey Nagel β-6-TBDM columns (25 m x 0.25 mm; temperature program, 50 °C (2 min), heating to 70 °C (20 min) with 0.5 °C min^{-1}; heating to 90 °C (20 min) with 0.5 °C min^{-1}; heating to 125 °C (0 min) with 1 °C min^{-1}) were used.

Odor Recognition Threshold Determination. For analysis, 11.38 mg of (3*S*,3a*S*,6*R*,7a*S*)-3,6-dimethyl-3a,4,5,6,7,7a-hexahydro-3*H*-1-benzofuran-2-one (**2a**) (93.5% purity, determined by GC−FID) and 11.22 mg of (*E*)-dec-2-enal (**1**) (chromatographic purity: 98.8%) were separately dissolved in 20 mL of ethyl acetate. Subsequently, a combined dilution series (2^x, whereby *x* corresponds to the number of 1:2 (v/v) dilutions) was prepared up to a dilution factor of 2^{31}, and the dilutions were analyzed via GC−FID−O (5 panelists, 3 males, and 2 females; ages between 22 and 29). The odor recognition threshold determination of (*R*)-1-*p*-menthene-8-thiol (**3**) was performed analogously, using 13.71 mg of **3** (92.3% purity, determined by GC−FID) and 11.72 mg of **1** (separately dissolved in ethyl acetate and combined afterward) up to a dilution factor of 2^{38}. Retention indices (RIs) were calculated according to van den Dool and Kratz.[17] For polynomial regression, OriginPro 2020 was used.

RESULTS AND DISCUSSION

Determination of FID/ODP Split Ratio Using GC−FID−O. As an alternative to the GC method used so far for odor threshold determination in air, the approach established herein offers the possibility of determining odor thresholds directly via GC−O, using only the analyte dissolved in a suitable solvent without the use of an internal standard. Due to the defined injection volume in combination with the usage of an on-column inlet, the injected mass of the analyte is directly known and can be used for further calculations. Prior to implementation of the novel method, two critical aspects were identified for subsequent odor threshold determination: the reproducibility of the injection and the accuracy of the splitting. The former was tested by repeated injection of an *n*-alkane series to verify the reproducibility over a broad range of volatility. The results showed relative standard deviations ≤1.1% for solely FID detection and ≤3.0% for repeated injections (six times each) using the μFlowManager. Especially regarding individual differences, which often account for at least a factor of 2 for a given compound, the achieved precision was judged to be sufficient. The second key aspect is that the presumed split ratio of the FID/ODP split is achieved. When systems with constantly heated external transfer lines are used, it is important to note that the FID/ODP split varies within a GC run. Using the method of Ullrich and Grosch, this problem arises particularly when there is a significant difference between the retention times of the internal standard and those of the analyte. In the method developed herein, this divergence is avoided, as the use of an internal standard is not required, and thus, only errors due to FID/ODP splitting of the analyte itself occur. However, one critical factor herein is that the two capillaries are heated differently after the μFlowManager splitter. The transfer capillary heading toward the FID is fully located inside the GC oven, and thus, the temperature equals the oven temperature. In contrast, only a minor part of the ODP transfer capillary is located inside the oven, whereas the major part is constantly tempered by the external transfer line heater. Its temperature, at least in the case of using a polar separation column, is usually set higher than the oven temperature. For the present study, it was set to 250 °C. The resulting difference in the backpressure causes the FID/ODP split ratio to vary depending on the actual GC oven temperature and tends to result in a reduced flow to the ODP. Therefore, the accurate FID/ODP split ratio was determined by repeated injection of an *n*-alkane standard solution, with

https://doi.org/10.1021/acs.jafc.3c08438
J. Agric. Food Chem. XXXX, XXX, XXX−XXX

and without splitting with a μFlowManager splitter (six times each), as a function of the retention index. Initially, measurements were carried out by connecting the column via the μFlowManager splitter with capillaries to the ODP and the FID. Subsequently, the ODP port was blocked by a sealing plug and the *n*-alkane standard was repeatedly injected again. The effect of the temperature on the FID/ODP split ratio was determined graphically (Figure 1) by plotting the retention

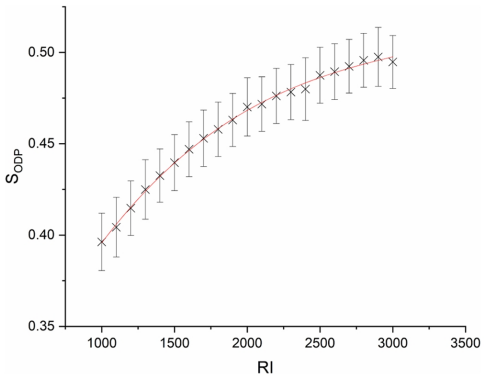

Figure 1. Determination of the accurate split ratio for the olfactory detection port (S_{ODP}) as a function of the retention index. Mean values for S_{ODP} (calculated according to eq 1) and standard deviations as well as polynomic fit ($S_{ODP} = 1.98 \times 10^{-4} \times RI - 5.46 \times 10^{-8} \times RI^2 + 5.50 \times 10^{-12} \times RI^3 + 0.247$; $R^2 = 0.9978$) are shown. Each injection (with and without splitting) was performed six times.

index against the observed split ratio for the ODP (S_{ODP}), calculated as follows:

$$S_{ODP} = 1 - \frac{\bar{A}_{i,FID/ODP}}{\bar{A}_{i,FID}} \quad (1)$$

in which $\bar{A}_{i,FID/ODP}$ represents the mean value of the FID peak area of *n*-alkane$_i$ with FID/ODP splitting; $\bar{A}_{i,FID}$ is the mean value of the peak area of *n*-alkane$_i$ without FID/ODP splitting.

The plot shows that the splitting ratio asymptotically approaches a maximum of nearly 0.5 (corresponding to a 1:1 split between FID and ODP) with increasing retention indices and thus increasing column oven temperatures (Figure 1). However, this splitting ratio is achieved only at high temperatures. A polynomic fit results in an R^2 value of 0.9978 and thus is suitable for the calculation of the actual splitting ratio depending on the respective retention index. Because of the variance in olfactory sensitivity caused by interindividual differences, a deviation of the detected last dilution step by only one dilution level directly results in a change of the odor threshold by a factor of 2. Therefore, the relatively small influence of the temperature program on the actual FID/ODP ratio can probably even be ignored with the method developed here (e.g., 1.1 ng L^{-1} air assuming a 1:1 split ratio vs 1.0 ng L^{-1} with the split ratio corrected according to eq 1 for **1**).

Odor Recognition Threshold Determination. As model compound (3*S*,3a*S*,6*R*,7a*S*)-3,6-dimethyl-3a,4,5,6,7,7a-hexahydro-3*H*-1-benzofuran-2-one (**2a**), which was recently identified as a fungal aroma compound with expected extremely low odor thresholds,[18] as well as the widely known and very potent aroma compound (*R*)-1-*p*-menthene-8-thiol (**3**), and the mentioned and often used internal standard (*E*)-dec-2-enal (**1**) (Figure 2) were selected.

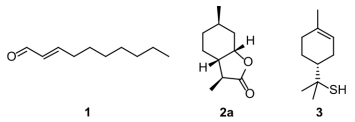

Figure 2. Model compounds used for odor recognition threshold determination in this study.

Whereas **1** is commercially available, lactone **2a** was synthesized by starting from (−)-isopulegol (Figure 3). The stereochemistry at C−OH was inverted by a Mitsunobu reaction followed by saponification of the formed nitrobenzoate **4**, affording (+)-neoisopulegol (**5**).[19,20] Subsequent hydroboration/oxidation gave *p*-menthane-3,9-diols **6** as a 2:1 mixture of diastereoisomers.[19,21,22] Final oxidation with potassium permanganate then gave a diastereomeric mixture of desired lactone **2** in 58% yield over four steps.[23] Diastereomer **2a** used for odor threshold determination was separated and further purified by preparative HPLC. Compound **3** was synthesized from (*R*)-α-terpineol through thionation with Lawesson's reagent.[24−27]

For odor recognition threshold determination, the substance to be analyzed as well as the internal standard were separately dissolved in ethyl acetate, subsequently diluted in a combined dilution series, and analyzed via GC−FID−O. The odor recognition threshold (OT) was calculated according to Ullrich and Grosch with an odor threshold of 2.7 ng L^{-1} for the internal standard and additionally by the novel method using the following equation:

$$OT = \frac{c_A V_I S_{ODP}}{D V_T} \quad (2)$$

in which c_A [μg μL^{-1}] represents the concentration of the analyte in the stock solution; V_I [μL] corresponds to the injection volume; S_{ODP} is the actual split ratio at the μFlowManager splitter calculated for the respective analyte based on the retention index; *D* refers to the highest dilution factor at which the compound was perceived ($D = 2^x$, where *x* is the highest dilution step); V_T [L] represents the tidal volume. Retention indices (RIs) were calculated according to van Den Dool and Kratz.[17] For the tidal volume, literature values of 0.4 L for females and 0.5 L for males were used,[28] to ensure the universal applicability and practicability of the method.

The odor recognition thresholds determined by the individual methods are summarized in Table 1. The obtained data revealed a difference of roughly a factor of 5 between the median odor threshold determined for **2a** using the novel method (1.9 × 10^{-6} ng L^{-1} air) and the previously published method (9.9 × 10^{-6} ng L^{-1} air). Accordingly, the new method provided comparable results, and the determination was possible without the use of an internal standard (Figure 4). Interindividual differences showed a stronger influence on the perception of lactone **2a** than the difference resulting from the two methods used, leading to deviations of several orders of

https://doi.org/10.1021/acs.jafc.3c08438
J. Agric. Food Chem. XXXX, XXX, XXX−XXX

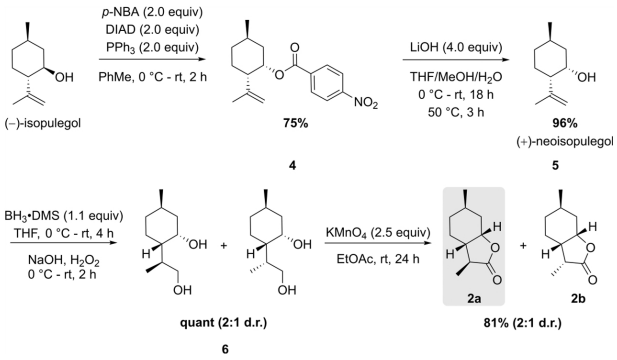

Figure 3. Synthesis of lactones 2 from (−)-isopulegol.

Table 1. Calculated Odor Thresholds (OT) for (*E*)-dec-2-enal (1), (3*S*,3a*S*,6*R*,7a*S*)-3,6-dimethyl-3a,4,5,6,7,7a-hexahydro-3*H*-1-benzofuran-2-one (2a) as well as (*R*)-1-*p*-menthene-8-thiol (3)[a]

proband	1[b] OT (ng L^{-1})[c]	2a OT (ng L^{-1})[c]	3 OT (ng L^{-1})[c]
1	1.0 ± 0.0	9.3×10^{-7} (2.5×10^{-6})	1.6×10^{-8} (4.4×10^{-8})
2	1.0 ± 0.0	3.0×10^{-5} (7.9×10^{-5})	1.6×10^{-8} (4.4×10^{-8})
3	0.7 ± 0.3	1.9×10^{-6} (9.9×10^{-6})	3.3×10^{-8} (8.8×10^{-8})
4	0.9 ± 0.3	2.3×10^{-6} (9.9×10^{-6})	5.1×10^{-9} (1.1×10^{-8})
5	1.8 ± 0.6	1.2×10^{-6} (1.2×10^{-6})	5.1×10^{-9} (1.1×10^{-8})

[a]Values in parentheses were determined employing the method previously reported by Ullrich and Grosch.[13] [b]Mean value and half range, calculated from the two determinations. [c]Calculated according to eq 2.

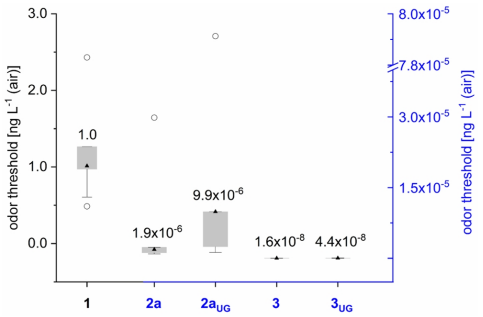

Figure 4. Box plot of odor thresholds, determined by five panelists, calculated according to eq 2 and according to Ullrich and Grosch (UG) for (*E*)-dec-2-enal (**1**) on left *y*-axis and for lactone (**2a**) and (*R*)-1-*p*-menthene-8-thiol (**3**) shown on the right *y*-axis. Median shown as triangle, outliers as circles, and Whiskers extending to ±1.5 × IQR.

magnitude. Likewise, the experimental data allowed for the calculation of the odor recognition threshold of **1** to be 1.0 ng L^{-1} in air. While the intensely minty and coconut-like smelling lactone **2a** was perceived up to a median *D*-value of 2^{28}, aldehyde **1** was only perceived up to a median *D*-value of 2^{9}. Thus, the odor threshold of internal standard **1** was several orders of magnitude higher compared to that of the aforementioned substance. For the grapefruit-like smelling (*R*)-1-*p*-menthene-8-thiol (**3**) odor thresholds of 1.6×10^{-8} ng L^{-1} air and 4.4×10^{-8} ng L^{-1} air (Ullrich and Grosch) were determined, thus resulting in a difference of roughly a factor of 3 between the two methods (Figure 4).

Overall, the newly developed method provided similar results compared with the published approach. However, at least for one participant, a strong difference in the perceptibility of the internal standard and lactone **2a** was noted. While this proband perceived the internal standard comparably well relative to the other participants, his *D*-value for the lactone was at least 2^{4} lower. This shows that the perception of specific compounds can vary greatly among different individuals and contradicts the use of a fixed value for the odor threshold of the internal standard, for example, **1**. This is especially evident when other published odor thresholds of the internal standard are compared to the value used for the calculation by Ullrich and Grosch. Hall and Anderson determined its threshold using a panel consisting of 12 persons by dynamic olfactometry.[29] Hereby, sensitivity varied across the panel, resulting in odor thresholds of 4.9 ng L^{-1} air (50% positive responses) and 7.9 ng L^{-1} air (75% positive responses). This additional source of error is now eliminated because an internal standard is no longer required. Furthermore, the novel method is less laborious. Especially for compounds that are not commercially available and must be synthesized or extracted from complex natural samples, the method additionally offers the advantage that the analytes are not blended by addition of an internal standard. Moreover, the novel method allows determining odor thresholds in parallel to aroma extract dilution analyses, which are commonly performed for complex aroma mixtures to identify the most potent and relevant compounds.

Compared with previously published odor thresholds for compound **2a**, the novel method provides comparable results. Buhr previously determined an odor threshold of 1×10^{-6} ng L^{-1} air for **2a**,[30] but analytical data partly differed from those described herein; therefore, an unequivocal assignment of the reported stereochemistry was not possible. With a median of 1.9×10^{-6} ng L^{-1} air determined within this study, compound

https://doi.org/10.1021/acs.jafc.3c08438
J. Agric. Food Chem. XXXX, XXX, XXX−XXX

2a indeed had an extraordinarily low threshold, which to the best of our knowledge is the lowest value reported for an aroma compound from a fungus. The investigations confirm that thiol **3** is arguably the most potent aroma compound known. The threshold values determined in this study for **3** (based on the method described herein and the method of Ullrich and Grosch) are still 2 orders of magnitude lower than for lactone **2a** (see above). A direct comparison with literature values for **3** is difficult, since data for its threshold in air are only available from one publication.[31] There, however, the lower threshold was attributed to the (*S*)-enantiomer with 6.6 × 10^{-6} ng L^{-1} (compared to 9.0 × 10^{-5} ng L^{-1} for the (*R*)-enantiomer). Since data on chiral analyses were not published by the authors, verification remains difficult. Disparities might also be attributed to differences in the optical purity. The synthetic route described within this study and the chiral separation on a *β*-6TBDM column showed an enantiomeric ratio of 90:10 in favor of the (*R*)-thiol.

Direct analysis of aroma compounds using GC−O enabled the establishment of a novel method for odor threshold determination in air without the need for an internal standard. The novel method reported herein has the major advantage of allowing the direct determination of extremely low odor thresholds in air. This method was applied to (3*S*,3a*S*,6*R*,7a*S*)-3,6-dimethyl-3a,4,5,6,7,7a-hexahydro-3*H*-1-benzofuran-2-one (**2a**) as well as (*R*)-1-*p*-menthene-8-thiol (**3**), compounds with the lowest known odor thresholds, for which internal standards with comparably low values are not available. The implementation requires: 1) a GC system equipped with an autosampler for reproducible injection and a flame ionization detector; 2) a cool on-column inlet to ensure complete and loss-free sample introduction to the GC column; 3) a splitting device for which the exact FID/ODP split ratios can be determined; 4) a heated transfer capillary to avoid delayed perception of aroma compounds; and 5) the analyte dissolved in a suitable solvent for gas chromatographic analysis. With this method in hand, compound **2a** was identified as the fungal aroma compound with the lowest odor threshold reported to date.

■ ASSOCIATED CONTENT

Supporting Information

The Supporting Information is available free of charge at https://pubs.acs.org/doi/10.1021/acs.jafc.3c08438.

Synthetic procedures for lactone **2a** and thiol **3** (PDF)

■ AUTHOR INFORMATION

Corresponding Author

Marco A. Fraatz − *Institute of Food Chemistry and Food Biotechnology, Justus Liebig University Giessen, Giessen 35392, Germany;* orcid.org/0000-0002-5028-9653; Phone: +49 (0) 641 99 349-02; Email: marco.fraatz@lcb.chemie.uni-giessen.de

Authors

Fabio F. Brescia − *Institute of Food Chemistry and Food Biotechnology, Justus Liebig University Giessen, Giessen 35392, Germany;* orcid.org/0000-0003-3182-3301

Jan Passinger − *Institute of Food Chemistry and Food Biotechnology, Justus Liebig University Giessen, Giessen 35392, Germany*

Raffael C. Wende − *Institute of Organic Chemistry, Justus Liebig University Giessen, Giessen 35392, Germany;* orcid.org/0000-0002-2242-4723

Peter R. Schreiner − *Institute of Organic Chemistry, Justus Liebig University Giessen, Giessen 35392, Germany;* orcid.org/0000-0002-3608-5515

Holger Zorn − *Institute of Food Chemistry and Food Biotechnology, Justus Liebig University Giessen, Giessen 35392, Germany; Fraunhofer Institute for Molecular Biology and Applied Ecology, Giessen 35392, Germany;* orcid.org/0000-0002-8383-8196

Complete contact information is available at: https://pubs.acs.org/10.1021/acs.jafc.3c08438

Notes

The authors declare no competing financial interest.

■ ACKNOWLEDGMENTS

The authors thank Jean-Philippe Kanter, Johanna Stein, and Victoria L. Hrazdil for their contribution to the sensory analysis as well as Thomas Albinus (GERSTEL GmbH & Co. KG) for fruitful discussions.

■ ABBREVIATIONS

er	enantiomeric ratio
O	olfactometry/olfactometric
ODP	olfactory detection port
RI	retention index/indices

■ REFERENCES

(1) International Organization for Standardization. Sensory analysis - Vocabulary; ISO 5492:2008. https://www.iso.org/standard/38051.html. (accessed February 16, 2024).

(2) Grosch, W. Evaluation of the key odorants of foods by dilution experiments, aroma models and omission. *Chem. Senses* **2001**, *26*, 533−545.

(3) Tanner, H.; Zanier, C.; Buser, H. R. 2,4,6-Trichloranisol: Eine dominierende Komponente des Korkgeschmacks. *Schweiz. Z. Obst-Weinbau* **1981**, *117*, 97−103.

(4) Leonardos, G.; Kendall, D.; Barnard, N. Odor threshold determinations of 53 odorant chemicals. *J. Air Pollut. Control Assoc.* **1969**, *19*, 91−95.

(5) Ohloff, G. *Riechstoffe und Geruchssinn*; Springer: Berlin Heidelberg, 1990.

(6) ASTM International. *Standard practice for determination of odor and taste thresholds by a forced-choice ascending concentration series method of limits*; ASTM E679−19: West Conshohocken, PA, 2019.

(7) Czerny, M.; Christlbauer, M.; Christlbauer, M.; Fischer, A.; Granvogl, M.; Hammer, M.; Hartl, C.; Hernandez, N. M.; Schieberle, P. Re-investigation on odour thresholds of key food aroma compounds and development of an aroma language based on odour qualities of defined aqueous odorant solutions. *Z. Lebensm. -Unters. Forsch.* **2008**, *228*, 265−273.

(8) Fischer, E.; Penzoldt, F. Über die Empfindlichkeit des Geruchssinnes. *Justus Liebigs Ann. Chem.* **1887**, *239*, 131−135.

(9) Nelson, P. E.; Hoff, J. E. Food Volatiles: Gas chromatographic determination of partition coefficients in water-lipid systems. *J. Food Sci.* **1968**, *33*, 479−482.

(10) Buttery, R. G.; Bomben, J. L.; Guadagni, D. G.; Ling, L. C. Some considerations of the volatilities of organic flavor compounds in foods. *J. Agric. Food Chem.* **1971**, *19*, 1045−1048.

(11) Buttery, R. G.; Guadagni, D. G.; Ling, L. C. Flavor compounds. Volatilities in vegetable oil and oil-water mixtures. Estimation of odor thresholds. *J. Agric. Food Chem.* **1973**, *21*, 198−201.

(12) Teranishi, R.; Buttery, R. G.; Guadagni, D. G. Odor quality and chemical structure in fruit and vegetable flavors. *Ann. N.Y. Acad. Sci.* **1974**, *237*, 209−216.
(13) Ullrich, F.; Grosch, W. Identification of the most intense volatile flavour compounds formed during autoxidation of linoleic acid. *Z. Lebensm. -Unters. Forsch.* **1987**, *184*, 277−282.
(14) Ullrich, F.; Grosch, W. Flavour deterioration of soya-bean oil: Identification of intense odour compounds formed during flavour reversion. *Fat Sci. Technol.* **1988**, *90*, 332−336.
(15) Ullrich, F.; Grosch, W. Identification of the most intense odor compounds formed during autoxidation of methyl linolenate at room temperature. *J. Am. Oil Chem. Soc.* **1988**, *65*, 1313−1317.
(16) Schieberle, P.; Grosch, W. Potent odorants of the wheat bread crumb: Differences to the crust and effect of a longer dough fermentation. *Z. Lebensm. -Unters. Forsch.* **1991**, *192*, 130−135.
(17) van Den Dool, H.; Kratz, P. D. A generalization of the retention index system including linear temperature programmed gas—liquid partition chromatography. *J. Chromatogr. A* **1963**, *11*, 463−471.
(18) Brescia, F. F.; Pitelas, W.; Yalman, S.; Popa, F.; Hausmann, H. G.; Wende, R. C.; Fraatz, M. A.; Zorn, H. Formation of diastereomeric dihydromenthofurolactones by *Cystostereum murrayi* and aroma dilution analysis based on dynamic headspace extraction. *J. Agric. Food Chem.* **2021**, *69*, 5997−6004.
(19) Chavan, S. P.; Zubaidha, P. K.; Dhondge, V. D. A short and efficient synthesis of (−) mintlactone and (+) iso-mintlactone. *Tetrahedron* **1993**, *49*, 6429−6436.
(20) Rigamonti, M. G.; Gatti, F. G. Stereoselective synthesis of hernandulcin, peroxylippidulcine A, lippidulcines A, B and C and taste evaluation. *Beilstein J. Org. Chem.* **2015**, *11*, 2117−2124.
(21) Schulte-Elte, K. H.; Ohloff, G. Über eine aussergewöhnliche Stereospezifität bei der Hydroborierung der Diastereomeren (1*R*)-Isopulegole mit Diboran. *Helv. Chim. Acta* **1967**, *50*, 153−165.
(22) Yadav, J. S.; Bhasker, E. V.; Srihari, P. Synthesis of a key intermediate for the total synthesis of pseudopteroxazole. *Tetrahedron* **2010**, *66*, 1997−2004.
(23) Gaudin, J.-M. Synthesis and organoleptic properties of *p*-menthane lactones. *Tetrahedron* **2000**, *56*, 4769−4776.
(24) Lecher, H. Z.; Greenwood, R. A.; Whitehouse, K. C.; Chao, T. H. The phosphonation of aromatic compounds with phosphorus pentasulfide. *J. Am. Chem. Soc.* **1956**, *78*, 5018−5022.
(25) Pedersen, B. S.; Scheibye, S.; Nilsson, N. H.; Lawesson, S.-O. Studies on organophosphorus compounds XX. Syntheses of thioketones. *Bull. Soc. Chim. Belges* **1978**, *87*, 223−228.
(26) Nishio, T. Direct conversion of alcohols into thiols. *J. Chem. Soc., Perkin Trans.* **1993**, *1*, 1113.
(27) Mardyukov, A.; Niedek, D.; Schreiner, P. R. Unravelling Lawesson's reagent: The structure of monomeric (4-methoxyphenyl)-phosphine disulfide. *Chem. Commun.* **2018**, *54*, 2715−2718.
(28) Hallett, S.; Toro, F.; Ashurst, J. V. Physiology, tidal volume. In *StatPearls*; StatPearls Publishing: Treasure Island (FL), 2022.
(29) Hall, G.; Andersson, J. Volatile fat oxidation products.: I. Determination of odour thresholds and odour intensity functions by dynamic olfactometry. *Lebensm. -Wiss. Technol.* **1983**, *16*, 354−361.
(30) Buhr, K.. *Untersuchungen zu Struktur-Geruchsbeziehungen von Lactonen*. Ph.D. Thesis; Bergische Universität Wuppertal: Wuppertal, 2006.
(31) Schoenauer, S.; Schieberle, P. Structure-odor activity studies on monoterpenoid mercaptans synthesized by changing the structural motifs of the key food odorant 1-*p*-menthene-8-thiol. *J. Agric. Food Chem.* **2016**, *64*, 3849−3861.

https://doi.org/10.1021/acs.jafc.3c08438
J. Agric. Food Chem. XXXX, XXX, XXX−XXX

6. **Chapter:** *O*- and *S*-methyltransferase from *Pleurotus sapidus* involved in flavor formation

A novel *O*- and *S*-methyltransferase from *Pleurotus sapidus* is involved in flavor formation

Brescia, F. F.; Korf, L.; Essen, L.-O.; Zorn, H.; Rühl, M.

J. Agr. Food Chem. **2024**, *72* (12), 6471–6480.

https://doi.org/10.1021/acs.jafc.3c08849

JOURNAL OF AGRICULTURAL AND FOOD CHEMISTRY

pubs.acs.org/JAFC Article

A Novel *O*- and *S*-Methyltransferase from *Pleurotus sapidus* Is Involved in Flavor Formation

Published as part of Journal of Agricultural and Food Chemistry virtual special issue "13th Wartburg Symposium on Flavor Chemistry and Biology".

Fabio Francesco Brescia, Lukas Korf, Lars-Oliver Essen, Holger Zorn,* and Martin Ruehl

Cite This: https://doi.org/10.1021/acs.jafc.3c08849 Read Online

ACCESS | Metrics & More | Article Recommendations | Supporting Information

ABSTRACT: Increasing consumer aversion to non-natural flavoring substances is prompting a heightened interest in enzymatic processes for flavor production. This includes methylation reactions, which are often performed by using hazardous chemicals. By correlation of aroma profile data and transcriptomic analysis, a novel *O*-methyltransferase (OMT) catalyzing a respective reaction within the formation of *p*-anisaldehyde was identified in the mushroom *Pleurotus sapidus*. Heterologous expression in *E. coli* followed by purification allowed for further characterization of the enzyme. Besides *p*-hydroxybenzaldehyde, the proposed precursor of *p*-anisaldehyde, the enzyme catalyzed the methylation of further hydroxylated aromatic compounds at the *meta*- and *para*-position. The K_m values determined for *p*-hydroxybenzaldehyde and *S*-adenosyl-L-methionine were 80 and 107 μM, respectively. Surprisingly, the studied enzyme enabled the transmethylation of thiol-nucleophiles, as indicated by the formation of 2-methyl-3-(methylthio)furan from 2-methyl-3-furanthiol. Moreover, the enzyme was crystallized at a resolution of 2.0 Å, representing the first published crystal structure of a basidiomycetous OMT.

KEYWORDS: *aroma, Basidiomycota, biocatalysis, fungi*

INTRODUCTION

The transfer of methyl groups, catalyzed by methyltransferases (MTs; EC 2.1.1.-) to a broad spectrum of molecules, occurs ubiquitously in all organisms. The biological significance of MTs includes the biosynthesis of complex molecules, detoxification, nucleic acid processing and repair, protein sorting and repair, signal transduction, and homeostasis.[1−3] Besides less often used cofactors like betaine, cobalamin, and tetrahydrofolic acid, the majority of MTs utilize *S*-adenosyl-L-methionine (known as AdoMet or SAM) as a cofactor.[4,5] As the byproduct of the methylation reaction with homocysteine (Hcy) as a methyl group acceptor, *S*-adenosyl-L-homocysteine (AdoHcy or SAH) is not regenerated and catabolized after the methyl-group transfer, and SAM is partly addressed as a cosubstrate.[2,4] Methylation reactions using SAM are energetically favorable (ΔG^0 = −17 kcal/mol for AdoMet + Hcy → AdoHcy + Met), which also explains its catalytic preference in comparison to other methyl-donors.[4,6,7] The methylation of the nucleophilic substrate thereby proceeds via an S_N2-like mechanism (Figure 1).[8]

Since the first structure of an AdoMet-dependent MT (DNA Methyltransferase *Hha*I) was published in 1993,[9] numerous structures were elucidated in the last decades and allowed for a classification based on structural motifs. A review published in 2003 proposed a classification into five different classes based on structural folds.[6] However, a more recent publication suggested four additional classes as a result of a study on the methyltransferases of *Saccharomyces cerevisiae*.[10] Additionally, a further categorization of MTs relies on the target atoms and

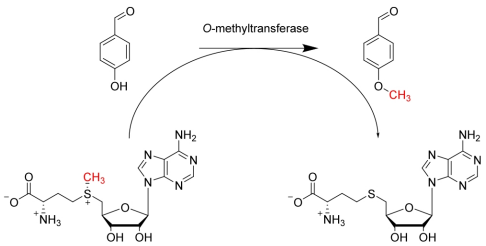

Figure 1. OMT-catalyzed transmethylation reaction of *p*-hydroxybenzaldehyde and SAM forming *p*-anisaldehyde and SAH.

acceptors of the methyl group. Most commonly, oxygen acts as the nucleophile (OMT) followed by nitrogen and carbon. However, also sulfur and halides[11] have been described as possible nucleophiles.[2] The target molecules include hormones, neurotransmitters, lipids, proteins, nucleic acids, glycans, and small molecules such as terpenoids or phenolic

Received: November 26, 2023
Revised: February 28, 2024
Accepted: February 28, 2024

compounds.[1,4,10,12,13] MTs acting on the latter group of compounds, also known as small-molecule or natural product MTs, play a key role in the biosynthesis of secondary plant metabolites as the resulting products like flavonoids, alkaloids, and phenylpropanoids are associated with plant growth, development, and defense.[12] In addition, methylated monolignols like coniferyl and sinapyl alcohol are essential for the biosynthesis of lignin.[14]

So far, less studied organisms, especially with regard to the presence of novel OMT activities toward small molecules, comprise fungi of the phylum Basidiomycota. However, due to their extremely versatile biocatalytic portfolio, Basidiomycota represent a highly promising source for such enzymes. To the best of our knowledge, only two small-molecule OMTs from *Phanerochaete chrysosporium* have been functionally expressed from Basidiomycota yet.[15] Especially for members of the white-rot fungi, such as *P. chrysosporium*, which are characterized by their ability to degrade lignin, OMTs are assumed as a detoxification mechanism of free phenolic groups formed during lignin degradation.[15−18] In cultures of the white-rot fungus *Bjerkandera adusta*, several methoxybenzylic compounds were identified, including *p*-anisaldehyde as an aroma compound. Lapadatescu et al. (2002) postulated a biosynthetic pathway starting from phenylalanine, in which *p*-anisaldehyde is formed via methylation of *p*-hydroxybenzaldehyde, which indicated the presence of an OMT.[19] Moreover, the formation of *p*-anisaldehyde was observed for several other Basidiomycota of the genus *Pleurotus*, including the intensely studied white-rot fungus *Pleurotus sapidus*.[20] In a recent study, *P. sapidus* produced up to 160 mg *p*-anisaldehyde per liter of culture medium, and further supplementation studies using labeled tyrosine revealed the formation of labeled *p*-anisaldehyde.[21] Thus, an analogous biosynthetic pathway compared to *B. adusta* and the presence of an OMT in the biosynthesis of *p*-anisaldehyde in *P. sapidus* seemed evident. However, enzymes involved in potential methylation reactions catalyzing the formation of *p*-anisaldehyde are so far unknown. The identification of OMTs in Basidiomycota in general may be highly interesting for the production of natural flavor substances, as chemically synthesized aroma compounds suffer from increased consumer rejection. This also applies for *p*-anisaldehyde, which is currently mainly produced by methylation and oxidation of *p*-cresol or by oxidation of anethole.[22] Biocatalytic applications allow, among other advantages, reduction of the use of hazardous chemicals used for such syntheses and, therefore, fulfill the principles of green chemistry. Thus, the aims of this study were to identify and characterize an OMT from *P. sapidus* involved in the formation of *p*-anisaldehyde by using an approach that combines molecular biology, analytical chemistry, and bioinformatics. The results of this study reveal a novel OMT that enables the methylation of various substrates and highlights the potential of Basidiomycota as a promising source for such enzymes.

MATERIALS AND METHODS

Chemicals. All chemicals used for the cultivation of *P. sapidus* strains, and also glycerol (99%), *p*-hydroxybenzaldehyde (98%), 6-hydroxycoumarin (96%), *o*-, *m*-, and *p*-hydroxybenzyl alcohol (all 99%), imidazole (99.5%), *m*-methoxybenzyl alcohol (98%), and *p*-methoxybenzyl alcohol (98%) were purchased from Sigma-Aldrich (Taufkirchen, Germany). Diethyl ether (99.5%) was supplied by BCH Bruehl-Chemikalien Handel (Bruehl, Germany). Ethanol (99.9%), 2-methoxybenzaldehyde (98%), and *n*-pentane (99%) were obtained from Th. Geyer (Hamburg, Germany). HPLC-grade methanol was obtained from J. T. Baker (Aventor Performance Materials, Gliwice, Poland). Ammonium acetate (99%) was purchased from VWR (Radnor Pennsylvania, USA). 2-Hydroxybenzaldehyde (99%), 3-hydroxybenzaldehyde (99%), and *m*-anisaldehyde (98%) were supplied by J&K Scientific (Pforzheim, Germany). *p*-Anisaldehyde (98%) and veratric aldehyde (99%) were obtained from Alfa Aesar (Kandel, Germany). *S*-Adenosyl-L-methionine disulfate tosylate (95%) was obtained from Fluorochem (Hadfield, United Kingdom). TRIzol was supplied by Life Technologies (Carlsberg, California, USA). Acetic acid (100%), agar−agar Kobe I, bovine albumin fraction V (98%), bromophenol blue (sodium salt), carbencillin disodium (98%), 3,4-dihydroxybenzaldehyde (98%), dimethyl sulfoxide (99.5%), disodium hydrogen phosphate dihydrate (98%), glycine (99%), hydrochloric acid (37%), isopropyl-β-D-thiogalactopyranoside (99%), LB-medium (Lennox), β-mercaptoethanol (99%), Rotiphorese Gel 40, sodium chloride (99.8%), sodium dihydrogen phosphate monohydrate (98%), sodium dodecyl sulfate (99%), tetramethylenediamine (TEMED), sodium sulfate (99%), tris(hydroxymethyl)-aminomethane (TRIS, 99%), TRIS-hydrochloride (99%), Tween 20 (Ph. Eur.), and vanillin (99%) were obtained from Carl Roth (Karlsruhe, Germany). Ammonium persulfate (100%) was obtained from Merck (Darmstadt, Germany), isovanillin (98%) from Acros Organics (Geel, Belgium), 7-hydroxycoumarin (98%) and thymol (95%) from TCI (Tokyo, Japan), Coomassie Brilliant Blue R250 and ethylenediaminetetraacetic acid (99%) from AppliChem (Karlsruhe, Germany), 6-methoxycoumarin (95%) from ABCR (Karlsruhe, Germany), Midori Green Direct from Nippon Genetics (Düren, Germany), and Agarose LE from Biozym (Oldendorf, Germany). Helium (5.0) was purchased from Praxair (Düsseldorf, Germany), and nitrogen (5.0) was from Air Liquide (Düsseldorf, Germany). All purity specifications represent the respective minimum.

Cultivation of Fungi and Sample Preparation. *Pleurotus sapidus* (DSM no. 8266) dikaryotic (DK5) strain was obtained from the German Collection of Microorganisms and Cell Cultures (Brunswick, Germany) and kept on malt extract (ME) agar (20 g of malt extract, 15 g of agar; per liter of ultrapure water) as stock cultures. Monokaryotic (MK) strain 57 was derived from the basidiospores of the DK strain and provided by the Institute of Food Chemistry of Leibniz University Hannover (Germany).[23] For the submerged cultivation, malt extract peptone (MEP) medium was used, containing 30 g of malt extract and 3 g of soy peptone (pH 5.6; respective compound per liter of ultrapure water). For precultures, a 0.5 cm × 0.5 cm piece of an 80% overgrown ME agar stock culture was transferred to a 100 mL-Erlenmeyer flask, containing 40 mL of MEP medium, and homogenized at 10,000 rpm for 30 s by means of an Ultra-Turrax T25 homogenizer (IKA, Staufen, Germany). Cultivation of precultures was carried out at 24 °C in darkness for 4 days on a rotary shaker (Orbitron, Infors, Einsbach, Germany) at 150 rpm (25 mm shaking diameter). For the inoculation of main cultures, two precultures were homogenized (Ultra-Turrax; 10,000 rpm, 30 s), pooled, and added to the main culture (ratio 1:10, v/v) containing MEP medium. Cultivation was carried out under the same conditions as those for the precultures. For each day of the four main culture days, triplicates of DK5 and MK57 were cultivated. Every main culture day, the respective triplicate from the two strains was harvested by centrifugation (3000*g*, 10 min, and 4 °C) and the separated mycelium stored at −80 °C. From each culture, 5 mL supernatants were transferred to sterile headspace vials (20 mL), sealed with silicone/PTFE caps, and stored at −20 °C.

Aroma Analysis. Prior to the aroma extraction, the supernatants were thawed at 4 °C and 50 μL of internal standard solution (thymol $3.144 \cdot 10^{-3}$ mg mL^{-1}) was added. The samples were extracted using 10 mm stir bars with 0.5 mm PDMS coating (Twister, GERSTEL, Mülheim an der Ruhr, Germany) at 4 °C and 1000 rpm for 1 h. After extraction, the stir bars were removed from the samples, rinsed with ultrapure water, dried with lint-free tissues, and placed in a conditioned Thermal Desorption Unit (TDU) liner (GERSTEL). Gas chromatographic analyses were performed using an Agilent 7890B gas chromatograph connected to an Agilent 5977B mass spectrometer (Agilent Technologies, Waldbronn, Germany). The

https://doi.org/10.1021/acs.jafc.3c08849
J. Agric. Food Chem. XXXX, XXX, XXX−XXX

system was equipped with a Thermal Desorption Unit 2 (TDU; GERSTEL) and a Cold Injection System 4 (CIS; GERSTEL). Aroma compounds were thermally desorbed in the TDU and cryo-focused in a CIS equipped with deactivated glass wool liner in solvent−vent mode. The TDU temperature was kept at 40 °C (0.5 min hold time) and then raised at 120 °C min^{-1} to 250 °C (10 min). For cryofocusing, the CIS was held at −70 °C (0.5 min; cooled with liquid nitrogen) and raised at 12 °C s^{-1} to 250 °C (5 min). For compound separation, a polar Agilent VF-WAXms [30 m × 0.25 mm; 0.25 μm film thickness; temperature program, 40 °C (3 min hold time), 5 °C min^{-1} to 240 °C (12 min); carrier gas, helium (1.56 mL min^{-1}, constant flow)] was used. After the GC column, the carrier gas flow was split by means of a μFlowManager Splitter (GERSTEL) into the mass spectrometer [transfer line temperature, 250 °C; electron ionization energy, 70 eV; ion source temperature, 230 °C; quadrupole temperature, 150 °C; scan range, m/z 33−300] and to a GERSTEL Olfactory Detection Port 3 (ODP) [transfer line temperature, 300 °C; mixing chamber temperature, 200 °C; mixing chamber gas, nitrogen] in a 1:1 ratio. For liquid injection, a split−splitless (S/SL) inlet (250 °C) equipped with a deactivated glass wool liner was used instead of the TDU/CIS system. The obtained mass spectra and retention indices (RI) calculated according to van den Dool and Kratz[24] were compared to published data, the National Institute of Standards and Technology (NIST) 2011 MS library, and to those of authentic reference compounds. For qualitative evaluation, MassHunter Qualitative Analysis (B.07.00) was used. Peak areas of the internal standard (qualifier: m/z 91 and m/z 150; quantifier m/z 135) and *p*-anisaldehyde (qualifier: m/z 107 and m/z 135; quantifier m/z 136) were determined using MassHunter Quantitative Analysis (B.07.01) from obtained TIC data.

RNA Isolation and Sequencing. For RNA extraction, frozen mycelium was ground into a powder using a mortar and pestle under liquid nitrogen. According to the instructions of the manufacturer, the total RNA was extracted using TRIzol. The extracted RNA was diluted in ultrapure water, and the concentration and purity were controlled by means of photometric analysis (Pearl nanophotometer, Implen, Munich, Germany) and agarose gel electrophoresis (Peqlab electrophoresis chamber; VWR Life Science). RNA samples were stored at −80 °C and shipped on dry ice to Novogene UK (Novogene, Cambridge, UK) for sequencing. Quality control as well as quantification were verified by Novogene using a capillary gel electrophoresis system (Bioanalyzer, Agilent, Waldbronn, Germany) and samples were sequenced by means of Illumina NovaSeq after library preparation using NEBNext Ultra RNA Library Prep Kit for Illumina (NEB, USA). Raw reads were processed as FastQ files using fastp (https://github.com/OpenGene/fastp) to obtain high quality clean reads.

Bioinformatics. Amino acid sequences of both characterized OMTs from *P. chrysosporium* (Uniprot accession numbers: P0CT89 and P0CT90) were blasted against the *P. sapidus* assembled and annotated genome (ASM2674385v1) using blastp within Geneious (Biomatters Inc., Auckland, New Zealand). Read counts of blastp hits with an expected value of < e^{-100} were compared to *p*-anisaldehyde concentrations of the respective samples (on day 1, day 2, and day 3 of the main cultivation). Only gene g12203 showed positively correlating transcripts.

Cloning and Heterologous Expression of OMT. The codon-optimized OMT gene g12203, cloned into the pColdI plasmid, was purchased from BioCat (BioCat, Heidelberg, Germany). For heterologous protein expression of the PSA-OMT1 (cf. Supporting Information S3), the plasmid was transformed into *E. coli* BL21 Gold (DE3) cells (New England Biolabs, Frankfurt, Germany) according to the protocol of the manufacturer. Cultivation was performed using lysogeny broth (LB) medium containing carbenicillin (100 μg mL^{-1}) as selection marker at 37 °C until an OD_{600} of 0.4−0.6 in baffled flasks. Expression was induced by the addition of isopropyl-β-D-thiogalactopyranoside to a final concentration of 0.1 mM. The cells were subsequently cultivated for 24 h at 16 °C, afterward harvested by centrifugation (4000*g*, 30 min, and 4 °C), and stored at −20 °C until further use.

Purification of OMT. For cell disruption, the harvested *E. coli* cells were thawed on ice, suspended in lysis-buffer (50 mM phosphate, 300 mM NaCl, 5% glycerol, pH 7.4; 20 to 25% solution (m/v)), and sonicated (Bandelin Sonoplus, Berlin, Germany) with 3 cycles (amplitude 40%; 60 s each, 60 s rest in between) on ice. Cell debris was removed by centrifugation (16,000*g*, 30 min, and 4 °C). Protein purification was accomplished via immobilized metal affinity chromatography using an NGC Quest 10 system (Bio-Rad Laboratories, Feldkirchen, Germany) and a 5 mL HisTrap column (GE Healthcare GmbH, Solingen, Germany) since the modified protein provides C- and N-terminal His_6-tags. Prior to purification, the column was washed with one column volume (CV) of lysis buffer (containing 120 mM imidazole). The supernatant was loaded onto the column and washed with 3.5 CV of imidazole lysis buffer, and the protein was eluted using 500 mM imidazole buffer (50 mM phosphate, 300 mM NaCl, 5% glycerol, pH 7.4). For desalting, three 5 mL HiTrap Desalting columns (GE Healthcare) and 50 mM phosphate buffer (elution buffer, pH 7.0) were used. The columns were equilibrated with the buffer and after the sample application washed with 1.5 CV of the elution buffer. Purified OMT was analyzed by sodium dodecyl sulfate polyacrylamide gel electrophoresis (SDS−PAGE) according to Laemmli[25] (4% stacking and 12% resolving gel, CBB R250 for staining) and Western Blot using a PerfectBlue Tank Electro Blotter Web S (Peqlab, Erlangen, Germany) and Towbin buffer (0.25 M Tris, 1.92 M glycine, and 5% (v/v) methanol)[26] for blotting (1000 mA, 75 min) on a polyvinylidene fluoride membrane (Carl Roth, Karlsruhe, Germany). The membrane was subsequently incubated in milk powder solution (5% milk powder in TBST buffer [50 mM TRIS (pH 7.5), 150 mM NaCl, and 0.1% Tween 20]) at 4 °C overnight. For staining of the His-tagged protein, the membrane was incubated overnight with Anti His-HRP antibody (Carl Roth) at 24 °C and stained utilizing an Opti-4CN Substrate Kit (Bio-Rad) according to the instructions of the manufacturer. Protein concentration was determined by means of a Bradford assay using ROTIQuant (Carl Roth) according to the manufacturer's manual. The molecular mass of PSA-OMT1 was calculated using the Expasy Compute pI/Mw tool.

Enzyme Assay. Enzymatic conversions were performed using headspace vials (20 mL) at a fixed enzyme concentration of 0.16 μM and a reaction volume of 5 mL on a rotary incubator (40 rpm, mixing angle of 70°; Stuart, Stone, UK) for 2 h in triplicate if not specified otherwise. The concentrations of SAM and of the respective substrate (dissolved in 30% ethanol or 100% DMSO for substrate screening, respectively) were fixed at 500 μM, unless specified otherwise. After conversion, the samples were cooled on ice and 100 μL 6 M HCl (HPLC analysis) and 200 μL 5 M HCl (GC analysis) was added. For GC analysis, the samples were extracted using 2 mL distilled *n*-pentane/diethyl ether (1:1.12; v/v) on the rotary shaker for 15 min. After extraction, the organic layer was removed, dried over anhydrous sodium sulfate, and directly used for GC−MS analysis. For HPLC analysis, the samples were filtered (polyester filter, 0.45 μm pore diameter) and directly used. If not indicated otherwise, measurements were performed by means of HPLC.

HPLC Method. HPLC analyses were performed using a Shimadzu LC-20 System (Shimadzu, Duisburg, Germany), equipped with a quaternary pump (LC20-AD), an autosampler (SIL-20ACHT), a column oven (CTO-20AC), and a photo diode array detector (SPD-M20A). For data analysis, LabSolution, ver. 5.93 (Shimadzu), was used. Separations were conducted utilizing a Waters AtlantisT3 column (100 mm × 3 mm; 5 μm particle size) at 25 °C, a flow rate of 1 mL min^{-1} (detection 200−600 nm, 1.5625 Hz, and 1.2 nm slit width) with 0.01 M (pH 4.2) ammonium acetate buffer (A) and methanol (B). The binary gradient was set as follows: 0 min, 75% A; 0−4 min ramp to 60% A; 4−9 min ramp to 30% A; 9−11 min ramp to 75% A; 11−14 min hold at 75% A. For quantitation, standards of the respective methylated products were measured ranging from 1 to 500 μM.

Determination of pH and Temperature Optima, Kinetic Parameters. The influence of pH values was studied using Davies Buffer (pH 2−12)[27] (measured via GC−MS) and phosphate buffer

https://doi.org/10.1021/acs.jafc.3c08849
J. Agric. Food Chem. XXXX, XXX, XXX−XXX

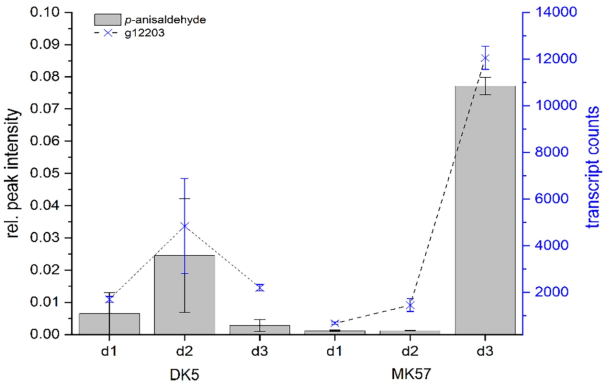

Figure 2. Correlation of the transcript count of g12203 (OMT) and the relative peak areas of *p*-anisaldehyde (referred to the internal standard) of submerged cultivated dikaryotic (DK5) and monokaryotic (MK57) strains of *P. sapidus*.

(100 mM, pH 6.2−8.2) at 24 °C and temperature at 14−44 °C with *p*-hydroxybenzaldehyde as the substrate. Kinetic parameters of the OMT were determined by variation of the SAM or *p*-hydroxybenzaldehyde concentration ranging from 25 to 400 μM and fixed concentration of either the substrate or SAM at 500 μM. The formation of *p*-anisaldehyde was quantified after a reaction time of 20 min. Enzyme kinetics were calculated using OriginPro 2020 (nonlinear fit, enzyme kinetics, Michaelis Menten, Levenberg−Marquardt) from biological triplicates of the respective conversion.

Crystallization and Structure Analysis of PSA-OMT1. Purified PSA-OMT1 in 25 mM Tris-HCl (pH 7.4) buffer (26.3 mg/mL) was filtered and crystallized in the presence of 15%(w/v) PEG 3K, 20%(v/v) 1,2,4-butanetriol, 1%(w/v) nondetergent sulfobetaine 256, 0.01 M of each spermine·4HCl, spermidine·3HCl, 1,4-diaminobutane·2HCl, DL-ornithine·HCl, and 0.1 M glycylglycine/2-amino-2-methyl-1,3-propanediol pH 8.5 (Morpheus II H9, *Nextal*), resulting in orthorhombic crystals. Protein crystallization was performed as sitting drop experiment in 96-well plates by mixing 300 nL of protein solution with 300 nL of crystallization condition. The data set for PSA-OMT1 was collected at the PXI beamline of the Swiss Light Source (SLS) at the Paul-Scherrer-Institute (PSI, Switzerland). The data set was corrected with the STARANISO server[28] to improve overall data range. PSA-OMT1 structure was solved at a resolution of 2.0 Å using molecular replacement with an AlphaFold2[29] search model based on the native sequence of PSA-OMT1. Structure refinements were done by multiple rounds of manual model building with Coot[30] followed by phenix.refine.[31]

RESULTS AND DISCUSSION

Correlation of Aroma Analysis and Transcriptomic Data. The aroma profile of a submerged culture of dikaryotic *P. sapidus* strain DSMZ 8266 (DK) containing numerous identified aroma compounds has been reported previously.[32] The identified compounds included rarely occurring terpenoids like dill ether and stereoisomers of the wine lactone, carbonyls such as 1-octen-3-one, and acrylic compounds such as benzaldehyde and *p*-anisaldehyde. In accordance with the findings described by Trapp et al. (2019), the formation of these compounds was also observed in this study. However, differences between the DK and the monokaryotic (MK) strain regarding the time point of occurrence and the intensity of distinct aroma compounds emerged. For *p*-anisaldehyde, the highest amounts formed by the DK strain were detected on the second main-culture day, with a decreasing intensity on the third day. In contrast, the *p*-anisaldehyde formation by the MK strain increased over the cultivation period, reaching its maximum on the third main-culture day (Figure 2). Moreover, the amount of *p*-anisaldehyde formed by the MK was 3-fold higher compared to that of the DK. To the best of our knowledge, differences between MK and DK strains of fungi with respect to aroma compound formation have rarely been published thus far. Omarini et al. (2014) demonstrated some MK strains of *P. sapidus* showed an improved biotransformation rate of (+)-valencene to (+)-nootkatone compared to the DK strain.[23] More recently, Bürger et al. (2022) determined differences in the aroma profile of *P. sapidus* MK and DK strains.[21] Furthermore, Krahe et al. (2021) showed differences in *p*-anisaldehyde formation via cleavage of *trans*-anethole between different *P. sapidus* strains as a result of variability of peroxidase gene expression and sequence alterations in the monokarya after meiosis.[33] Thus, differential enzyme expression seemed evident to be the cause of the different *p*-anisaldehyde formation of DK and MK strains.

In order to identify the OMT involved in the formation of *p*-anisaldehyde, RNA was extracted from the mycelium of the DK and MK strains used in this study on three different culture days and subsequently sequenced. The transcriptomic data revealed a differentially expressed gene (g12203) between the MK and the DK strains, which was annotated as an *O*-methyltransferase (PSA-OMT1) in the genome of *P. sapidus* (Figure 2). The transcript pattern correlated well with the determined relative peak areas of *p*-anisaldehyde. Therefore, involvement of the coding enzyme (PSA-OMT1) in the biogenesis of *p*-anisaldehyde was assumed.

Heterologous Expression of *P. sapidus* O-Methyltransferase in *E. coli*. For heterologous protein expression of the PSA-OMT1 in the pColdI vector, the *E. coli* strain BL21 Gold(DE3) was used. SDS−PAGE analysis as well as western blotting using the anti-His antibody with conjugated horseradish peroxidase revealed successful soluble enzyme expression of PSA-OMT1 (53.6 kDa) at 16 °C using 0.1 mM IPTG (Figure 3). The enzyme activity was confirmed by GC-MS and HPLC measurement of the conversion of *p*-hydroxybenzaldehyde and SAM forming *p*-anisaldehyde. Thus, far, the formation of *p*-anisaldehyde by methylation of *p*-hydroxybenzaldehyde by Basidiomycota such as *Bjerkandera*

https://doi.org/10.1021/acs.jafc.3c08849
J. Agric. Food Chem. XXXX, XXX, XXX−XXX

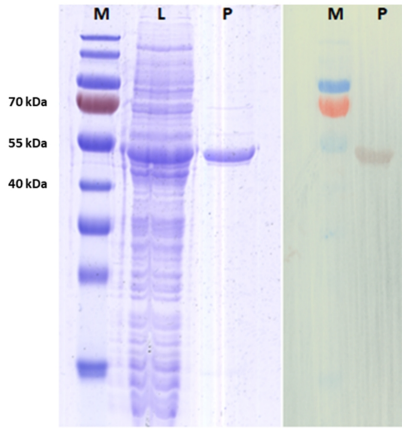

Figure 3. SDS-PAGE analysis of OMT (L: Lysate of *E. coli*; P: Protein after purification using Ni-NTA) and western blot membrane (anti-His tag antibody).

adusta has only been postulated without any known enzyme being able to catalyze the respective reaction.

Besides two OMTs of *P. chrysosporium*, other basidiomycetous OMTs have not been functionally expressed and characterized so far. In contrast, for plants such as alfalfa (*Medicago sativa* L.),[34] loquat (*Eriobotrya japonica*),[35] rice (*Oryza sativa* L.),[36] grape vine (*Vitis vinifera* L.)[37] and others, several OMTs have been characterized and published. However, the approach described in this study for the identification of an OMT based on the correlation of aroma analysis data as secondary metabolite products in combination with the corresponding transcriptomic data has not been applied thus far.

Determination of pH and Temperature Optima. Effects on the conversion of *p*-hydroxybenzaldehyde using PSA-OMT1 were studied in Davies universal buffer ranging from pH 2−12 at 24 °C for an estimation of the optimal pH-value for the reaction (cf. Supporting Information S1). The GC data revealed that no activity was present below pH 6 and above pH 9, with an optimum between pH 6 and 8. For a more precise determination, enzymatic conversions were performed using phosphate buffer ranging from pH 6.2 to 8.2 at 24 °C. The highest yields of *p*-anisaldehyde were obtained at pH 7.4, with higher pH values leading to a greater loss of activity than more acidic conditions. The optimized pH condition was applied for temperature testing, whereby 34 °C proved to be the temperature optimum of the studied reaction (Supporting Information S1).

The optimal pH conditions determined for PSA-OMT1 were comparable to the data reported for the two heterologously expressed OMTs of *P. chrysosporium* (pH 7.5 for Mtrase#1 and pH 8.0 for Mtrase#2) using coniferyl alcohol as a substrate.[15] In two previous publications, Coulter et al. (1993) and Jeffers et al. (1997) investigated the influence of the pH value and temperature on the catalytic activity of two different OMTs, which were purified from *P. chrysosporium* mycelium. The *p*-OMT investigated by Coulter et al. showed the highest activity toward 3-methoxy-*p*-hydroxyacetophenone at pH 8.0 and 45 °C.[18] Contrary, for the 3-OMT studied by Jeffers et al., the pH and temperature optima for the conversion of 3-hydroxy-4-methoxybenzoic acid were determined to be pH 7.5 and 37 °C and, thus, more similar to those of PSA-OMT1.[17] Kirita et al. isolated an OMT from the mycelium of *Flammulina velutipes*, which converted (−)-epigallocatechin-3-*O*-gallate to the respective methylated products at optima of pH 7.0 and 37 °C.[38] Furthermore, Wat and Towers (1974) isolated an OMT from the mycelium of the brown-rot fungus *Neolentinus lepideus* (syn. *Lentinus lepideus*) that is involved in the formation of methyl 4-methoxycinnamate.[39] For the enzymatic conversion of methyl 4-hydroxycinnamate to the respective methylated product, a pH value of 7.0 was found to be optimal. Accordingly, the determined optima for PSA-OMT1 were consistent with the data described for other fungal OMTs. The enhancing effect of bivalent cations such as Mg^{2+} on the activity described for some plants and animal OMTs was also tested; however, this did not result in an increased formation of *p*-anisaldehyde by PSA-OMT1 (data not shown), suggesting an independence from bivalent cations, which needs to be further confirmed by chelating experiments. However, this preliminary result was in agreement with those of other fungal OMTs previously listed.[15,17,18,39]

Enzyme Kinetic Parameters. Kinetic parameters for fungal OMTs have rarely been described in the literature. Coulter et al. (1993) determined a K_m value for *p*-OMT of 34 μM for acetovanillone and 99 μM for the cofactor SAM.[39] Jeffers et al. (1997) cited a K_m value of 76 μM for isovanillic acid (111 μM for SAM) and of 108 μM for 3,4-dihydroxybenzoic acid (107 μM for SAM) for a 3-OMT.[17] Thus, the K_m values of 80.3 and 107.0 μM for *p*-hydroxybenzaldehyde and SAM, respectively, determined in this study were comparable to those described in the literature (Table 1, cf. Supporting Information S2).

Table 1. Determination of Enzyme Kinetic Parameters of PSA-OMT1 for *p*-Hydroxybenzaldehyde and SAM

parameter[a]	*p*-hydroxybenzaldehyde	SAM
Michaelis−Menten constant, K_m (μM)	80.3 ± 6.9	107.0 ± 16.9
maximum reaction speed, v_{max} (mU mg^{-1})	44.6 ± 2.0	54.4 ± 3.5
catalytic constant, k_{cat} (s^{-1})	0.04	0.05
catalytic efficiency, k_{cat}/K_m (s^{-1} μM^{-1})	0.0005	0.0005

[a]Calculated using OriginPro 2020 from biological triplicates of the respective conversion.

Determination of Conversion Rates. In the standard assay (0.16 μM enzyme, 2 h conversion time), about 17 μM *p*-anisaldehyde was formed. Conversions using an increased enzyme concentration of 1 μM and varying equimolar concentrations of *p*-hydroxybenzaldehyde and SAM (50, 100, and 500 μM) over 24 h under optimal pH and temperature conditions led to a conversion rate of 12−14%. An increase in the product yield to 22% was achieved within 24 h by omitting the homogenization of the reaction mixture (Figure 4). The lower conversion while using the rotary incubator rate might be due to mechanical stress and enzyme denaturation resulting thereof. Generally, it should be noted that SAH is known to be a strong inhibitor of OMTs and, thus, might affect the reaction.

https://doi.org/10.1021/acs.jafc.3c08849
J. Agric. Food Chem. XXXX, XXX, XXX−XXX

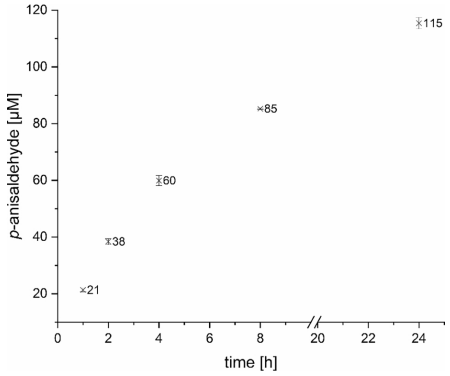

Figure 4. Time-dependent formation of *p*-anisaldehyde over 24 h starting from *p*-hydroxybenzaldehyde. Reactions were performed in triplicate and error bars represent the respective standard deviation.

Conversion of Different Substrates. As the substrate specificity of the OMTs can vary depending on the enzyme studied, the regioselectivity of methylation was tested using substrates with altered positions of the hydroxyl group. The two OMTs studied by Pham and Kim (2016) were, for example, able to convert 3- and 4-hydroxy-substituted substrates.[15] Accordingly, *o*-, *m*-, and *p*-hydroxy-substituted benzaldehydes were used for conversion with PSA-OMT1 (Figure 5). In addition, the significance of the presence of an electron-withdrawing group was tested by using the corresponding alcohols instead of aldehydes. The data revealed that PSA-OMT1 did not convert *o*-substituted substrates under the studied conditions. The highest concentrations were detected for *p*-anisaldehyde (37 μM) followed by *p*-methoxybenzyl alcohol (8 μM) and *m*-anisaldehyde (3 μM). For *m*-hydroxybenzyl alcohol, no conversion was detected under the applied conditions. As the concentration of *m*-anisaldehyde formed was lower compared to that of *p*-methoxybenzyl alcohol, a preference toward *p*-substituted substrates was observed. The influence of the electron-withdrawing group is thus apparently weaker compared to that of the position of the substitution. This was also confirmed in the conversion of vanillin and isovanillin. While vanillin was converted to veratric aldehyde (13 μM), no conversion was observed for isovanillin. As bicyclic substrates, 6- and 7-hydroxycoumarin were tested, and again, a conversion to the respective methylated product was detected only for the *p*-substituted compound (23 μM). As a dihydroxylated substrate, 3,4-dihydroxybenzaldehyde was tested; however, no conversion to vanillin, isovanillin, or veratric aldehyde was detected under the applied conditions. Overall, PSA-OMT1 successfully converted monohydroxylated compounds at *m*- and *p*-position, comparable to previously described fungal OMTs.

In addition to the methylation of compounds containing one specific acceptor atom, at least one enzyme has been reported to accept multiple nucleophiles.[40] Apart from the conversion of hydroxyl groups, methylation of sulfur groups would be interesting for the production of aroma compounds. The formation of such methylated sulfurous aroma compounds by Basidiomycota has recently been reported for three species of the genus *Laetiporus*, namely, *L. sulphureus*, *L. montanus*, and *L. persicinus*. During the cultivation of these fungi, the meaty-like smelling aroma compounds 2-methyl-3-(methylthio)furan and 2-methyl-3-furanthiol were identified.[41] The latter compound is known to be responsible for the meaty-odor of chicken broth.[42] The corresponding thioether derivate possesses similar odor properties and is known to be a character impact compound of cooked meat;[43] however, it offers the advantage of being more stable as disulfide bridges cannot be formed. It is thus better suited for industrial applications. For the formation of 2-methyl-3-(methylthio)furan by fungi, the authors suggested an SMT to be present; however, this remained unproven. To examine whether the substrate spectrum of the OMT from *P. sapidus* includes other aroma relevant nucleophiles, the formation of 2-methyl-3-(methylthio)furan from the proposed precursor 2-methyl-3-furanthiol was studied. The GC-data revealed a significant difference in the formation of the methylated product compared to the enzyme blank and the chemical blank (Figure 6). Hence, PSA-OMT1 was able to catalyze the methylation of the thiol group to the respective thioether derivative. To the best of our knowledge, a fungal OMT that also accepts thiol-groups and, therefore, acts as SMT has not been described in the literature so far. Moreover, the biocatalytic conversion of 2-methyl-3-furanthiol

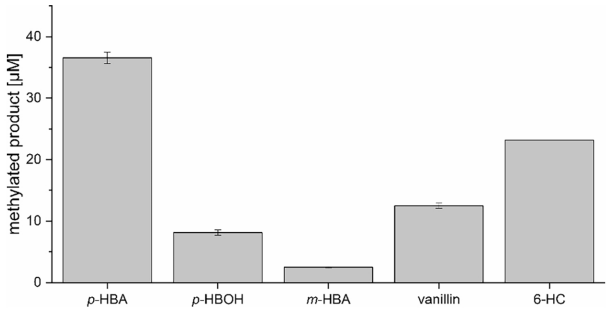

Figure 5. Conversion of different substrates using PSA-OMT1 under standard conditions without homogenization of the reaction mixture. *p*-hydroxybenzaldehyde (*p*-HBA) converted to *p*-anisaldehyde; *p*-hydroxybenzyl alcohol (*p*-HBOH) converted to *p*-methoxybenzyl alcohol; *m*-hydroxybenzaldehyde (*m*-HBA) converted to *m*-anisaldehyde; vanillin converted to veratric aldehyde; 6-hydroxycoumarin (6-HC) converted to 6-methoxycoumarin (standard deviation 0.03 μM). Reactions were performed in triplicate and error bars represent the respective standard deviation.

https://doi.org/10.1021/acs.jafc.3c08849
J. Agric. Food Chem. XXXX, XXX, XXX−XXX

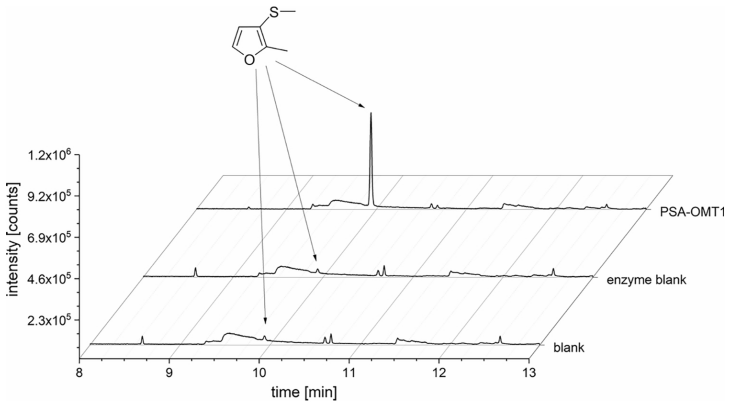

Figure 6. GC-MS chromatograms (total ion count) from the conversion of 2-methyl-3-furanthiol using PSA-OMT1 (sample) compared to a chemical blank (without addition of enzyme) and an enzyme blank (thermally deactivated enzyme at 100 °C for 20 min).

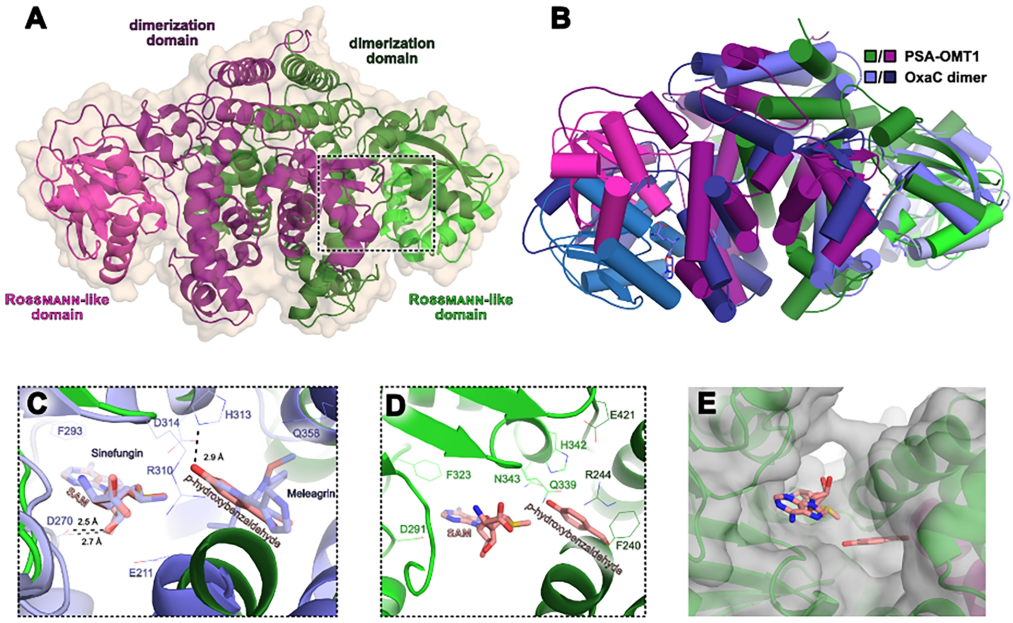

Figure 7. Crystal structure of PSA-OMT1 with structural comparison and potential substrate interaction modeling. (A) Overall structure of the PSA-OMT1 dimer (PDB: 8PHA), the two chains are colored in purple and green and the Rossmann-like fold is highlighted by lighter coloring. (B) Superposition of the dimers of PSA-OMT1 (purple/green) and OxaC (slate/blue) shows good alignment for their individual monomers with some orientational deviation within the dimer due to the substrate-bound state of OxaC. Superposition is displayed as a simplified cartoon. (C) View on the substrate-binding pockets of PSA-OMT1 and OxaC; the latter showing a SAM analog (sinefungin) and the OxaC substrate meleagrin in blue. For comparison, we included SAM and *p*-hydroxybenzaldehyde (salmon), the substrates of PSA-OMT1, at analogous positions as in OxaC. This gives a model how substrate binding may occur in PSA-OMT1. (D) Model of the PSA-OMT1-substrate complex. Residues, which potentially correspond to the substrate interacting residues of OxaC, are highlighted for PSA-OMT1 and shown with green labels. (E) Surface view of the substrate binding pocket of PSA-OMT1 shows the large open cavity that is formed by PSA-OMT1 allowing for promiscuous substrate binding.

to the thioether derivative has so far only been described for *Laetiporus* species and for an SMT from rat liver.[44]

Crystal Structure of PSA-OMT1. Crystals of PSA-OMT1 were obtained in an orthorhombic crystal form containing two OMT dimers per asymmetric symmetry unit. The structure

https://doi.org/10.1021/acs.jafc.3c08849
J. Agric. Food Chem. XXXX, XXX, XXX−XXX

was solved by molecular replacement and refined at 2.0 Å resolution (cf. Supporting Information S4). The dimeric organization of PSA-OMT1 (Figure 7A) is caused by an N-terminal, all-α helical domain with an overall large and complex interface (5841 Å^2) that is followed by the C-terminal catalytic domain with a Rossmann-like fold. This architecture is found in fungal SAM-dependent class I *O*-methyltransferases. Accordingly, this structure is similar to ascomycetal enzymes (Figure 7B) like the multifunctional SAM-dependent OMT-like pericyclase LepI from *Aspergillus flavus*[45] with an rmsd of 3.73 Å for 373 Cα atoms (PDB: 6IX8), the pericyclase PdxI from *A. bombycis*[46] (rmsd 3.24 Å for 357 Cα atoms, PDB: 7BQL), Hpil from *Hymenoscyphus scutula*[46] (3.17 Å, 351 Cα atoms, PDB: 7BQP), and OxaC from *Penicillium oxalicum*[47] (4.80 Å, 334 Cα atoms, PDB: 5W7S).

By structural comparison with these enzymes, the substrate binding site of PSA-OMT1 can be delineated (Figure 7C,D). A comparison with OxaC, a methyltransferase involved in the biosynthesis of the antiproliferative secondary metabolite oxaline, shows a high degree of conservation for residues involved in SAM binding. For example, D291 of PSA-OMT1 corresponds to D270 in OxaC, which forms two hydrogen bonds with the 2′ and 3′ hydroxyl groups of the ribose moiety of SAM (Figure 6C). Likewise, F323 (PSA-OMT1) can be predicted to form $\pi-\pi$ stacking to the adenine group of SAM as observed for F293 in OxaC. In comparison, the degree of conservation for the binding site of *p*-hydroxybenzaldehyde in PSA-OMT1 is rather low, given the high diversity of substrates, which are transformed by this fungal subfamily of methyltransferases. Notably, H342 is suitably positioned in PSA-OMT1 to act as a general base for catalysis at the hydroxyl or thiol group to be methylated (Figure 7D). In OxaC, its counterpart, H313, forms a hydrogen bond to the hydroxyl group of the substrate that is opposite to the methyl group of SAM. This residue is well conserved within this MT subfamily of fungal SAM-dependent class I *O*-methyltransferases. Furthermore, the substrate binding site of PSA-OMT1 is voluminous (Figure 7E), apparently a hallmark of these fungal MT enzymes and hence compatible for accepting the wide range of substrates as found in this study. Here, the observed regioselectivity for para-substituted phenol derivatives may be caused by a recognition of the phenyl substituent by the residues R244 and Q339 nearby.

Overall, the correlation of aroma and transcriptome data allowed the identification of a new OMT that enabled the methylation of several phenolic and one sulfur-containing aroma precursor. The approach used combined molecular biological, chemical-analytical, and bioinformatic methods to identify a new enzyme in fungi. Further work, such as cocrystallization experiments with substrates, could help to elucidate the catalytic mechanism. In addition, site-specific mutagenesis might increase enzyme efficiency, leading to possible industrial applications in the future.

■ ASSOCIATED CONTENT

Supporting Information

The Supporting Information is available free of charge at https://pubs.acs.org/doi/10.1021/acs.jafc.3c08849.

S1: effects of the reaction pH and temperature on the conversion of *p*-hydroxybenzaldehyde; S2: determination of enzyme kinetic parameters for *p*-hydroxybenzaldehyde and SAM; S3: amino acid sequence of the recombinantly produced PSA-OMT1; S4: data collection and refinement statistics of PSA-OMT1 (PDF)

■ AUTHOR INFORMATION

Corresponding Author

Holger Zorn − *Institute of Food Chemistry and Food Biotechnology, Justus Liebig University Giessen, Giessen 35392, Germany; Fraunhofer Institute for Molecular Biology and Applied Ecology, Giessen 35392, Germany;* orcid.org/0000-0002-8383-8196; Phone: +49 (0) 641 99 34900; Email: holger.zorn@uni-giessen.de

Authors

Fabio Francesco Brescia − *Institute of Food Chemistry and Food Biotechnology, Justus Liebig University Giessen, Giessen 35392, Germany;* orcid.org/0000-0003-3182-3301

Lukas Korf − *Institute of Biochemistry, Philips University Marburg, Marburg 35032, Germany*

Lars-Oliver Essen − *Institute of Biochemistry, Philips University Marburg, Marburg 35032, Germany*

Martin Ruehl − *Institute of Food Chemistry and Food Biotechnology, Justus Liebig University Giessen, Giessen 35392, Germany; Fraunhofer Institute for Molecular Biology and Applied Ecology, Giessen 35392, Germany*

Complete contact information is available at: https://pubs.acs.org/10.1021/acs.jafc.3c08849

Funding

Part of the work done by Martin Rühl was funded by the Fraunhofer society within the Attract project "Terpenoids from fungi".

Notes

The authors declare no competing financial interest.

■ ACKNOWLEDGMENTS

The authors would like to thank Paula Baar for her assistance with the experimental work.

■ ABBREVIATIONS USED

CIS, Cold Injection System; DK, dikaryotic strain; ME(P), malt extract soy peptone; MK, monokaryotic strain; ODP, olfactory detection port; OMT, *O*-methyltransferase; RI, retention index/indices; SAH, *S*-adenosyl-L-homocysteine; SAM, *S*-adenosyl-L-methionine; SMT, *S*-methyltransferase; TDU, Thermal Desorption Unit

■ REFERENCES

(1) Martin, J. SAM (dependent) I AM: the *S*-adenosylmethionine-dependent methyltransferase fold. *Curr. Opin. Struct. Biol.* **2002**, *12*, 783−793.

(2) Liscombe, D. K.; Louie, G. V.; Noel, J. P. Architectures, mechanisms and molecular evolution of natural product methyltransferases. *Nat. Prod. Rep.* **2012**, *29*, 1238−1250.

(3) Cai, X.-C.; Kapilashrami, K.; Luo, M. Synthesis and assays of inhibitors of methyltransferases. *Methods Enzymol.* **2016**, *574*, 245−308.

(4) Klimasauskas, S.; Lukinavicius, G. AdoMet-Dependent Methyltransferases, Chemistry of. In *Wiley Encyclopedia of Chemical Biology*; Begley, T. P., Ed.; John Wiley & Sons, Inc: Hoboken, NJ, USA, 2007.

(5) Matthews, R. G.; Koutmos, M.; Datta, S. Cobalamin-dependent and cobamide-dependent methyltransferases. *Curr. Opin. Struct. Biol.* **2008**, *18*, 658−666.

(6) Schubert, H. L.; Blumenthal, R. M.; Cheng, X. Many paths to methyltransfer: A chronicle of convergence. *Trends Biochem. Sci.* **2003**, *28*, 329−335.
(7) Krishnamohan, A.; Jackman, J. E. A family divided: Distinct structural and mechanistic features of the SpoU-TrmD (SPOUT) methyltransferase superfamily. *Biochemistry* **2019**, *58*, 336−345.
(8) O'Hagan, D.; Schmidberger, J. W. Enzymes that catalyse S_N2 reaction mechanisms. *Nat. Prod. Rep.* **2010**, *27*, 900−918.
(9) Cheng, X.; Kumar, S.; Posfai, J.; Pflugrath, J. W.; Roberts, R. J. Crystal structure of the Hhal DNA methyltransferase complexed with *S*-adenosyl-L-methionine. *Cell* **1993**, *74*, 299−307.
(10) Wlodarski, T.; Kutner, J.; Towpik, J.; Knizewski, L.; Rychlewski, L.; Kudlicki, A.; Rowicka, M.; Dziembowski, A.; Ginalski, K. Comprehensive structural and substrate specificity classification of the *Saccharomyces cerevisiae* methyltransferome. *PloS one* **2011**, *6*, No. e23168.
(11) Wuosmaa, A. M.; Hager, L. P. Methyl chloride transferase: A carbocation route for biosynthesis of halometabolites. *Science* **1990**, *249*, 160−162.
(12) Ibrahim, R. K.; Bruneau, A.; Bantignies, B. Plant *O*-methyltransferases: molecular analysis, common signature and classification. *Plant Mol. Biol.* **1998**, *36*, 1−10.
(13) Lam, K. C.; Ibrahim, R. K.; Behdad, B.; Dayanandan, S. Structure, function, and evolution of plant *O*-methyltransferases. *Genome* **2007**, *50*, 1001−1013.
(14) Lewis, N. G.; Yamamoto, E. Lignin: Occurrence, biogenesis and biodegradation. *Annu. Rev. Plant Physiol. Plant Mol. Biol.* **1990**, *41*, 455−496.
(15) Pham, L. T. M.; Kim, Y. H. Discovery and characterization of new O -methyltransferase from the genome of the lignin-degrading fungus Phanerochaete chrysosporium for enhanced lignin degradation. *Enzyme Microb. Technol.* **2016**, *82*, 66−73.
(16) Pham, L. T. M; Eom, M.-H.; Kim, Y. H. Inactivating effect of phenolic unit structures on the biodegradation of lignin by lignin peroxidase from *Phanerochaete chrysosporium*. *Enzyme Microb. Technol.* **2014**, *61*−*62*, 48−54.
(17) Jeffers, M. R.; McRoberts, W. C.; Harper, D. B. Identification of a phenolic 3-*O*-methyltransferase in the lignin-degrading fungus *Phanerochaete chrysosporium*. *Microbiology (Reading, Engl.)* **1997**, *143*, 1975−1981.
(18) Coulter, C.; Kennedy, J. T.; McRoberts, W. C.; Harper, D. B. Purification and properties of an *S*-adenosylmethionine: 2,4-Disubstituted phenol *O*-methyltransferase from *Phanerochaete chrysosporium*. *Appl. Environ. Microbiol.* **1993**, *59*, 706−711.
(19) Lapadatescu, C.; Giniès, C.; Le Quéré, J. L.; Bonnarme, P. Novel scheme for biosynthesis of aryl metabolites from L-phenylalanine in the fungus *Bjerkandera adusta*. *Appl. Environ. Microbiol.* **2000**, *66*, 1517−1522.
(20) Gutiérrez, A.; Caramelo, L.; Prieto, A.; Martínez, M. J.; Martínez, A. T. Anisaldehyde production and aryl-alcohol oxidase and dehydrogenase activities in ligninolytic fungi of the genus *Pleurotus*. *Appl. Environ. Microbiol.* **1994**, *60*, 1783−1788.
(21) Bürger, F.; Koch, M.; Fraatz, M. A.; Omarini, A. B.; Berger, R. G.; Zorn, H. Production of an anise- and woodruff-like aroma by monokaryotic strains of *Pleurotus sapidus* grown on citrus side streams. *Molecules* **2022**, *27*, 651.
(22) Burdock, G. A. *Fenaroli's handbook of flavor ingredients*, 6th ed.; CRC Press, Taylor & Francis Group: Boca Raton, 2010.
(23) Omarini, A. B.; Plagemann, I.; Schimanski, S.; Krings, U.; Berger, R. G. Crosses between monokaryons of *Pleurotus sapidus* or *Pleurotus florida* show an improved biotransformation of (+)-valencene to (+)-nootkatone. *Bioresour. Technol.* **2014**, *171*, 113−119.
(24) van den Dool, H.; Kratz, P. D. A generalization of the retention index system including linear temperature programmed gas-liquid partition chromatography. *J. Chromatogr. A* **1963**, *11*, 463−471.
(25) Laemmli, U. K. Cleavage of structural proteins during the assembly of the head of bacteriophage T4. *Nature* **1970**, *227*, 680−685.
(26) Towbin, H.; Staehelin, T.; Gordon, J. Electrophoretic transfer of proteins from polyacrylamide gels to nitrocellulose sheets: procedure and some applications. *Proc. Natl. Acad. Sci. U. S. A.* **1979**, *76*, 4350−4354.
(27) Davies, M. T. A universal buffer solution for use in ultra-violet spectrophotometry. *Analyst* **1959**, *84*, 248.
(28) Vonrhein, C.; Tickle, I. J.; Flensburg, C.; Keller, P.; Paciorek, W.; Sharff, A.; Bricogne, G. Advances in automated data analysis and processing within autoPRO, combined with improved characterisation, mitigation and visualisation of the anisotropy of diffraction limits using STARANISO. *Acta Crystallogr., Sect. A: Found. Adv.* **2018**, *74*, a360−a360.
(29) Jumper, J.; Evans, R.; Pritzel, A.; Green, T.; Figurnov, M.; Ronneberger, O.; Tunyasuvunakool, K.; Bates, R.; Žídek, A.; Potapenko, A.; et al. Highly accurate protein structure prediction with AlphaFold. *Nature* **2021**, *596*, 583−589.
(30) Emsley, P.; Lohkamp, B.; Scott, W. G.; Cowtan, K. Features and development of Coot. *Acta Crystallogr., Sect. D: Biol. Crystallogr.* **2010**, *66*, 486−501.
(31) Afonine, P. V.; Grosse-Kunstleve, R. W.; Echols, N.; Headd, J. J.; Moriarty, N. W.; Mustyakimov, M.; Terwilliger, T. C.; Urzhumtsev, A.; Zwart, P. H.; Adams, P. D. Towards automated crystallographic structure refinement with phenix.refine. *Acta Crystallogr., Sect. D: Biol. Crystallogr.* **2012**, *68*, 352−367.
(32) Trapp, T.; Zajul, M.; Ahlborn, J.; Stephan, A.; Zorn, H.; Fraatz, M. A. Submerged cultivation of *Pleurotus sapidus* with molasses: Aroma dilution analyses by means of solid phase microextraction and stir bar sorptive extraction. *J. Agric. Food Chem.* **2018**, *66*, 2393−2402.
(33) Krahe, N.-K.; Berger, R. G.; Witt, M.; Zorn, H.; Omarini, A. B.; Ersoy, F. Monokaryotic *Pleurotus sapidus* strains with intraspecific variability of an alkene cleaving DyP-type peroxidase activity as a result of gene mutation and differential gene expression. *Int. J. Mol. Sci.* **2021**, *22*, 1363 DOI: 10.3390/ijms22031363.
(34) Kota, P.; Guo, D.; Zubieta, C.; Noel, J.; Dixon, R. A. *O*-Methylation of benzaldehyde derivatives by "lignin specific" caffeic acid 3-*O*-methyltransferase. *Phytochemistry* **2004**, *65*, 837−846.
(35) Koeduka, T.; Kajiyama, M.; Furuta, T.; Suzuki, H.; Tsuge, T.; Matsui, K. Characterization of an *O*-methyltransferase specific to guaiacol-type benzenoids from the flowers of loquat (*Eriobotrya japonica*). *J. Biosci. Bioeng.* **2016**, *122*, 679−684.
(36) Koshiba, T.; Hirose, N.; Mukai, M.; Yamamura, M.; Hattori, T.; Suzuki, S.; Sakamoto, M.; Umezawa, T. Characterization of *S*-hydroxyconiferaldehyde *O*-methyltransferase in *Oryza sativa*. *Plant Biotechnol.* **2013**, *30*, 157−167.
(37) Busam, G.; Junghanns, K. T.; Kneusel, R. E.; Kassemeyer, H. H.; Matern, U. Characterization and expression of caffeoyl-coenzyme A 3-*O*-methyltransferase proposed for the induced resistance response of *Vitis vinifera* L. *Plant Physiol.* **1997**, *115*, 1039−1048.
(38) Kirita, M.; Tanaka, Y.; Tagashira, M.; Kanda, T.; Maeda-Yamamoto, M. Purification and characterization of a novel *O*-methyltransferase from *Flammulina velutipes*. *Biosci., Biotechnol., Biochem.* **2014**, *78*, 806−811.
(39) Wat, C.-K.; Towers, G. Phenolic *O*-methyltransferase from *Lentinus lepideus* (basidiomycete). *Phytochemistry* **1975**, *14*, 663−666.
(40) Schmidberger, J. W.; James, A. B.; Edwards, R.; Naismith, J. H.; O'Hagan, D. Halomethane biosynthesis: Structure of a SAM-dependent halide methyltransferase from *Arabidopsis thaliana*. *Angew. Chem., Int. Ed. Engl.* **2010**, *49*, 3646−3648.
(41) Yalman, S.; Trapp, T.; Vetter, C.; Popa, F.; Fraatz, M. A.; Zorn, H. Formation of a meat-like flavor by submerged cultivated *Laetiporus montanus*. *J. Agric. Food Chem.* **2023**, *71*, 8083−8092.
(42) Jayasena, D. D.; Ahn, D. U.; Nam, K. C.; Jo, C. Flavour chemistry of chicken meat: A review. *Asian-Australas. J. Anim. Sci.* **2013**, *26*, 732−742.
(43) Fan, M.; Xiao, Q.; Xie, J.; Cheng, J.; Sun, B.; Du, W.; Wang, Y.; Wang, T. Aroma compounds in chicken broths of Beijing Youji and commercial broilers. *J. Agric. Food Chem.* **2018**, *66*, 10242 DOI: 10.1021/acs.jafc.8b03297.

https://doi.org/10.1021/acs.jafc.3c08849
J. Agric. Food Chem. XXXX, XXX, XXX−XXX

(44) Lake, B. G.; Price, R. J.; Walters, D. G.; Phillips, J. C.; Young, P. J.; Adams, T. B. Studies on the metabolism of the thiofurans furfuryl mercaptan and 2-methyl-3-furanthiol in rat liver. *Food Chem. Toxicol.* **2003**, *41*, 1761−1770.
(45) Cai, Y.; Hai, Y.; Ohashi, M.; Jamieson, C. S.; Garcia-Borras, M.; Houk, K. N.; Zhou, J.; Tang, Y. Structural basis for stereoselective dehydration and hydrogen-bonding catalysis by the SAM-dependent pericyclase LepI. *Nat. Chem.* **2019**, *11*, 812−820.
(46) Ohashi, M.; Jamieson, C. S.; Cai, Y.; Tan, D.; Kanayama, D.; Tang, M.-C.; Anthony, S. M.; Chari, J. V.; Barber, J. S.; Picazo, E.; et al. An enzymatic Alder-ene reaction. *Nature* **2020**, *586*, 64−69.
(47) Newmister, S. A.; Romminger, S.; Schmidt, J. J.; Williams, R. M.; Smith, J. L.; Berlinck, R. G. S.; Sherman, D. H. Unveiling sequential late-stage methyltransferase reactions in the meleagrin/oxaline biosynthetic pathway. *Org. Biomol. Chem.* **2018**, *16*, 6450−6459.

https://doi.org/10.1021/acs.jafc.3c08849
J. Agric. Food Chem. XXXX, XXX, XXX−XXX